The Theory of High Field Transport and its Application to the Properties of Small Band Gap Semiconductors

A thesis presented by
Thomas Y. Stokoe
to the
University of St. Andrews
in application for the Degree of
Doctor of Philosophy

August 1972

Declaration

The accompanying thesis is my own composition. It is based on work carried out by me and no part of it has previously been presented in application for a Higher Degree.

J Stobbe.

I was admitted as a research student under Ordinance General No. 12 in October 1969, and as a candidate for the degree under this ordinance in October 1970.

Certificate

I certify that the conditions of the Ordinance and Regulations have been fulfilled.

J.F. Cornell

Research Supervisor

Acknowledgements

I should like to express my thanks to the following:

Dr. J.F. Cornwell, my research supervisor, for his constant interest and encouragement, and many suggestions which are unacknowledged in the thesis.

Professor R.B. Dingle, for the facilities made available to me in the Department of Theoretical Physics.

Mr. J.W. Allen, for valuable and informative discussion, particularly in the earlier chapters of this thesis.

The Science Research Council, which provided financial support throughout the course of this work.

Abstract

The theory of high field transport is applied to the properties of small band gap semiconductors. To describe the transport properties of small band gap semiconductors it is necessary to include the full effects of the lattice periodicity on the electron. Consequently the relaxation times and collision integrals for the various scattering mechanisms require generalisation, since the usual derivation of these quantities only consider the effect of the bulk properties of the lattice on the electrons. The theoretical methods which are developed will be concerned with this generalisation.

This thesis is principally concerned with the properties of polar semiconductors for which the traditional relaxation time approximation is inapplicable. Two methods of solution are discussed with regards to a description of the high field transport properties of n-InSb. The first method, the drifted Maxwellian approach, is based on the approximation that the functional form of the carrier distribution function is determined by carrier-carrier interactions. The simplicity of this approach is shown to provide a convenient starting point for calculation of semiconductor transport properties. Various scattering mechanisms are considered in a single energy band model of InSb, and reasonable semi-quantitative agreement with experiment is obtained when suitable material constants are chosen.

The second theoretical method considered is based on the solution of the Boltzmann equation by iteration, and is therefore essentially exact. The properties of the integral equations involved are discussed, with particular emphasis being placed on the numerical aspects of convergence. This method is applied to InSb where the effects of intervalley scattering are included producing good agreement with experiment.

Finally the two methods are compared, and a discussion is presented concerning the extension of the two theories to more realistic problems.

CONTENTS

CHAPTER 1

INTRODUCTION

Interest in the high field transport properties of solids first arose in connection with the dielectric breakdown of insulators [2]. Only at very high fields was it possible to produce any current flow in these materials. In the case of semiconductors, the application of a high field can result in a very large increase in the carrier energies, without any significant increase in carrier concentration. Thus, it is possible to deduce directly the effect of a high field on the carriers. A review of the subject has recently been published by E. M. Conwell [1], where a fairly extensive account of the high field transport properties of semiconductors is presented. The application of a high field to a metal does not produce any substantial change in the electron energies, and in general does not lead to any phenomena which do not occur at lower fields.

The definition of what can be regarded as a high field in a semiconductor will now be made: When the carriers of a non-degenerate system are in thermodynamic equilibrium, they will assume a Maxwellian energy distribution of the form

$$f(\underset{\sim}{k}) \propto \exp\left(-E(\underset{\sim}{k})/k_B T_0\right) \qquad 1.1.1$$

where E and $\underset{\sim}{k}$ are the carrier energy and momentum respectively, and T_0 is the temperature of the system.

If a small field is applied to this system, the carriers will drift in the direction of the field, and introduce an asymmetric component into the distribution function. This leads to the assumption which is adopted in the theory of low field transport, for which the distribution function is taken to be of the form

$$f(\underset{\sim}{k}) = f_0(E) + \cos\gamma\, f_1(E) \qquad 1.1.2$$

$$\text{with } f_1(E) \ll f_0(E),$$

where $f_0(E)$ is defined by equation 1.1.1, $f_1(E)$ is the asymmetric contribution, and γ is the angle between the carrier momentum and the field. This equation can be used in conjunction with the Boltzmann equation to derive the low field mobility of the carriers

provided details of the relevant scattering processes are known [46]. The mobility is expressed in terms of $f_0(\varepsilon)$ and is thus constant. At higher fields the average carrier energy begins to increase, and it is no longer possible to represent the spherically symmetric part of the distribution function by equation 1.1.1. If the "carrier heating" is not too large, this function may be given as

$$f_0(\varepsilon) \propto (1 + g(\varepsilon)) \exp(-\varepsilon/k_B T_0), \qquad 1.1.3$$

where $g(\varepsilon)$ represents a polynomial expansion in powers of the carrier energy. When equation 1.1.3 is substituted into equation 1.1.2, the resulting distribution function corresponds to what is termed the "warm electron" region, and it describes the onset of non-ohmic behaviour. At higher fields still, where the increase in carrier energy is large in comparison to the thermal equilibrium carrier energy, the function defined by equation 1.1.3 would become inappropriate and requires too many terms in order to represent the spherically symmetric part of the distribution function; this defines the "hot electron" region. When the dominant scattering processes of a system are essentially elastic the relaxation time approximation is applicable [1], and only the first two terms in the Legendre expansion of the distribution function as defined by equation 1.1.2 need be considered, even at high fields. But for the case of inelastic scattering, as for example when short wavelength acoustic phonons or optical phonons are present, this approximation is no longer valid and further terms in the Legendre expansion may be needed. The solution of the inelastic scattering problem will be of special interest in the chapters which follow.

The transport theory of semiconductors at low fields is concerned with carriers located in the close vicinity of specific symmetry points of the Brillouin zone. In the case of III-V compounds, this region of interest lies at the centre of the B.Z., but for materials such as Ge and Si the region of interest consists of a set of equivalent valleys located on the surface of the B.Z.. At higher fields carriers may become sufficiently energetic to redistribute themselves throughout large regions of the B.Z.. Consequently, band structure peculiarities become more evident than at lower fields; in Ge for example, the many valley band structure produces anisotropy in the carrier mobility for the different crystal orientations. A

phenomenon of particular interest arises in materials such as GaAs, and InSb [5] with higher valleys which lie a few tenths of an electron volt above the conduction band edge. Electrons with sufficient energy may be excited into these valleys, and thus radically change the average carrier mobility. In order to describe the transport properties of small band gap semiconductors accurately even at low fields, it has been necessary to include the effects of band structure non-parabolicity [22]. The following chapters will be concerned with the inclusion of these effects on the transport properties of small band gap semiconductors at high fields.

In recent years three methods have been applied to the solution of the high field transport problem in polar semiconductors. Firstly, an approximate method based on the assumption that the carrier distribution function can be represented by a transformed Maxwellian which was originally suggested by Fröhlich [3], and has been applied to the case of polar semiconductors by Stratton [21], Hammar and Weissglas [10], and others [8,9]. The simplicity of the method provides a convenient though inexact treatment of the transport problem, and Chapter 3 will be concerned with its generalisation to include the effects of band structure non-parabolicity, and other effects resulting from the periodicity of the crystal lattice. The theory is then applied to the material InSb in Chapter 4, in an attempt to understand the important scattering processes for various temperatures and fields. Most of the work presented in these two chapters has recently been published [11,12].

Two other methods which have been developed involve the solution of Boltzmann's equation by numerical means. Firstly, Monte Carlo techniques have been introduced by Kurosawa [4] and Boardman, Fawcett and Rees [5], where the properties of a single electron travelling through the crystal are simulated and averaged. It has been proved [5] that these Monte Carlo methods generate the Boltzmann solution. Secondly, a method for solving the Boltzmann equation by iteration from a trial distribution function has been discussed by Rees [6,7]. This approach provides a more comprehensive treatment of transport phenomena than the Monte Carlo technique since it is possible, for example, to include the effects of carrier-carrier scattering, and time varying effects in a straightforward manner. However, complex problems associated with the time independent solution of the Boltzmann equation can be treated more efficiently by the Monte Carlo approach.

Chapter 4 is concerned with the derivation of the Boltzmann equation and the associated collision integrals including the effects of band structure non-parabolicity, and Chapter 5 will involve the time dependent and time independent solutions of this equation for InSb at 77°K using Rees' iterative method. Since Rees' approach yields the exact result for the carrier transport in a semiconductor, it was possible to evaluate the electron mobility in InSb at very high fields with confidence. At such fields the effects of inter-valley scattering are shown to be important, and the results are in good agreement with a recent Monte Carlo calculation which has been made by Fawcett and Ruch [62]. Finally in Chapter 5 a comparison is made between the solution of the high field transport problem by the drifted Maxwellian approach of Chapters 2 and 3, and by the iterative solution of the Boltzmann equation given in Chapter 5.

CHAPTER 2

THE GENERAL THEORY OF THE DRIFTED MAXWELLIAN APPROACH

2.1 Introduction

The problem of evaluating the transport properties of electrons in solids can be considerably simplified if the distribution function of the particular system is known. Under the condition that carrier-carrier collisions are predominant, the distribution function is of the form [3]

$$f(\underset{\sim}{k}) \propto \exp\left[-\hbar^2(\underset{\sim}{k}-\underset{\sim}{k}_o)^2/(2m^* k_B T_e)\right], \qquad 2.1.1$$

where the electrons are out of thermal equilibrium with the lattice at a temperature T_e, and $\underset{\sim}{k}_o$ is the displacement of the electron distribution function in momentum space due to the applied field. In the case of small band gap semiconductors it is necessary to generalise the above function in order to include the effects of band structure non-parabolicity. Licea [13-16] assumed a displaced Maxwellian of the form

$$f(\underset{\sim}{k}) \propto \exp\left[-E(|\underset{\sim}{k}-\underset{\sim}{k}_o|)/k_B T_e\right], \qquad 2.1.2$$

which is the solution of Boltzmann's equation (4.6), but for a non-parabolic band structure there is no simple relationship between $\underset{\sim}{k}_o$ and the average drift velocity of the carriers. A more suitable expression for the solution to the Boltzmann equation is the drifted Maxwellian

$$f(\underset{\sim}{k}) \propto \exp\left[-(E(\underset{\sim}{k})-\hbar \underset{\sim}{V}_D.\underset{\sim}{k})/k_B T_e\right], \qquad 2.1.3$$

suggested by Hammar and Weissglas [10] . With this form the electrons assume a Maxwellian distribution function at a temperature T_e, in a reference frame moving at a velocity $\underset{\sim}{V}_D$ relative to that of the lattice.

There are a number of ways of obtaining the mobility-field characteristic of a particular system with a known distribution function. The usual method is to average the electron energy and momentum over the change of the distribution function with time due to

collis ion with the different scattering mechanisms. The resulting equations are [1]

$$\left.\begin{aligned} -\int E\left(\frac{\partial f}{\partial t}\right)_c d^3\underset{\sim}{k} &= e\underset{\sim}{V}_D \cdot \underset{\sim}{F} \\ -\int \hbar \underset{\sim}{k}\left(\frac{\partial f}{\partial t}\right)_c d^3\underset{\sim}{k} &= e\underset{\sim}{F} \end{aligned}\right\} \qquad 2.1.4$$

where $\underset{\sim}{F}$ is the applied field, and $\underset{\sim}{V}_D$ is the resultant drift velocity. An alternative but entirely equivalent method (cf. [1,10]) is to average the rate of loss of energy and the rate of loss of momentum due to the different scattering mechanisms, giving

$$\left.\begin{aligned} -\int \frac{dE}{dt} f(\underset{\sim}{k})\, d^3\underset{\sim}{k} &= e\underset{\sim}{V}_D \cdot \underset{\sim}{F} \\ -\int \frac{d}{dt}(\hbar \underset{\sim}{k}) f(\underset{\sim}{k})\, d^3\underset{\sim}{k} &= e\underset{\sim}{F} \end{aligned}\right\} \qquad 2.1.5$$

Both these methods involve a triple intergration over the momentum space associated with the scattering mechanisms, followed by a triple integration over the momentum space associated with the electrons. Since equations 2.1.5 do not involve the distribution function until the final triple integration, it will be shown that this leads to a simpler and more generally applicable formulation than that of equations 2.1.4. Thus using the distribution function 2.1.3 in equations 2.1.5 it is possible to evaluate the mobility-field characteristic resulting from various combinations of scattering mechanisms in closed integral form.

The following sections of this chapter will be concerned with the derivation of equations 2.1.5 for lattice scattering due to polar optical and acoustic phonons, and ionised impurity scattering. The equations are expressed in terms of a generalised band structure which is spherically symmetric in $\underset{\sim}{k}$ space, and the effects of the mixing of the Bloch states and spin reversal scattering are included in each case.

It has been usual to approximate the distribution functions 2.1.1 - 2.1.3 by expanding the drift term in the exponential to

first order, in order to make subsequent calculations tractable. This is equivalent to assuming that the ratio of the drift velocity to the "thermal" velocity of the electrons is small, which is not true in all circumstances [9] . This assumption is not made throughout the following theory.

2.2 Polar Optical Scattering

The rate of loss of energy and momentum by electrons as a consequence of interacting with the polar optical phonon field have been calculated for a parabolic band by Conwell [17] and Paranjape [18] , and for a simplified Kane band structure [19] by Hammar and Weissglas [10] . They will now be evaluated for a generalised band structure.

The rate of loss of energy by an electron in a state $\underset{\sim}{k}$ is given by

$$\frac{dE}{dt} = \sum_{q} \hbar\omega_q \left[P_a(\underset{\sim}{k} \rightarrow \underset{\sim}{k}+\underset{\sim}{q}) - P_e(\underset{\sim}{k} \rightarrow \underset{\sim}{k}-\underset{\sim}{q})\right], \qquad 2.2.1$$

where $P_a(\underset{\sim}{k} \rightarrow \underset{\sim}{k}+\underset{\sim}{q})$ is the absorption probability, and $P_e(\underset{\sim}{k} \rightarrow \underset{\sim}{k}-\underset{\sim}{q})$ is the emission probability, $\hbar\omega_q$ is the phonon energy, and $\underset{\sim}{q}$ is the phonon wave vector. Similarly the rate of loss of momentum in the direction $\underset{\sim}{k}$ is

$$\frac{d(\hbar\underset{\sim}{k})}{dt} = \sum_{q} \hbar q_k \left[P_a(\underset{\sim}{k} \rightarrow \underset{\sim}{k}+\underset{\sim}{q}) - P_e(\underset{\sim}{k} \rightarrow \underset{\sim}{k}-\underset{\sim}{q})\right], \qquad 2.2.2$$

where $q_k = (\hat{k}.\underset{\sim}{q})\,\hat{k}$, with $\hat{k}$ defining the unit vector.

According to Fröhlich [20] , the matrix element for s-type wave functions for polar optical scattering is given by

$$|(\underset{\sim}{k} \pm \underset{\sim}{q}|H'_{po}|\underset{\sim}{k})|^2 = \frac{2\pi\hbar\omega e^2}{4\pi\varepsilon_0 V q^2}\left(\frac{1}{\varepsilon_\infty} - \frac{1}{\varepsilon_s}\right)\left(N+\tfrac{1}{2}\mp\tfrac{1}{2}\right), \qquad 2.2.3$$

where $N = (exp(\hbar\omega/k_B T_0) - 1)^{-1}$, V is the crystal volume, ω is the frequency of the longitudinal phonons (taken as constant), T_0 is the lattice temperature, ε_∞ and ε_s are the high and low frequency dielectric constants respectively, and ε_0 the permittivity of free space.

2.2.(a) Rate of loss of energy

The parabolic case is described by Conwell [1] p.156. It will now be generalised for an arbitrary band structure. Assuming the validity of perturbation theory, equation 2.2.1 can be written as

$$\frac{dE}{dt} = \frac{2\pi}{\hbar}\sum_{q} \hbar\omega\left[|(\underset{\sim}{k}+\underset{\sim}{q}|H'_{po}|\underset{\sim}{k})|^2 \delta(E_{\underset{\sim}{k}+\underset{\sim}{q},N-1} - E_{\underset{\sim}{k},N}) - |(\underset{\sim}{k}-\underset{\sim}{q}|H'_{po}|\underset{\sim}{k})|^2 \delta(E_{\underset{\sim}{k}-\underset{\sim}{q},N+1} - E_{\underset{\sim}{k},N})\right] \qquad 2.2.4$$

with the usual transformation

$$\sum_{q} \longrightarrow \frac{V}{8\pi^3}\iiint q^2 \sin\theta \, dq \, d\theta \, d\phi \qquad 2.2.5$$

2.2.3 and 2.2.5 give

$$\frac{dE}{dt} = \frac{e^2(\hbar\omega)^2 N}{(4\pi\varepsilon_0)\,2\pi\hbar}\left(\frac{1}{\varepsilon_\infty} - \frac{1}{\varepsilon_s}\right)\iiint \Big[\delta\left(E((\underset{\sim}{k}+\underset{\sim}{q})^2) - E(k^2) - \hbar\omega\right)$$

$$- \exp(\hbar\omega/k_B T_0)\,\delta\left(E((\underset{\sim}{k}-\underset{\sim}{q})^2) - E(k^2) + \hbar\omega\right)\Big] \sin\theta \, dq \, d\theta \, d\phi .$$

Thus

$$\frac{dE}{dt} = \frac{e^2(\hbar\omega)^2 N}{4\pi\varepsilon_0 \hbar}\left(\frac{1}{\varepsilon_\infty} - \frac{1}{\varepsilon_s}\right)\left\{ I_+(E) - \exp\left(\frac{\hbar\omega}{k_B T_0}\right) I_-(E)\right\}, \qquad 2.2.6$$

where

$$I_+(E) = \iint \delta\left(E((\underset{\sim}{k}+\underset{\sim}{q})^2) - E(k^2) - \hbar\omega\right) \sin\theta \, d\theta \, dq ,$$

and

$$I_-(E) = \iint \delta\left(E((\underset{\sim}{k}-\underset{\sim}{q})^2) - E(k^2) + \hbar\omega\right) \sin\theta \, d\theta \, dq .$$

To facilitate the evaluation of these integrals the function $F(E)$ is defined such that $k^2 = F(E)$ is the inverse of $E = E(k^2)$. Thus, taking $F'(E) = dF/dE$ and letting

$$x = E((\underset{\sim}{k}+\underset{\sim}{q})^2),$$

then

$$k^2 + 2kq\cos\theta + q^2 = F(x),$$

and

$$-2kq \sin\theta \, d\theta = F'(x)\, dx .$$

By substitution

$$I_+(E) = \iint_{E(k^2+q^2)}^{E((\underset{\sim}{k}-\underset{\sim}{q})^2)} -\frac{F'(x)}{2kq}\,\delta(x - (E+\hbar\omega))\, dx\, dq ,$$

which when intergrated results in

$$I_+(E) = \frac{F'(E+\hbar\omega)}{2\sqrt{F(E)}} \int_{q_{min}}^{q_{max}} \frac{dq}{q} \quad . \qquad 2.2.7$$

The limits for the integration over q must satisfy the conditions defined in the argument of the δ function in equation 2.2.4, i.e.

$$E((\underset{\sim}{k}+\underset{\sim}{q})^2) = E(k^2) + \hbar\omega \, .$$

Thus

$$(\underset{\sim}{k}+\underset{\sim}{q})^2 = F(E+\hbar\omega) \, .$$

Defining $k' = \sqrt{F(E+\hbar\omega)}$ then $\underset{\sim}{k}' = \underset{\sim}{k}+\underset{\sim}{q}$ which results in

$q_{min}^{max} = |\underset{\sim}{k}'| \pm |\underset{\sim}{k}|$, since q must be positive.

Hence

$$q_{min}^{max} = \sqrt{F(E+\hbar\omega)} \pm \sqrt{F(E)} \qquad 2.2.8$$

which when substituted into the limits of equation 2.2.7 produces

$$I_+(E) = \frac{F'(E+\hbar\omega)}{2\sqrt{F(E)}} \log \frac{\sqrt{F(E+\hbar\omega)}+\sqrt{F(E)}}{\sqrt{F(E+\hbar\omega)}-\sqrt{F(E)}} \, .$$

By a similar calculation

$$I_-(E) = \frac{F'(E-\hbar\omega)}{2\sqrt{F(E)}} \log \frac{\sqrt{F(E)}+\sqrt{F(E-\hbar\omega)}}{\sqrt{F(E)}-\sqrt{F(E-\hbar\omega)}} \, ,$$

and

$$\frac{dE}{dt} = \frac{e^2(\hbar\omega)^2 N}{8\pi\varepsilon_0 \hbar\sqrt{F(E)}} \left(\frac{1}{\varepsilon_\infty} - \frac{1}{\varepsilon_s}\right) \left\{ F'(E+\hbar\omega) \log \frac{\sqrt{F(E+\hbar\omega)}+\sqrt{F(E)}}{\sqrt{F(E+\hbar\omega)}-\sqrt{F(E)}} \right. \qquad 2.2.9$$

$$\left. - \exp\left(\frac{\hbar\omega}{k_B T_0}\right) F'(E-\hbar\omega) \log \frac{\sqrt{F(E)}+\sqrt{F(E-\hbar\omega)}}{\sqrt{F(E)}-\sqrt{F(E-\hbar\omega)}} \right\} .$$

2.2.(b) Rate of loss of momentum

The derivation of the rate of loss of momentum follows closely that of the rate of loss of energy. Thus, substituting equations 2.2.3 and 2.2.5 into equation 2.2.2 and

$$\frac{d}{dt}(\hbar\underset{\sim}{k}) = \frac{e^2\hbar\omega N}{(4\pi\varepsilon_0)2\pi\hbar} \left(\frac{1}{\varepsilon_\infty} - \frac{1}{\varepsilon_s}\right) \iiint \hbar\underset{\sim}{q}_{tR} \left[\delta(E_{\underset{\sim}{k}+\underset{\sim}{q},N-1} - E_{\underset{\sim}{k},N}) \right.$$

$$- \exp\left(\frac{\hbar\omega}{k_B T_0}\right) \delta\left(E_{\underline{k}-\underline{q},N+1} - E_{\underline{k},N}\right) \Big] \sin\theta \, d\theta \, dq \, d\phi ,$$

where $\underline{q}_{\underline{k}} = q \cos\theta \, \hat{\underline{k}}$. Therefore

$$\frac{d}{dt}(\hbar \underline{k}) = \frac{e^2 \hbar \omega N}{4\pi \varepsilon_0 \sqrt{F(E)}} \underline{k} \left(\frac{1}{\varepsilon_\infty} - \frac{1}{\varepsilon_0}\right) \left\{ M_+(E) - \exp\left(\frac{\hbar\omega}{k_B T_0}\right) M_-(E) \right\} \qquad 2.2.10$$

where

$$M_+(E) = \iint q \cos\theta \, \delta\left(E((\underline{k}+\underline{q})^2) - E(k^2) - \hbar\omega\right) \sin\theta \, d\theta \, dq ,$$

and

$$M_-(E) = \iint q \cos\theta \, \delta\left(E((\underline{k}-\underline{q})^2) - E(k^2) + \hbar\omega\right) \sin\theta \, d\theta \, dq .$$

These integrals can be evaluated using the method described earlier by defining the function $k^2 = F(E)$ as the inverse of $E = E(k^2)$. Therefore if $X = E((\underline{k}+\underline{q})^2)$, then

$$\cos\theta = \frac{1}{2kq} \left(F(x) - k^2 - q^2 \right), \qquad 2.2.11$$

and as before

$$- 2kq \sin\theta \, d\theta = F'(x) \, dx .$$

Hence

$$M_+(E) = - \iint_{E((\underline{k}+\underline{q})^2)}^{E((\underline{k}-\underline{q})^2)} \frac{F'(x)}{4k^2 q} \left(F(x) - k^2 - q^2\right) \delta\left(x - E - \hbar\omega\right) dx \, dq$$

which gives

$$M_+(E) = \frac{F'(E+\hbar\omega)}{4F(E)} \int \frac{F(E+\hbar\omega) - F(E)}{q} - q \, . \, dq .$$

The limits for this integration are given by equation 2.2.8, and

$$M_+(E) = \frac{F'(E+\hbar\omega)}{4F(E)} \left\{ \left[F(E+\hbar\omega) - F(E)\right] \log \frac{\sqrt{F(E+\hbar\omega)} + \sqrt{F(E)}}{\sqrt{F(E+\hbar\omega)} - \sqrt{F(E)}} \right.$$

$$\left. - 2\sqrt{F(E+\hbar\omega)}\sqrt{F(E)} \right\} .$$

Similarly

$$M_{-}(E) = \frac{F'(E-\hbar\omega)}{4F(E)}\left\{\left[F(E)-F(E-\hbar\omega)\right]\log\frac{\sqrt{F(E)}+\sqrt{F(E-\hbar\omega)}}{\sqrt{F(E)}-\sqrt{F(E-\hbar\omega)}} + 2\sqrt{F(E-\hbar\omega)}\sqrt{F(E)}\right\},$$

which results in

$$\frac{d}{dt}(\hbar\underset{\sim}{k}) = \frac{e^2\hbar\omega N}{16\pi\varepsilon_0 F(E)^{3/2}}\underset{\sim}{k}\left(\frac{1}{\varepsilon_\infty}-\frac{1}{\varepsilon_s}\right)\left\{F'(E+\hbar\omega)\left(\left[F(E+\hbar\omega)-F(E)\right]\right.\right.$$
$$\times\log\frac{\sqrt{F(E+\hbar\omega)}+\sqrt{F(E)}}{\sqrt{F(E+\hbar\omega)}-\sqrt{F(E)}} - 2\sqrt{F(E+\hbar\omega)}\sqrt{F(E)}\Big) - \exp\left(\frac{\hbar\omega}{k_B T_0}\right)F'(E-\hbar\omega) \qquad 2.2.12$$
$$\left.\times\left(\left[F(E)-F(E-\hbar\omega)\right]\log\frac{\sqrt{F(E)}+\sqrt{F(E-\hbar\omega)}}{\sqrt{F(E)}-\sqrt{F(E-\hbar\omega)}} + 2\sqrt{F(E-\hbar\omega)}\sqrt{F(E)}\right)\right\}.$$

2.2.(c) Averaging the rates of loss of energy and momentum

Averaging the rate of loss of energy over the drifted Maxwellian distribution function defined by equation 2.1.3 and

$$\left\langle\frac{dE}{dt}\right\rangle = \frac{\int_0^{2\pi}\int_0^{\pi}\int_0^{\chi'}\frac{dE}{dt}\exp\left[-\frac{1}{k_B T_e}\left(E(k^2)-\hbar\underset{\sim}{V}_D\cdot\underset{\sim}{k}\right)\right]k^2\sin\gamma\,dk\,d\gamma\,d\psi}{\int_0^{2\pi}\int_0^{\pi}\int_0^{\chi'}\exp\left[-\frac{1}{k_B T_e}\left(E(k^2)-\hbar\underset{\sim}{V}_D\cdot\underset{\sim}{k}\right)\right]k^2\sin\gamma\,dk\,d\gamma\,d\psi}$$

where χ' is the upper limit of the band. Hence

$$\left\langle\frac{dE}{dt}\right\rangle = \frac{\int_0^{\chi}Y(E,V_D,T_e)\frac{dE}{dt}\sqrt{F(E)}\,F'(E)\exp\left(-\frac{E}{k_B T_e}\right)dE}{\int_0^{\chi}Y(E,V_D,T_e)\sqrt{F(E)}\,F'(E)\exp\left(-\frac{E}{k_B T_e}\right)dE}, \qquad 2.2.13$$

where $Y(E,V_D,T_e) = \frac{\sinh a}{a}$, and $a = \frac{\hbar V_D\sqrt{F(E)}}{k_B T_e}$.

Similarly averaging the rate of loss of momentum in the $\hat{V}_D$ direction,

$$\left\langle\frac{d(\hbar\underset{\sim}{k})}{dt}\right\rangle = \hat{V}_D\frac{\int_0^{2\pi}\int_0^{\pi}\int_0^{\chi'}\left(\frac{d(\hbar\underset{\sim}{k})}{dt}\cdot\hat{V}_D\right)\exp\left[-\frac{1}{k_B T_e}\left(E(k^2)-\hbar\underset{\sim}{V}_D\cdot\underset{\sim}{k}\right)\right]k^2\sin\gamma\,dk\,d\gamma\,d\psi}{\int_0^{2\pi}\int_0^{\pi}\int_0^{\chi'}\exp\left[-\frac{1}{k_B T_e}\left(E(k^2)-\hbar\underset{\sim}{V}_D\cdot\underset{\sim}{k}\right)\right]k^2\sin\gamma\,dk\,d\gamma\,d\psi},$$

hence

$$\left\langle \frac{d(\hbar k_\beta)}{dt} \right\rangle = \frac{\hbar V_D}{3 k_B T_e} \frac{\int_0^\chi Z(E, V_D, T_e) \left| \frac{d(\hbar k_\beta)}{dt} \right| F(E) F'(E) \exp\left(-\frac{E}{k_B T_e}\right) dE}{\int_0^\chi Y(E, V_D, T_e) \sqrt{F(E)}\, F'(E) \exp\left(-\frac{E}{k_B T_e}\right) dE}, \qquad 2.2.14$$

where $Z(E, V_D, T_e) = \frac{3}{a^3}(a\cosh a - \sinh a)$.

Thus, averaging equations 2.2.9 and 2.2.12 as indicated above, taking the limits of integration over the energy from 0 to $\chi - \hbar\omega$ for absorption, and from $\hbar\omega$ to χ for emission,

$$\left\langle \frac{dE}{dt} \right\rangle = - \frac{e^2 (\hbar\omega)^2 N}{8\pi\varepsilon_0 \hbar} \left(\frac{1}{\varepsilon_\infty} - \frac{1}{\varepsilon_s}\right) \frac{I_1}{I_N} \qquad 2.2.15$$

and

$$\left\langle \frac{d(\hbar k_\beta)}{dt} \right\rangle = - \hbar V_D \frac{e^2 \hbar\omega N}{48\pi\varepsilon_0 k_B T_e} \left(\frac{1}{\varepsilon_\infty} - \frac{1}{\varepsilon_s}\right) \frac{I_2 + I_3}{I_N}, \qquad 2.2.16$$

where

$$I_1 = \int_0^\chi \left(Y(b) \exp\left(\frac{\hbar\omega}{k_B T_0} - \frac{\hbar\omega}{k_B T_e}\right) - Y(a) \right) F'(E+\hbar\omega) F'(E) \times \log \frac{\sqrt{F(E+\hbar\omega)} + \sqrt{F(E)}}{\sqrt{F(E+\hbar\omega)} - \sqrt{F(E)}} \exp\left(-\frac{E}{k_B T_e}\right) dE,$$

$$I_2 = \int_0^\chi R_-(E, V_D, T_e)\, F'(E+\hbar\omega) F'(E) [F(E+\hbar\omega) - F(E)] \times \log \frac{\sqrt{F(E+\hbar\omega)} + \sqrt{F(E)}}{\sqrt{F(E+\hbar\omega)} - \sqrt{F(E)}} \exp\left(-\frac{E}{k_B T_e}\right) dE,$$

$$I_3 = \int_0^\chi 2 R_+(E, V_D, T_e)\, F'(E+\hbar\omega) F'(E) \sqrt{F(E+\hbar\omega)} \sqrt{F(E)} \exp\left(-\frac{E}{k_B T_e}\right) dE,$$

$$I_N = \int_0^\chi Y(a) \sqrt{F(E)}\, F'(E) \exp\left(-\frac{E}{k_B T_e}\right) dE,$$

$$R_{\pm}(E, V_D, T_e) = \left\{ Z(b) \exp\left(\frac{\hbar\omega}{k_B T_0} - \frac{\hbar\omega}{k_B T_e}\right) \pm Z(a) \right\},$$

$b = \frac{\hbar V_D}{k_B T_e} \sqrt{F(E+\hbar\omega)}$, Y, Z and a are defined above.

If we assume that the drift parameter in the distribution function is small, taking a first order approximation it can be seen that Y and Z tend to unity. Choosing $F(E) = 2m^*E/\hbar^2$, as is the case for a parabolic band where m^* is the effective mass at the centre of the B.Z., equations 2.1.15 and 2.1.16 reduce to those given by Stratton [21] . For an approximated Kane band structure [19] , where $F(E) = 2m^*E(1+E/G)/\hbar^2$, G is the band gap, equations 2.1.15 and 2.1.16 reduce to those given by Hammar and Weissglas [10] . (A factor of $1/Ak_BT_e$ is missing from equation (8) in reference [10] , but is included in the subsequent calculation of that paper).

2.2.(d) Inclusion of the mixing of Bloch states and spin-reversal scattering

When the full effect of the periodic lattice is taken into account, not only is the band structure non-parabolic, but the electron energy eigen functions are not pure plane waves. The latter part requires the insertion on the right-hand side of equation 2.2.3 a multiplicative factor $G(k, k', y)$ as shown by Ehrenreich [22] , where

$$G(k, k', y) = \frac{1}{2} \sum_{\mu,\mu'} \left| \int_0 \Phi_{\mu' k'}(\underline{r}) \, \Phi_{\mu k}(\underline{r}) \, d\underline{r} \right| \qquad 2.2.17$$

$\Phi_{\mu k}$ are the cell periodic parts of the Bloch wave functions, and μ , μ' are spin labels. Kane [19] has evaluated these functions in the case of compounds with a conduction band minimum at the centre of the B.Z., which results in an expansion of the form

$$G(k, k', y) = g(k, k') + \rho(k, k')\, y + \sigma(k, k')\, y^2 \qquad 2.2.18$$

where $\underline{k}' = \underline{k} \pm \underline{q}$ and $y = \hat{k} \cdot \hat{k}'$.

The rate of loss of energy can be derived in the same way as

plane wave case in sub-section 2.2.(a). Thus

$$\frac{dE}{dt} = \frac{e^2(\hbar\omega)^2 N}{4\pi\varepsilon_0 \hbar}\left(\frac{1}{\varepsilon_\infty} - \frac{1}{\varepsilon_s}\right)\left\{ I_{sp+}(E) - \exp\left(\frac{\hbar\omega}{k_B T_0}\right) I_{sp-} \right\}, \qquad 2.2.19$$

by analogy with equation 2.2.6. Now

$$I_{sp+}(E) = \iint G(k,k',y)\,\delta\left(E((\underline{k}+\underline{q})^2) - E(k^2) - \hbar\omega\right)\sin\theta\, d\theta\, dq$$

where $\underline{k}' = \underline{k} + \underline{q}$, and $y = \hat{k}.\hat{k}' = (k + q\cos\theta)/k'$. Defining $x = E((\underline{k}+\underline{q})^2)$ in the usual way and $y = \frac{k^2 + F(x) - q^2}{2k\sqrt{F(x)}}$, which leads to

$$I_{sp+}(E) = \frac{1}{2k}\iint \frac{F'(x)}{q}\left\{ g(k,\sqrt{F(x)}) + \rho(k,\sqrt{F(x)})\left(\frac{k^2 + F(x) - q^2}{2k\sqrt{F(x)}}\right) + \sigma(k,\sqrt{F(x)})\left(\frac{k^2 + F(x) - q^2}{2k\sqrt{F(x)}}\right)^2 \right\} \delta(x - (E+\hbar\omega))\, dx\, dq.$$

Hence with $k' = \sqrt{F(E+\hbar\omega)}$

$$I_{sp+}(E) = \frac{F'(E+\hbar\omega)}{2\sqrt{F(E)}} \int_{q_{min}}^{q_{max}} \left[\frac{Q(k,k')}{q} - R(k,k')q + S(k,k')q^3 \right] dq,$$

where

$$Q(k,k') = g(k,k') + \frac{k'^2 + k^2}{2k'k}\rho(k,k') + \frac{(k'^2 + k^2)^2}{4k'^2k^2}\sigma(k,k'),$$

$$R(k,k') = \frac{\rho(k,k')}{2kk'} + \frac{k'^2 + k^2}{2k'^2k^2}\sigma(k,k'),$$

and

$$S(k,k') = \frac{\sigma(k,k')}{4k'^2k^2}.$$

Hence using the limits of integration from equation 2.2.8 and

$$I_{sp+}(E) = \frac{F'(E+\hbar\omega)}{2\sqrt{F(E)}}\left\{ Q \log\frac{k'+k}{k'-k} - 2Rk'k + 2Skk'(k'^2 + k^2) \right\},$$

$$I_{sp+}(E) = \frac{F'(E+\hbar\omega)}{2\sqrt{F(E)}}\, T(E, E+\hbar\omega).$$

Similarly

$$I_{sp-}(E) = \frac{F'(E-\hbar\omega)}{2\sqrt{F(E)}}\, T(E-\hbar\omega, E).$$

The rate of loss of momentum can be calculated in exactly the same manner giving

$$\frac{d(\hbar \underset{\sim}{k})}{dt} = \frac{e^2 \hbar \omega N}{4\pi \varepsilon_0 \sqrt{F(E)}} \underset{\sim}{k} \left(\frac{1}{\varepsilon_\infty} - \frac{1}{\varepsilon_s}\right) \left\{ M_{sp+}(E) - \exp\left(\frac{\hbar\omega}{k_B T_0}\right) M_{sp-}(E) \right\}, \qquad 2.2.20$$

where

$$M_{sp\pm}(E) = \iint q \cos\theta \, G(k, k', y) \, \delta\left(E((\underset{\sim}{k} + \underset{\sim}{q})^2) - E(k^2) - \hbar\omega\right) \sin\theta \, d\theta \, dq.$$

Integrating over θ as for $I_{sp\pm}(E)$ and

$$M_{sp\pm}(E) = \frac{F'(E+\hbar\omega)}{4F(E)} \int \frac{1}{q} \left((k'^2 - k^2) - q^2\right)\left(Q - Rq^2 + Sq^4\right) dq.$$

This reduces to

$$M_{sp\pm}(E) = \frac{F'(E+\hbar\omega)}{4F(E)} \left\{ (k'^2 - k^2)\left[Q \log \frac{k'+k}{k'-k} - 2Rkk' + 2Skk'(k'^2 + k^2) \right] \right.$$
$$\left. - 2\left[Qkk' - Rkk'(k'^2 + k^2) + Skk'\left(k'^4 + \frac{10}{3} k'^2 k^2 + k^4\right) \right] \right\},$$

where Q, R, and S are defined above.

Thus

$$M_{sp+}(E) = \frac{F'(E+\hbar\omega)}{4F(E)} \left\{ \left[F(E+\hbar\omega) - F(E)\right] T(E, E+\hbar\omega) - 2U(E, E+\hbar\omega) \right\},$$

and

$$M_{sp-}(E) = \frac{F'(E-\hbar\omega)}{4F(E)} \left\{ \left[F(E) - F(E-\hbar\omega)\right] T(E-\hbar\omega, E) + 2U(E-\hbar\omega, E) \right\}.$$

Equations 2.2.19 and 2.2.20 can be averaged in exactly the same way as equations 2.2.9 and 2.2.12, resulting in modified forms of equations 2.2.15 and 2.2.16.

2.3 Acoustic Phonon Scattering

Acoustic phonon scattering can be treated in a similar way to polar optical phonon scattering. The s-type matrix element that is analogous to that of equation 2.2.3 is given by Conwell [1] p.108, where

$$|\langle \underset{\sim}{k} \pm \underset{\sim}{q} | H_q' | \underset{\sim}{k} \rangle|^2 = \frac{E_1^2 \hbar \omega_q}{2\rho u^2 V} \left(N_q + \tfrac{1}{2} \mp \tfrac{1}{2} \right), \qquad 2.3.1$$

$N_q = (\exp(\hbar\omega_q/k_B T_0) - 1)^{-1}$, E_1 is the deformation potential, u the average longitudinal sound velocity, and ρ the crystal density. The remaining parameters have been defined earlier.

A linear dispersion relation $\omega_q = uq$ will be assumed for the longitudinal acoustic phonon spectrum. For most materials of interest at temperatures greater than about 20°K the acoustic phonon energy is much less than the average energy of the carriers, so it will be assumed that $\hbar\omega_q \ll k_B T_0$ throughout the following calculations. This in fact defines the condition of equipartition of energy for the lattice oscillators [1] p.9.

2.3.(a) Rate of loss of energy

The parabolic case is described in [1] chapter 3. It will now be calculated for a generalised band structure, thus, substituting equations 2.2.5 and 2.3.1 into equation 2.2.1 gives

$$\frac{dE}{dt} = \frac{2\pi}{\hbar} \cdot \frac{V}{8\pi^3} \iiint \frac{E_1^2 (\hbar\omega_q)^2}{2\rho u^2 V} \Big\{ N_q \, \delta(E((\underset{\sim}{k}+\underset{\sim}{q})^2) - E(\underset{\sim}{k}^2) - \hbar\omega_q)$$

$$- (N_q + 1) \, \delta(E((\underset{\sim}{k}-\underset{\sim}{q})^2) - E(\underset{\sim}{k}^2) + \hbar\omega_q) \Big\} q^2 \sin\theta \, dq \, d\theta \, d\phi .$$

Now $N_q = k_B T_0 / \hbar\omega_q - \frac{1}{2}$ since $\hbar\omega_q \ll k_B T_0$, thus

$$\frac{dE}{dt} = \frac{E_1^2}{4\pi\rho u^2} \Big\{ J_+(E) - J_-(E) \Big\},$$

where

$$J_+(E) = \iint q^3 \left(k_B T_0 - \frac{\hbar u q}{2} \right) \delta(E((\underset{\sim}{k}+\underset{\sim}{q})^2) - E(\underset{\sim}{k}^2) - \hbar u q) \sin\theta \, d\theta \, dq,$$

and

$$J_-(E) = \iint q^3 \left(k_B T_0 + \frac{\hbar u q}{2} \right) \delta(E((\underset{\sim}{k}-\underset{\sim}{q})^2) - E(\underset{\sim}{k}^2) + \hbar u q) \sin\theta \, d\theta \, dq .$$

Substituting $\underset{\sim}{k}^2 = F(E)$ and $X = E((\underset{\sim}{k}+\underset{\sim}{q})^2 - \hbar u q$ where

$$F(x+\hbar u q) = F(x) + \hbar u q F'(x) = k^2 + 2kq\cos\theta + q^2,$$

and

$$\left[F'(x) + \hbar u q F''(x)\right] dx = -2kq\cos\theta\, d\theta$$

leads to

$$J_+(E) = \iint \frac{q^2}{2k}\left(k_B T_0 - \frac{\hbar u q}{2}\right)\delta(x-E)\left(F'(x) + \hbar u q F''(x)\right) dx\, dq.$$

Thus

$$J_+(E) = \int_{q_{min}}^{q_{max}} \frac{q^2}{2k}\left(k_B T_0 - \frac{\hbar u q}{2}\right)\left(F'(E) + \hbar u q F''(E)\right) dq,$$

where the limits of integration must satisfy the equation

$$E((k+q)^2) = E(k^2) + \hbar u q,$$

therefore

$$(k+q)^2 = F(E+\hbar u q) \doteq F(E) + \hbar u q F'(E),$$

and

$$q\left(q + \left(2\sqrt{F(E)} - \hbar u F'(E)\right)\right) = 0$$

Since q must take a positive value the allowed range of integration is

$$\left.\begin{aligned} q_{min} &= 0, \\ \text{and} \qquad q_{max} &= 2\sqrt{F(E)} + \hbar u F'(E). \end{aligned}\right\} \qquad 2.3.2$$

Integrating over q results in

$$J_+(E) = \frac{1}{2\sqrt{F(E)}}\left\{\frac{\left(2\sqrt{F(E)} + \hbar u F'(E)\right)^3}{3} k_B T_0 F'(E) + \frac{\left(2\sqrt{F(E)} + \hbar u F'(E)\right)^4}{4} \hbar u \left(k_B T_0 F''(E) - \frac{F'(E)}{2}\right)\right\},$$

Similarly

$$J_-(E) = \frac{1}{2\sqrt{F(E)}}\left\{\frac{\left(2\sqrt{F(E)} - \hbar u F'(E)\right)^3}{3} k_B T_0 F'(E) - \frac{\left(2\sqrt{F(E)} - \hbar u F'(E)\right)^4}{4} \hbar u \left(k_B T_0 F''(E) - \frac{F'(E)}{2}\right)\right\},$$

which when subtracted from $J_+(E)$ produces

$$J_+(E) - J_-(E) = \frac{4\hbar u}{\sqrt{F(E)}}\left[F(E)F'^2(E) k_B T_0 + F^2(E)\left(k_B T_0 F''(E) - \frac{F'(E)}{2}\right)\right]$$

after retaining first order terms. Thus

$$\frac{dE}{dt} = \frac{E_1^2 \hbar\sqrt{F(E)}}{\pi\rho}\left[k_B T_0\left(F'^2(E) + F(E)F''(E)\right) - \frac{F(E)F'(E)}{2}\right]. \qquad 2.3.3$$

For a parabolic band structure, and $E \gg k_B T_0$, the above formula reduces to equation (3.4.27) in Conwell [1].

2.3.(b) Rate of loss of momentum

Substituting into equation 2.2.2 in the usual way, and

$$\frac{d(\hbar k)}{dt} = \frac{2\pi}{\hbar}\cdot\frac{V}{8\pi^3}\iiint \frac{E_1^2\hbar\omega_q}{2\rho u^2 V}\hbar q_{kk}\Big\{N_q\,\delta(E((k+q)^2)-E(k^2)-\hbar\omega_q) - (N_q+1)\,\delta(E((k-q)^2)-E(k^2)+\hbar\omega_q)\Big\}q^2\sin\theta\,dq\,d\theta\,d\phi.$$

this can be written as

$$\frac{d(\hbar k)}{dt} = \frac{E_1^2\,k}{4\pi\rho u^2\sqrt{F(E)}}\left(L_+(E)-L_-(E)\right),$$

where

$$L_+(E) = \iint q^3\cos\theta\left(k_BT_0-\frac{\hbar uq}{2}\right)\delta(E((k+q)^2)-E(k^2)-\hbar uq)\sin\theta\,d\theta\,dq,$$

and

$$L_-(E) = \iint q^3\cos\theta\left(k_BT_0+\frac{\hbar uq}{2}\right)\delta(E((k-q)^2)-E(k^2)+\hbar uq)\sin\theta\,d\theta\,dq.$$

Substituting $k^2 = F(E)$ and $x = E((k+q)^2)-\hbar uq$ where

$$\cos\theta = (F(x)-k^2+\hbar uqF'(x)-q^2)/2kq$$

leads to

$$L_+(E) = \iint\frac{q}{4F(E)}\left(k_BT_0-\frac{\hbar uq}{2}\right)\left(F(x)-k^2+\hbar uqF'(x)-q^2\right)\left(F'(x)+\hbar uqF''(x)\right)\delta(x-E)\,dx\,dq$$

$$= \frac{1}{4F(E)}\int q^2\left(k_BT_0-\frac{\hbar uq}{2}\right)\left(\hbar uqF'(E)-q^2\right)\left(F'(E)+\hbar uqF''(E)\right)dq.$$

The limits for this integration are given by equation 2.3.2. Thus

$$L_+(E) = \frac{1}{4F(E)}\left[-\frac{(2\sqrt{F(E)}+\hbar uF(E))^4}{4}k_BT_0F'(E)+\hbar u\left\{\frac{(2\sqrt{F(E)}+\hbar uF(E))^3}{3}k_BT_0F'^2(E)\ldots\right\}\right],$$

and similarly

$$L_-(E) = \frac{1}{4F(E)}\left[\frac{(2\sqrt{F(E)}-\hbar uF'(E))^4}{k_BT_0}k_BT_0F'(E)+\hbar u\left\{\frac{(2\sqrt{F(E)}-\hbar uF'(E))^3}{3}k_BT_0F'^2(E)\ldots\right\}\right],$$

Hence

$$L_+(E)-L_-(E) = -2F(E)F'(E)k_BT_0$$

after retaining only first order terms. This results in

$$\frac{d(\hbar k)}{dt} = -\frac{E_1^2k_BT_0}{2\pi\rho u^2}\,\underset{\sim}{k}\,\sqrt{F(E)}\,F'(E) \qquad 2.3.4$$

Divide through by $\hbar k$, assume a parabolic band structure and equation 2.3.4 reduces to the momentum relaxation time given by Conwell [1] , equation 3.1.11.

2.3.(c) Inclusion of the mixing of Bloch states and spin-reversal scattering

When the factor $G(k,k',y)$ defined by equation 2.2.17 is inserted in the right-hand side of equation 2.3.1 the effect of the periodicity of the lattice on the electron is accounted for [23] . Thus it is necessary to replace $J_+(E)$ of Section 2.3.(a) by $J_{sp+}(E)$, where

$$J_{sp+}(E) = \frac{1}{2\sqrt{F(E)}} \iint q^2 \left(k_B T_0 - \frac{\hbar u q}{2}\right)\left(F'(E) + \hbar u q F''(E)\right) G(k, |k+q|, y) \sin\theta \, d\theta \, dq .$$

Since we assume that the acoustic phonon energy is much larger than the electron energy, the terms which appear in $G(k,k',y)$ will be expanded to first order with respect to the phonon energy, thus

$$\left.\begin{aligned} \beta(k,k') &= A(E) + \hbar u q\, B(E), \quad \rho(k,k') = C(E) + \hbar u q\, D(E), \\ \alpha(k,k') &= G(E) + \hbar u q\, H(E), \quad y = P(E,q) + \hbar u q\, Q(E,q). \end{aligned}\right\} \qquad 2.3.5$$

Thus by substitution, including only first order terms in the phonon energy for $G(k,k',y)$ and

$$J_{sp+}(E) = \frac{1}{2\sqrt{F(E)}} \iint q^2 \left(k_B T_0 - \frac{\hbar u q}{2}\right)\left(F'(E) + \hbar u q F''(E)\right)\left[A + CP + GP^2 + \hbar u q \left(B + CQ + PD + 2GPQ + HP^2\right)\right] \sin\theta \, d\theta \, dq .$$

Now y is defined in equation 2.1.18 as $\hat{k}.(\hat{k}+\hat{q})$, thus

$$y = \frac{k + q\cos\theta}{|k+q|} = \left(1 + \frac{q}{k}\cos\theta\right)\left(1 - \frac{\hbar u q}{2k^2} F'(E)\right). \qquad 2.3.6$$

The integration over θ can now be performed in the usual way giving

$$J_{sp+}(E) = \frac{1}{2\sqrt{F(E)}} \int q^2 \left[k_B T_0 F'(E) - \hbar u q \left(k_B T_0 - \frac{F'(E)}{2}\right)\right]\left\{(A + C + G) - \frac{q^2}{2k^2}(C + 2G) + \frac{q^4}{4k^4} G + \hbar u q \left[B + D + H - \frac{q^2}{2k^2}\left(D + 2H - (C+2G)\frac{F'(E)}{2k^2}\right) + \frac{q^4}{4k^2}\left(H - \frac{G F'(E)}{k^2}\right)\right]\right\} dq .$$

Using the normalisation condition which is imposed upon $G(k,k',y)$ where $A+C+G=1$ the integrand results in

$$J_{sp+}(E) = \frac{1}{2\sqrt{F(E)}} \int q^2 \Big\{ k_B T_0 F(E)\left(1 - \frac{q^2}{2k^2}(C+2G) + \frac{q^4}{4k^4}G\right) + \hbar u q \Big[\left(k_B T_0 F''(E) - \frac{F'(E)}{2}\right)(\ldots) + k_B T_0 F'(E)(B+D+H\ldots) \Big] \Big\} dq.$$

The limits for this integration are given by equations 2.3.2, which produces after some calculation

$$J_{sp+}(E) = \frac{1}{2\sqrt{F(E)}} \Big\{ k_B T_0 F'(E)\Big[\frac{(W+X)^3}{3} - \frac{(W+X)^5}{10k^2}(C+2G) + \frac{(W+X)^7}{28k^4}G\Big] + \hbar u \Big[\left(k_B T_0 F''(E) - \frac{F'(E)}{2}\right)\left(\frac{(W+X)^4}{4} - \frac{(W+X)^6}{12k^2}(C+2G) + \frac{(W+X)^8}{32k^4}G\right)\Big] + k_B T_0 F'(E)\left((B+D+H)\frac{(W+X)^4}{4} - \left(D+2H-(C+2G)\frac{F'(E)}{2k^2}\right)\frac{(W+X)^6}{12k^2} + \left(H - \frac{GF'(E)}{k^2}\right)\frac{(W+X)^8}{32k^4}\Big]\Big\},$$

where $W = 2\sqrt{F(E)}$, and $X = \hbar u F'(E)$.

By a similar calculation

$$J_{sp-}(E) = \frac{1}{2\sqrt{F(E)}} \Big\{ k_B T_0 F'(E)\Big[\frac{(W-X)^3}{3} - \frac{(W-X)^5}{10k^2}(C+2G) + \frac{(W-X)^7}{28k^4}G\Big] - \hbar u \Big[\left(k_B T_0 F''(E) - \frac{F'(E)}{2}\right)\left(\frac{(W-X)^4}{4} - \frac{(W-X)^6}{12k^2}(C+2G) + \frac{(W-X)^8}{32k^4}G\right)\Big] + k_B T_0 F'(E)\left((B+D+H)\frac{(W-X)^4}{4} - \left(D+2H-(C+2G)\frac{F'(E)}{2k^2}\right)\frac{(W-X)^6}{12k^2} + \left(H - \frac{GF'(E)}{k^2}\right)\frac{(W-X)^8}{32k^2}\Big]\Big\}.$$

Hence

$$J_{sp+}(E) - J_{sp-}(E) = 4\sqrt{F(E)}\,\hbar u \Big\{ k_B T_0 F'^2(E)(1-2C) + F'(E)\left(k_B T_0 F''(E) - \frac{F'(E)}{2}\right)\left(1 - \frac{4C+2G}{3}\right) + F(E) k_B T_0 F'(E)\left(B - \frac{D+H}{3} + \frac{2F'(E)}{3F(E)}(C-G)\right)\Big\}.$$

This result in a similar expression to that given by equation 2.3.3 where

$$\frac{dE}{dt} = \frac{E_1^2 \hbar \sqrt{F(E)}}{\pi \rho} \left\{ \left[k_B T_0 \left(F'^2(E) + F(E) F''(E) \right) - \frac{F(E) F'(E)}{2} \right] \right. \qquad 2.3.7$$

$$\left. \times \left(1 - \frac{2}{3}(2C+G) \right) + k_B T_0 F(E) F'(E) \left(B + \frac{1}{3}(D-H) \right) \right\}.$$

The rate of loss of momentum can be obtained by the inclusion of an additional factor $G(k,k',y)$ in the derivation of equation 2.3.4. It can be seen that terms involving the phonon energy can be ignored, therefore

$$L_{sp+}(E) = \frac{1}{4F(E)} \int - q^3 k_B T_0 F'(E) \left(1 - \frac{q^2}{2k^2}(C+2G) + \frac{q^4}{4k^4} G \right) dq.$$

On integration

$$L_{sp+}(E) = \frac{F'(E) k_B T_0}{4F(E)} \left[- \frac{(W+X)^4}{4} + \frac{(W+X)^6}{12k^2}(C+2G) - \frac{(W+X)^8}{32k^4} K \right],$$

also

$$L_{sp-}(E) = \frac{F'(E) k_B T_0}{4F(E)} \left[\frac{(W-X)^4}{4} - \frac{(W-X)^6}{12k^2}(C+2G) + \frac{(W-X)^8}{32k^4} K \right]$$

where $W = 2\sqrt{F(E)}$ and $X = \hbar u F'(E)$. Hence

$$L_{sp+}(E) - L_{sp-}(E) = -2F(E) F'(E) k_B T_0 \left(1 - \frac{2}{3}(2C+G) \right),$$

and

$$\frac{d(\hbar k)}{dt} = - \frac{E_1^2 k_B T_0}{2\pi \rho u^2} k \sqrt{F(E)} F'(E) \left(1 - \frac{2}{3}(2C+G) \right). \qquad 2.3.8$$

Equations 2.3.3 and 2.3.4, 2.3.7 and 2.3.8 can be averaged by direct substitution in equations 2.2.13 and 2.2.14.

The inclusion of p-type electron wave functions result in the possibility of scattering by transverse acoustic phonons. Also it would be expected that the non-parabolicity of the energy band would result in some variation of the deformation potential. These effects are discussed by Korenblit and Sherstobitov [24] and are expected to be small.

2.4 Ionised Impurity Scattering

Ionised impurity scattering has been considered by many previous authors, and in most cases of interest which arise in semiconductors the determination of the scattering matrix by the Born approximation is found to be satisfactory [25] . Thus, if the electron-impurity interaction takes place via a screened Coulomb interaction, the appropriate s-type matrix element is given by

$$|(\underset{\sim}{k}|H_I'|\underset{\sim}{k}-\underset{\sim}{q})|^2 = \frac{(4\pi)^2 e^4}{(4\pi\varepsilon_0\varepsilon_s)^2 V}\cdot\frac{1}{(\lambda^2+q^2)^2}\ , \qquad 2.4.1$$

where $1/\lambda$ is the screening length of the impurity, and the remaining parameters have been defined earlier.

The mass of the ionised impurity is much greater than that of an electron, so it will be assumed that the electron-impurity collisions are elastic.

2.4.(a) Rate of loss of momentum

The impurity ions will be assumed stationary so the electrons can only lose momentum. Thus, substituting equation 2.4.1 into equation 2.2.2 taking N_I as the impurity concentration results in

$$\frac{d}{dt}(\hbar\underset{\sim}{k}) = -\frac{2\pi}{\hbar}\frac{\underset{\sim}{k}}{\sqrt{F(\epsilon)}}\frac{V}{8\pi^3}N_I\iiint\frac{q^2(4\pi)^2e^4\hbar q\cos\theta}{(4\pi\varepsilon_0\varepsilon_s)^2V(\lambda^2+q^2)^2}$$
$$\times\delta(E((\underset{\sim}{k}-\underset{\sim}{q})^2)-E(k^2))\sin\theta\,dq\,d\theta\,d\phi .$$

This equation reduces to

$$\frac{d}{dt}(\hbar\underset{\sim}{k}) = -\underset{\sim}{k}\frac{2\pi N_I e^4 F'(\epsilon)}{(4\pi\varepsilon_0\varepsilon_s)^2\sqrt{F^3(\epsilon)}}\int_{q_{min}}^{q_{max}}\frac{q^3}{(\lambda^2+q^2)^2}\,dq .$$

The limits for this integration must satisfy the equation

$E((\underset{\sim}{k}-\underset{\sim}{q})^2) = E(k^2)$, so that $q_{min}=0$ and $q_{max}=2\sqrt{F(\epsilon)}$.

Hence

$$\frac{d}{dt}(\hbar\underset{\sim}{k}) = -\underset{\sim}{k}\frac{\pi N_I e^4 F'(\epsilon)}{(4\pi\varepsilon_0\varepsilon_s)^2\sqrt{F^3(\epsilon)}}B(z)\ , \qquad 2.4.2$$

where $z=4F(\epsilon)/\lambda^2$, and $B(z)=\log(1+z)-z/(1+z)$ defines the Brooks-Herring function [25] .

The resulting momentum relaxation time from equation 2.4.2 agrees with that of Barrie [26] .

2.4.(b) Inclusion of the mixing of Bloch states and spin-reversal scattering

The appropriate matrix element was first derived by Ehrenreich [22] and is the product of equations 2.4.1 and 2.2.17. This can be substituted into the rate of loss of momentum defined by equation 2.2.2 in a similar manner to that described in Section 2.4.(a) producing

$$\frac{d}{dt}(\hbar \underset{\sim}{k}) = -\underset{\sim}{k}\,\frac{2\pi N_I e^4 F'(E)}{(4\pi\varepsilon_0\varepsilon_s)^2\sqrt{F^3(E)}}\int_0^{2\sqrt{F(E)}}\frac{q^3}{(\lambda^2+q^2)^2}(1-Rq^2+Sq^4)\,dq,$$

where R and S are defined by equation 2.2.19. Thus, integrating

$$\frac{d}{dt}(\hbar \underset{\sim}{k}) = -\underset{\sim}{k}\,\frac{\pi N_I e^4 F'(E)}{(4\pi\varepsilon_0\varepsilon_s)^2\sqrt{F^3(E)}}\left\{B(z)-\lambda^2 R(E)\left[z-\frac{z}{1+z}-2B(z)\right]+\lambda^4 S(E)\left[\frac{z^2}{2}-2z+\frac{2z}{1+z}+3B(z)\right]\right\}. \qquad 2.4.3$$

Equations 2.4.2 and 2.4.3 can be averaged by direct substitution in equation 2.2.14.

CHAPTER 3

THE APPLICATION OF THE DRIFTED MAXWELLIAN APPROACH TO n-InSb

3.1. Introduction

A theory of the high field transport properties of semiconductors that is based on the drifted Maxwellian distribution function was developed in Chapter 2. In this chapter the theory will be applied to InSb, and the results of numerical calculations on several model band structures, particularly those of Kane [19] , will be descibed. It will be shown that even though the drifted Maxwellian distribution function may not be the Boltzmann solution, good semi-quantitative agreement with experiment can be obtained for a large range of temperatures and electric fields.

In Chapter 2 the effect of the periodicity of the lattice on the electron is taken into account. This manifests itself not only in the non-parabolicity of the band structure, but also in the non-planar form of the Bloch wave functions. For InSb spin-orbit coupling leads to the possibility of spin-reversal scattering. This is included in the mixing of Bloch states. It is found that for small band gap semiconductors, these factors can significantly alter their transport properties. With their inclusion it is possible to obtain better agreement between theory and experiment for high and low field transport properties. In particular the high field drift-velocity field characteristics of InSb at 20°K and 77°K, and the low field mobility-field characteristic between 20°K and 500°K are considered. Optical polar, acoustic and ionised impurity scattering mechanisms are included with suitably chosen values of the material constants of InSb.

A great deal of experimental work has been done on the low and high field transport properties of InSb over a wide range of temperatures [8,9,27-30] . Difficulties have been encountered in interpreting these results. These arise not only from doubts about theoretical methods applied, but also from uncertainties about the relative strengths of the various scattering mechanisms in InSb, as these depend on imprecisely known physical constants. Experimental values of the static dielectric constant range from 17.50 to 18.7, [32-35]. This leads to a change in the coupling constant of polar mode scattering by as much as 50%. Similarly, Ehrenreich [22] suggested

a value of -7.2eV for the acoustic deformation potential, but other evidence has suggested a value of -30eV [28,36,37] . This would increase the coupling constant of acoustic mode deformation potential scattering by a factor of about 17. To help clarify this situation a comparative study is presented of the transport properties of InSb, over a wide range of lattice temperatures and fields in an attempt to resolve the contradictions resulting from these uncertainties. It will be shown that greater consistency between theory and experiment can be achieved by taking the most recent value of the static dielectric constant given by Sanderson [35] of 17.50, with Ehrenreich's value for the acoustic mode deformation potential of -7.2eV.

The effect of expanding the drift parameter of the drifted Maxwellian distribution function to first order is investigated in Section 3.2. It is shown that the approximation leads to the disappearence of the region in which the electron temperature T_e is less than the lattice temperature T_0 without significantly affecting the mobility-field characteristic.

3.2 Discussion of the Method through its Application to InSb at 77° K

The low field mobility of InSb has been calculated by Ehrenreich [22] for a wide range of lattice temperatures and scattering mechanisms. He concluded that polar optical mode scattering was dominant from relatively low temperatures up to about 400°K. Using this assumption at 77°K, many previous workers [8,9,10,38,39] have utilised the displaced Maxwellian and the drifted Maxwellian approaches to calculate its high field transport properties. Experimental high field characteristics are given by [8,9,30], and a review assuming a parabolic band structure is given by [39].

In Chapter 2 if equations 2.2.15 and 2.2.16 are substituted into equations 2.1.5 to form a set of simultaneous equations with two unknowns it is straightforward to compute the drift velocity V_D, and field E corresponding to a particular electron temperature T_e. All that remains is the choice of a suitable band structure. Kane [19] has obtained the band structure of InSb using a $k.p$ perturbation calculation, and his results are summarised in Appendix 1. This predicts a band model of the form

$$F(E) = \frac{2m^*}{\hbar^2} \frac{E(E+G)(E+G+\Delta)(G+\frac{2}{3}\Delta)}{G(G+\Delta)(E+G+\frac{2}{3}\Delta)} , \qquad 3.2.1$$

where m^* is the effective mass of an electron at the centre of the B.Z., G is the band gap, and Δ is the spin-orbit splitting of the valence band. This formula is valid provided $m^* \ll m$, where m is the free electron mass, and will be called the Kane (1) band structure hereafter. If $\Delta \gg G, E$ a good approximation to this formula is

$$F(E) = \frac{2m^*}{\hbar^2} E(1 + E/G) . \qquad 3.2.2$$

This will be called the Kane (2) band structure. If the band gap G is much greater than the electron energy E then this further reduces to the parabolic band strucure for which

$$F(E) = \frac{2m^*}{\hbar^2} E . \qquad 3.2.3$$

Taking a first order expansion in the drift parameter of the distribution function, as described in Section 2.2.(c), plots 1, 2 and 3 result for the band structures 3.2.1, 3.2.2 and 3.2.3 respectively in Fig.1 and Fig.2. For the purpose of comparison the

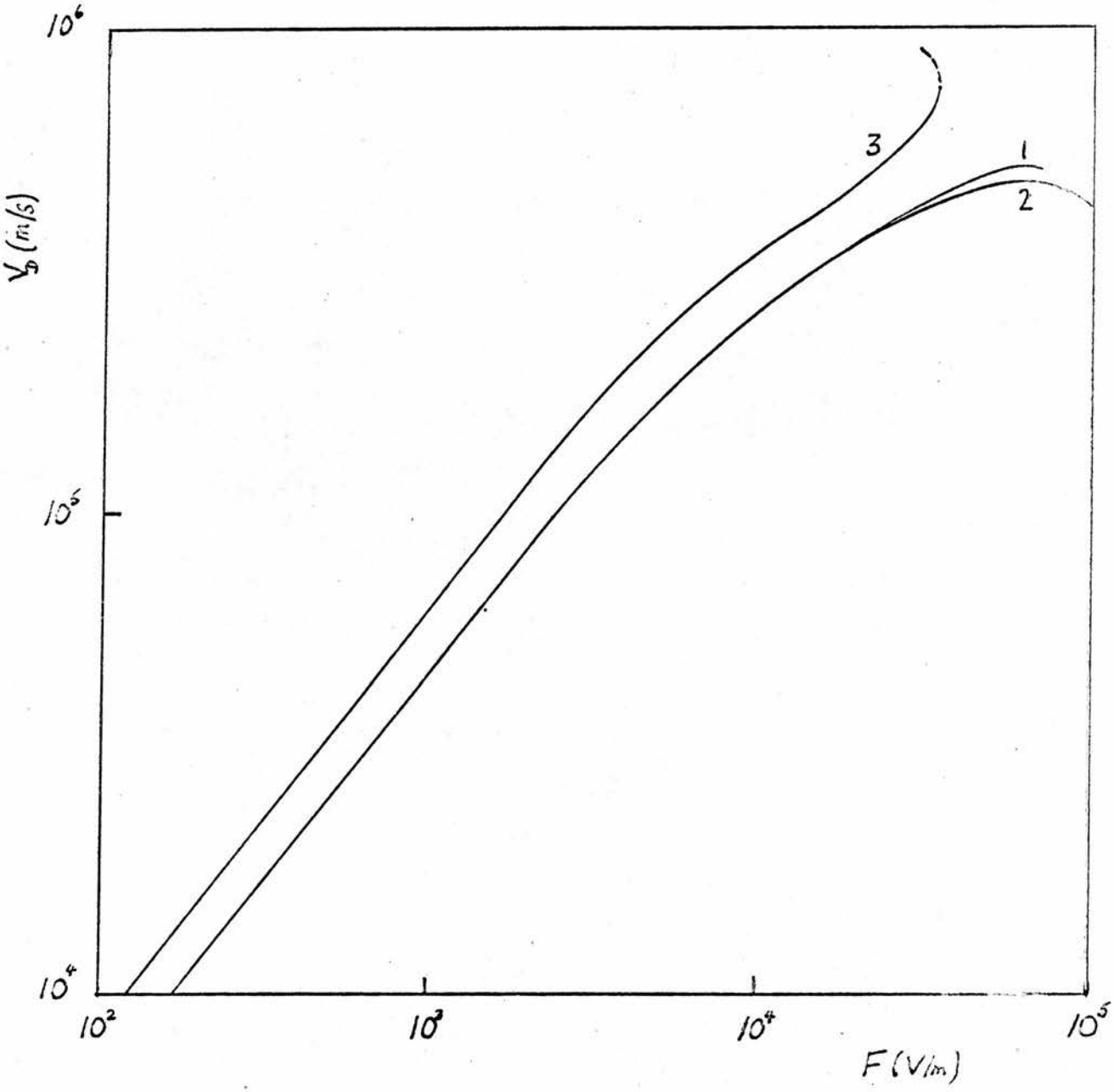

FIG. 1.

The variation of drift velocity with field for InSb at 77°K assuming in plots 1, 2, and 3; Kane (1), Kane (2), and parabolic band structures respectively. The approximated distribution function is assumed.

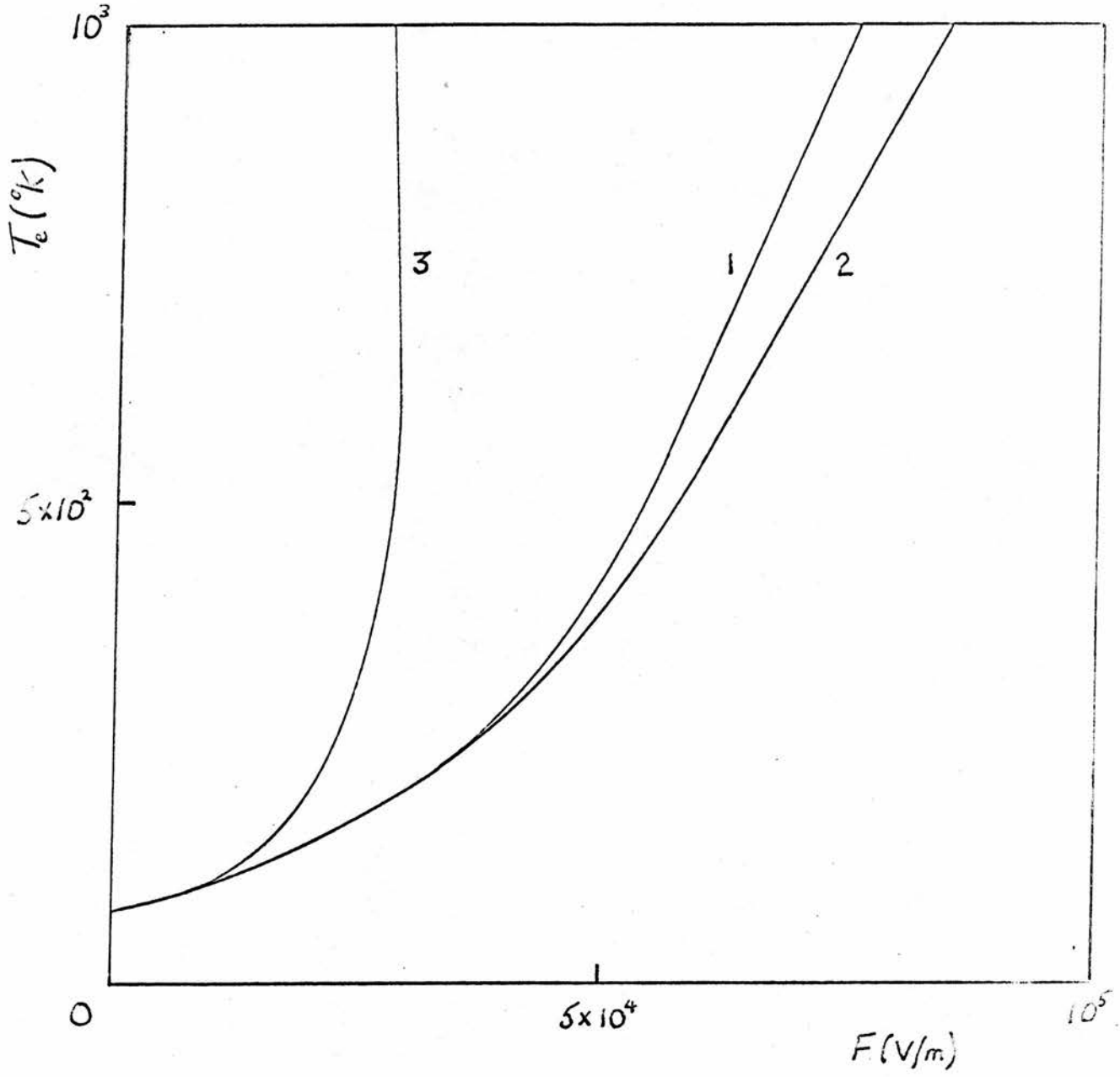

FIG. 2.

The variation of electron temperature with field for InSb at 77°K assuming in plots 1, 2, and 3; Kane (1), Kane (2), and parabolic band structures respectively. The approximated distribution function is assumed.

the material constants of InSb are initially taken from Glicksman and Hicinbothem [9], which are $m^* = 0.013m$, $\varepsilon_\infty = 15.7$, $\varepsilon_s = 18.7$ and the ~~Debye~~ temperature θ is taken to be 260°K. It is assumed that the longitudinal optical phonon energy is constant such that $\hbar\omega = k_B\theta$. The values for the band gap G and the spin-orbit splitting Δ of the valence band are 0.23eV and 0.98eV respectively [40]. Plots 2 and 3 in Fig.1 and Fig.2 agree with those given in references [17] and [27]. The effect of spin-orbit splitting appears to be relatively small, as can be seen by comparing plots 1 and 2.

By choosing a suitable iterative method it is possible to compute transport characteristics for the exact drifted Maxwellian distribution function. For the Kane (1) band structure this leads to plot 2, Fig.3 and Fig.4. The same result, but with the drift parameter of the distribution function expanded to first order is included for comparison in plot 1.

It can be seen from Fig.4 that equations 2.2.15 and 2.2.16 can be satisfied when the electron temperature T_e is less than the lattice temperature T_o . This arises simply out of the definition of the distribution function [38,41,42] and can be seen as follows. It is straightforward to evaluate the average carrier energy for a system with an exact drifted Maxwellian distribution function assuming a parabolic band structure, and it is given by

$$\langle E \rangle = \frac{3}{2} k_B T_e + \frac{1}{2} m^* V_D^2 . \qquad 3.2.4$$

When the carriers are heated this everage energy must be greater than the average thermal equilibrium carrier energy $\frac{3}{2} k_B T_o$. The contribution of the second term on the right-hand of equation 3.2.4 leads to the possibility that the electron temperature T_e can be less than the lattice temperature T_o . It should be noted that the expansion of the drift parameter of the distribution function to first order is equivalent to approximating the average carrier energy by $\frac{3}{2} k_B T_e$ and hence the elimination of the region where $T_e < T_o$.

When the drift parameter $\hbar V_D k / k_B T_e$ is small, the approximated and exact distribution functions are most similar. This is true when V_D is small and when V_D and T_e are large, so that when V_D assumes an intermediate value the approximation is least applicable. This is confirmed by Fig.3 and Fig.4. The resulting drift-velocity-field characteristic of Fig.3 shows that there is little difference

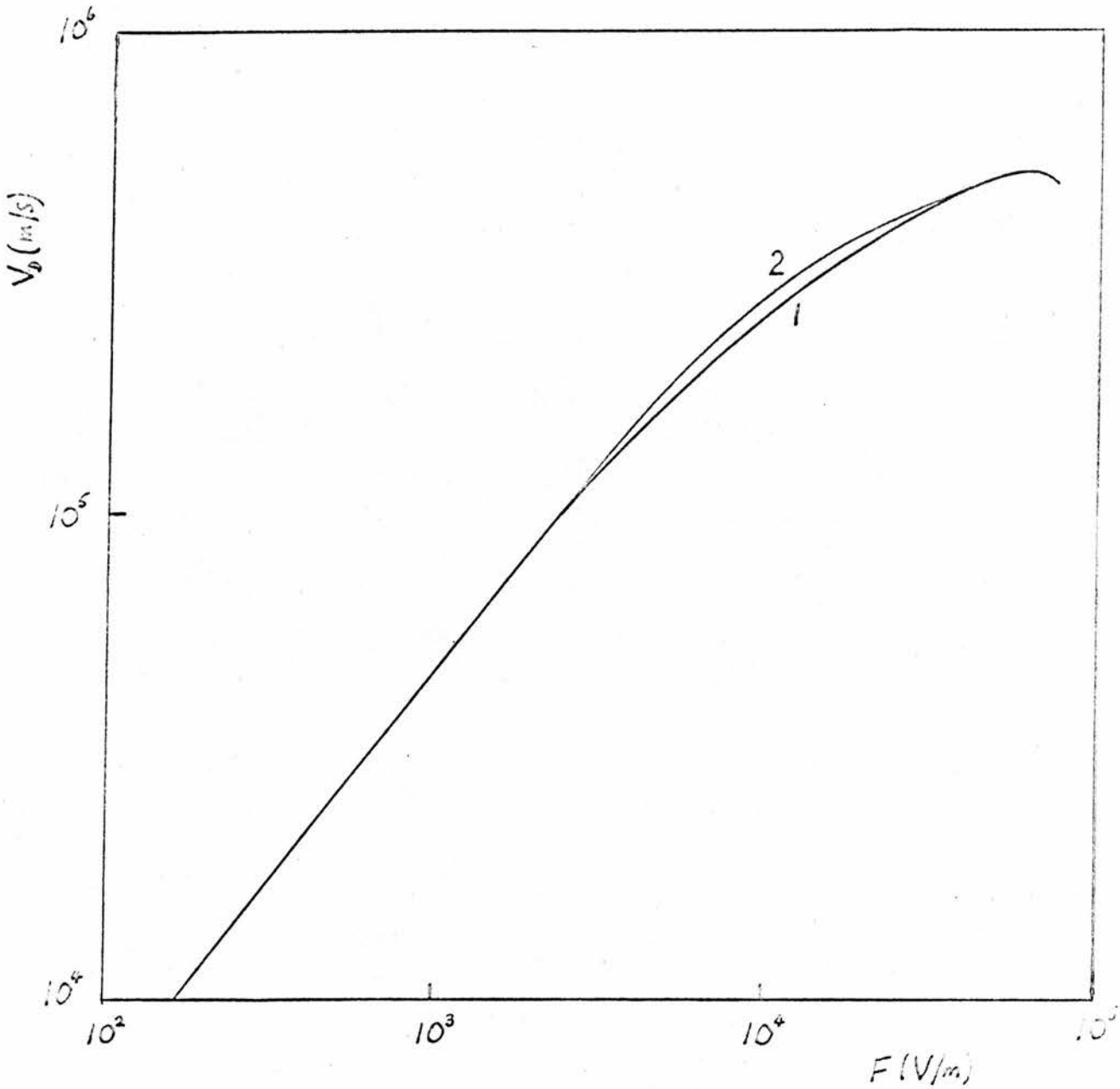

FIG. 3.

The variation of drift velocity with field for InSb at 77°K taking the approximated and exact distribution functions in plots 1 and 2 respectively.

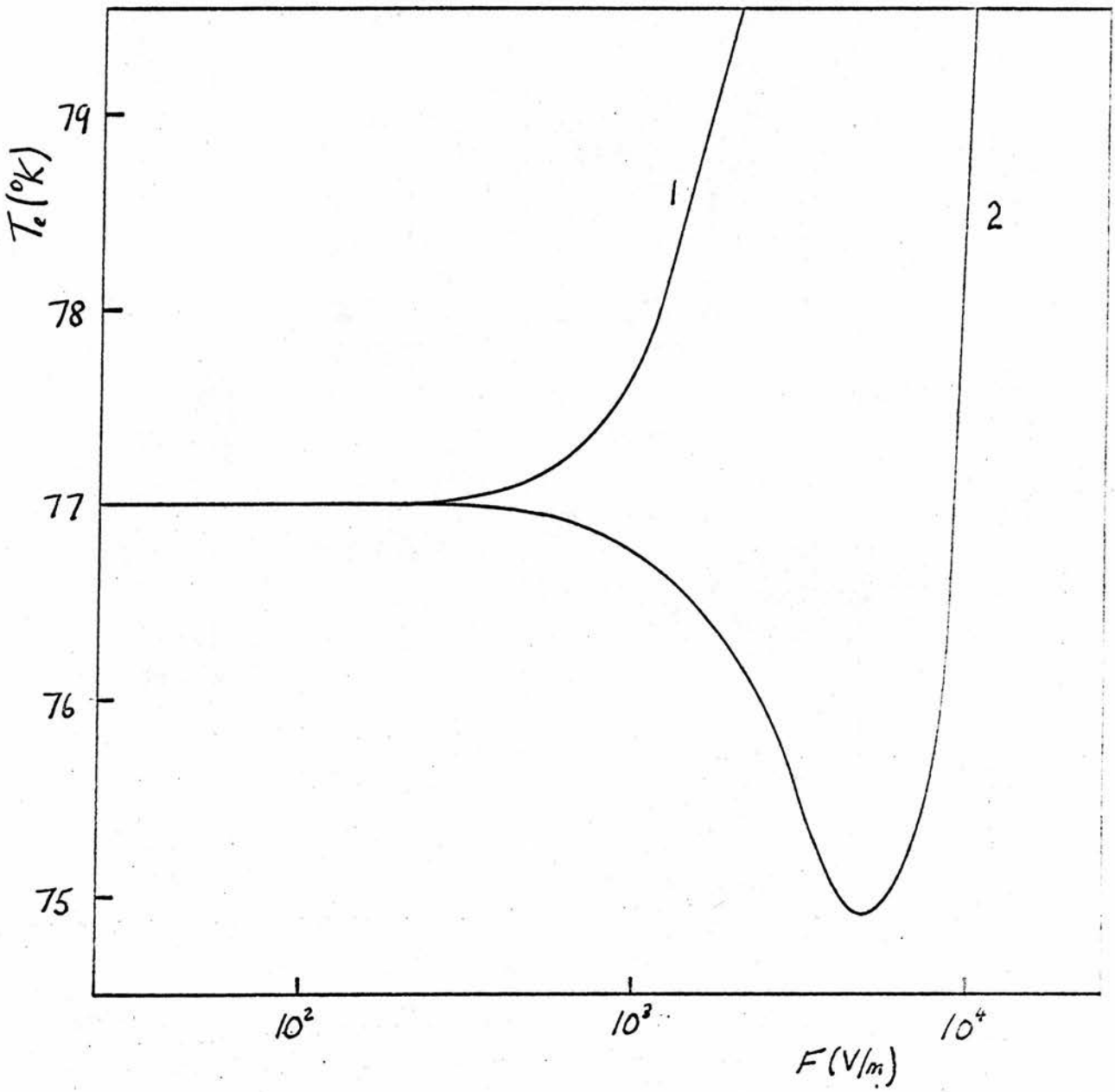

FIG. 4.

The variation of electron temperature with field for InSb at 77°K taking the approximated and exact distribution functions in plots 1 and 2 respectively.

between the calculation of the exact and approximated distribution functions. This conclusion was also reached by Mukhopadhyay and Nag for the parabolic case [39]. So all remaining calculations of this chapter will assume the approximated distribution function.

In Section 2.2.(d), the inclusion of the mixing of Bloch states and spin-reversal scattering in the formula for polar optical scattering is considered in detail. For InSb the function $G(k,k',y)$ defined by equation 2.2.17 can be evaluated using Kane's model, and gives

$$G(k,k',y) = a_k^2 a_{k'}^2 + 2a_k a_{k'}(b_k b_{k'} + c_k c_{k'})y + (b_k b_{k'} + c_k c_{k'})^2 y^2 + \left[\tfrac{1}{4} b_k^2 b_{k'}^2 + \tfrac{1}{2}(b_k b_{k'} + c_k c_{k'})^2 - \tfrac{1}{\sqrt{2}} b_k b_{k'}(b_k c_{k'} + c_k b_{k'})\right](1-y^2) \qquad 3.2.5$$

as shown by Matz [43]. Thus, the functions β, ε and α of equation 2.2.18 can be obtained by comparison since a_k, b_k and c_k are given by equation (15) of Kane's paper. The calculation for the Kane (1) band structure with the inclusion of the mixing of Bloch states and spin-reversal scattering results in plot 2, Fig.5 and Fig.6, with the straightforward plane wave calculation plot 1 being shown for comparison.

The factors a_k, b_k and c_k are discussed in Appendix 1, and in the limit where the spin-orbit splitting of the valence band becomes infinite

$$a_k = \left(\frac{G+E}{G+2E}\right)^{1/2}, \quad b_k = c_k/\sqrt{2} = \left(\frac{E}{3(G+2E)}\right)^{1/2}. \qquad 3.2.6$$

When the mixing of Bloch states is taken into account to first order $a_k = 1$ and $b_k = c_k = 0$. Thus, $R = S = 0$ and $Q = a_{k'}^2$ in equation 2.2.20. This results in an extra factor of $a_{k'}^2 \simeq (G+\hbar\omega)/(G+2\hbar\omega)$ in the rate of loss of momentum which does not appear in the plane wave calculation. The ratio $\hbar\omega/G$ for InSb is about 0.1 which leads to an increase in the low field mobility of 10%. An exact calculation gives an increase of 17% as shown in Table 1, Section 3.3. Thus it should be emphasised that for narrow band gap polar semiconductors, the effect of the mixing of Bloch states and spin-reversal scattering on their transport properties can be significant.

The low field mobility for acoustic scattering assuming a parabolic band structure which can be deduced from equation 2.3.4, differs from that given by Madelung [40] by a factor $32/9\pi = 1.13$. Fig.7 compares the mobility-electron temperature characteristics

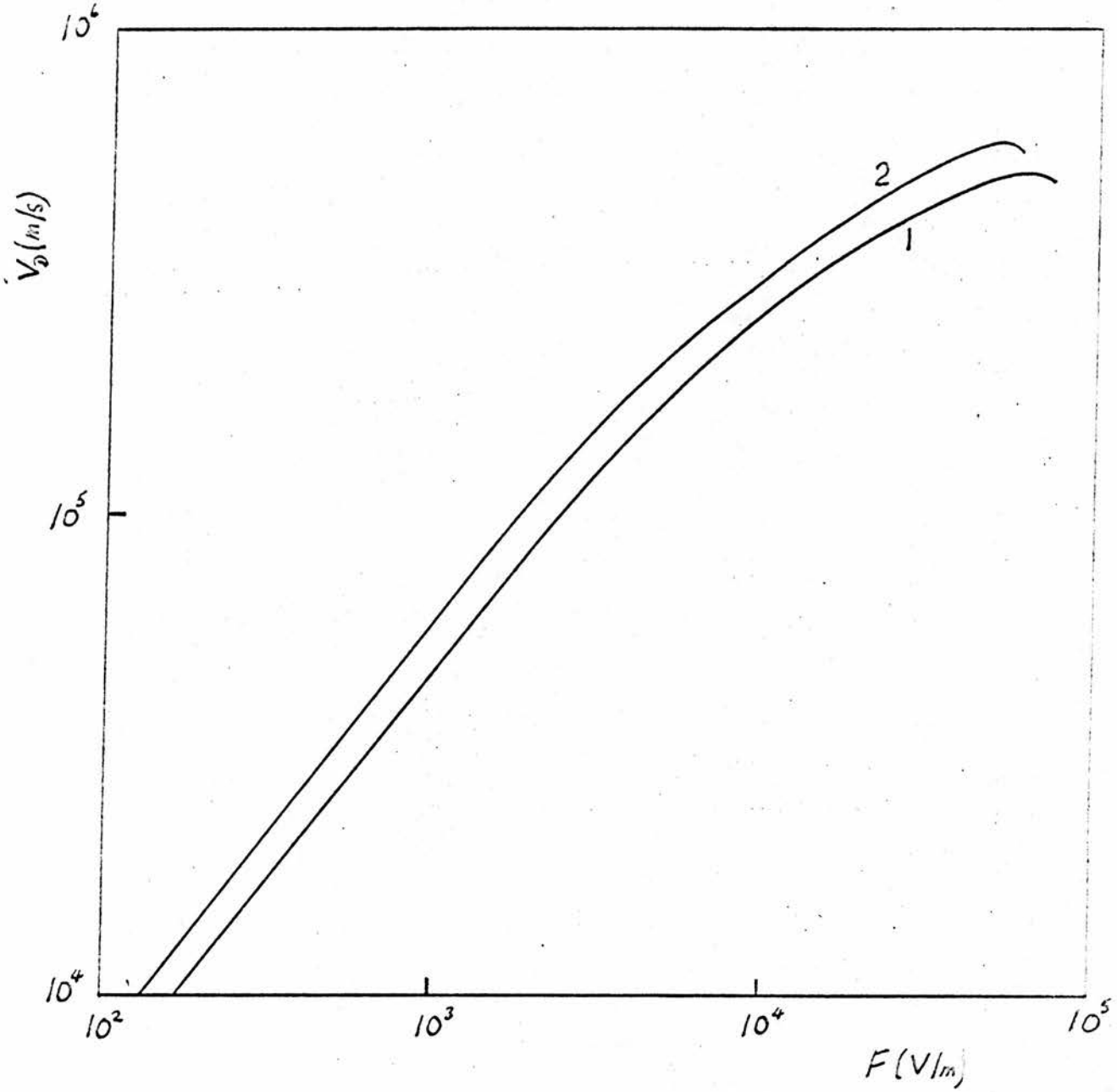

FIG. 5.

The variation of drift velocity with field for InSb at 77°K assuming a Kane (1) band structure with and without the inclusion of s–p mixing in plots **2** and **1** respectively.

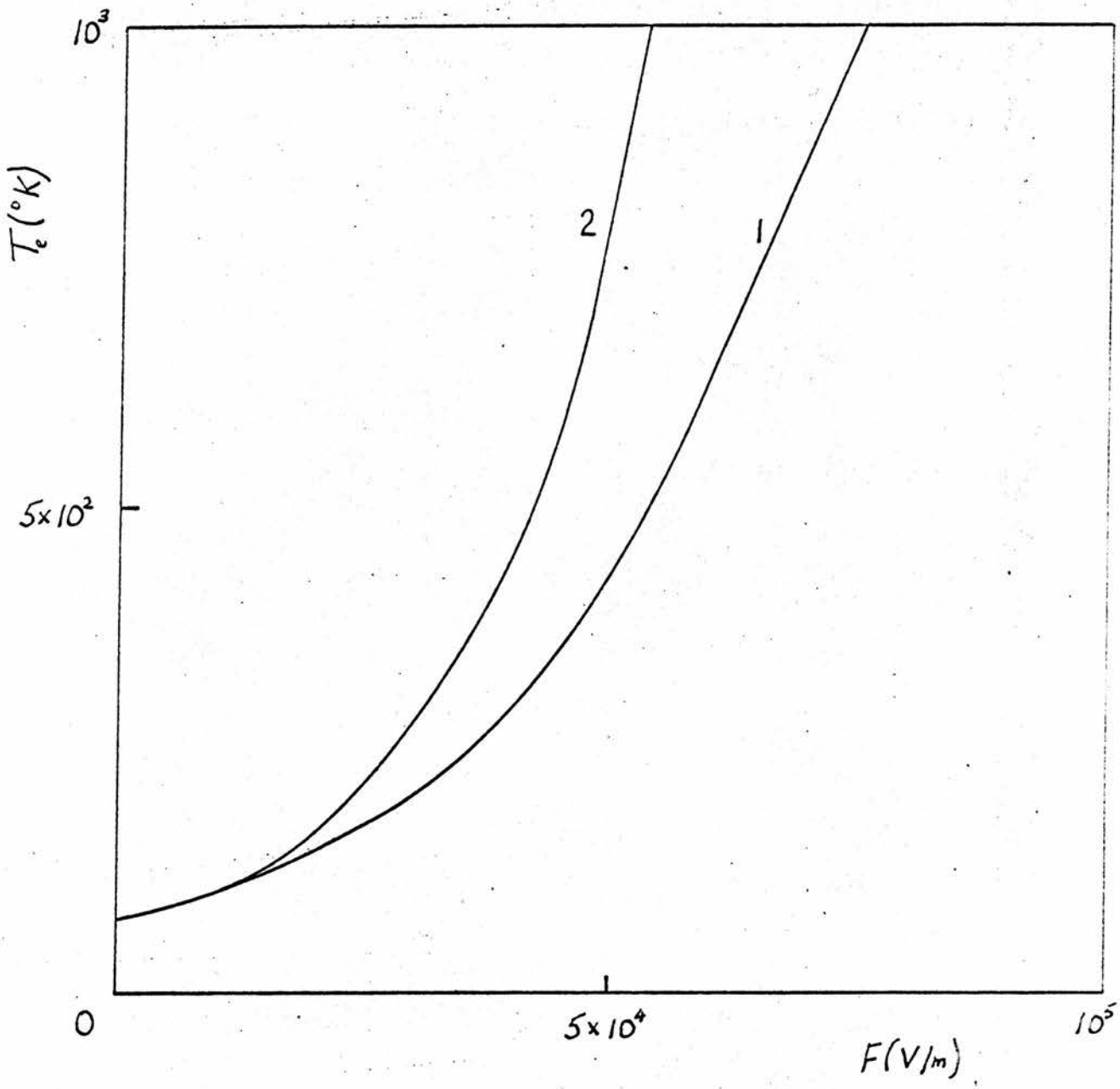

FIG. 6.

The variation of electron temperature with field for InSb at 77°K assuming a Kane (1) band structure with and without the inclusion of s-p mixing in plots **2** and **1** respectively.

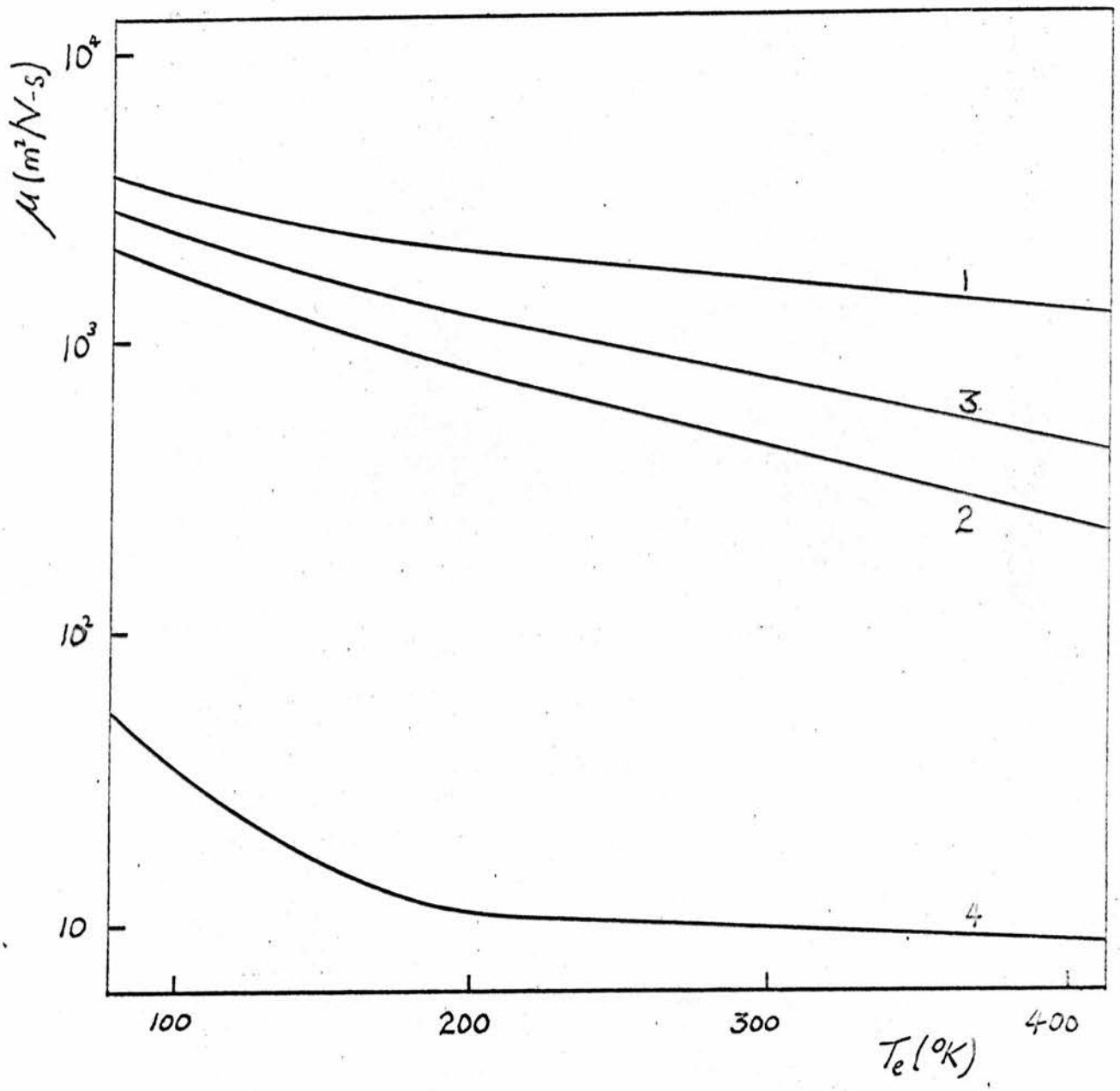

FIG. 7.

The variation of mobility with electron temperature for InSb at 77°K for acoustic scattering assuming a parabolic band structure, and a Kane (2) band structure with and without s-p mixing in plots 1, 2, and 3 respectively. Plot 4 shows the polar case for a Kane (2) band structure.

of the acoustic and optical polar modes of scattering. Plots 1, 2 and 3, Fig.7 describe the parabolic, the Kane (1) and the Kane (2) with the inclusion of the mixing of Bloch states cases for acoustic scattering. Further details are given in Appendix 1. Plot 4, Fig.7 shows the polar optical characteristic for the Kane (2) band structure. The material constants of InSb used for this calculation assume an acoustic deformation potential of -7.2eV, a longitudinal sound velocity of 3,700m/s and a crystal density of 5.79gm/cm^3.

The rate of loss of energy by an electron to the acoustic phonon field is much less than the loss to the optical polar phonon field even assuming an acoustic deformation potential of -30eV, so the electric field at a particular electron temperature is principally determined by the polar optical scattering mechanism.

For ionised impurity scattering the mobility- electron temperature chatacteristic can be deduced from equations 2.4.2 and 2.4.3. The resulting low field mobility for the parabolic case differs from that given by Madelung [40] by a factor $32/3\pi = 3{\cdot}4$ and by the form of the integral in which the Brooks-Herring function arises. Usually the integral is approximated by substituting in the Brooks-Herring function the value of E at which the remaining integrand has a maximum. This value is $3k_BT_o$ in the formula given by Madelung [40]. However, this cannot be done for the mobility resulting from equation 2.4.2 because when the Brooks-Herring function is removed from the integral, the remaining integrand does not possess a maximum value. Using Dingle's suggestion [44], the value of E substituted in the Brooks-Herring function is taken as that at which the remaining integral has a mean value. This value of E is $\log_e 2 . k_BT_o$ for the above case. Thus, plot 1, Fig.8 shows the mobility-electron temperature characteristic for a parabolic band, approximating the integral according to Dingle's method. Plot 2 shows the exact calculation for a Kane (2) band structure. The effects of the mixing of Bloch states was found to be small.

For this calculation it is assumed that the system is non-degenerate and the impurities are completely ionised, so that the Debye screening length $1/\lambda$ is given by [44]

$$\lambda^2 = \frac{4\pi n e^2}{4\pi \varepsilon_o \varepsilon_s k_B T_o} , \qquad 3.2.7$$

where T_o is 77°K, the carrier concentration n is taken as $5 \times 10^{19}/m^3$ and the impurity concentration N_I as $1 \times 10^{20}/m^3$. It should be

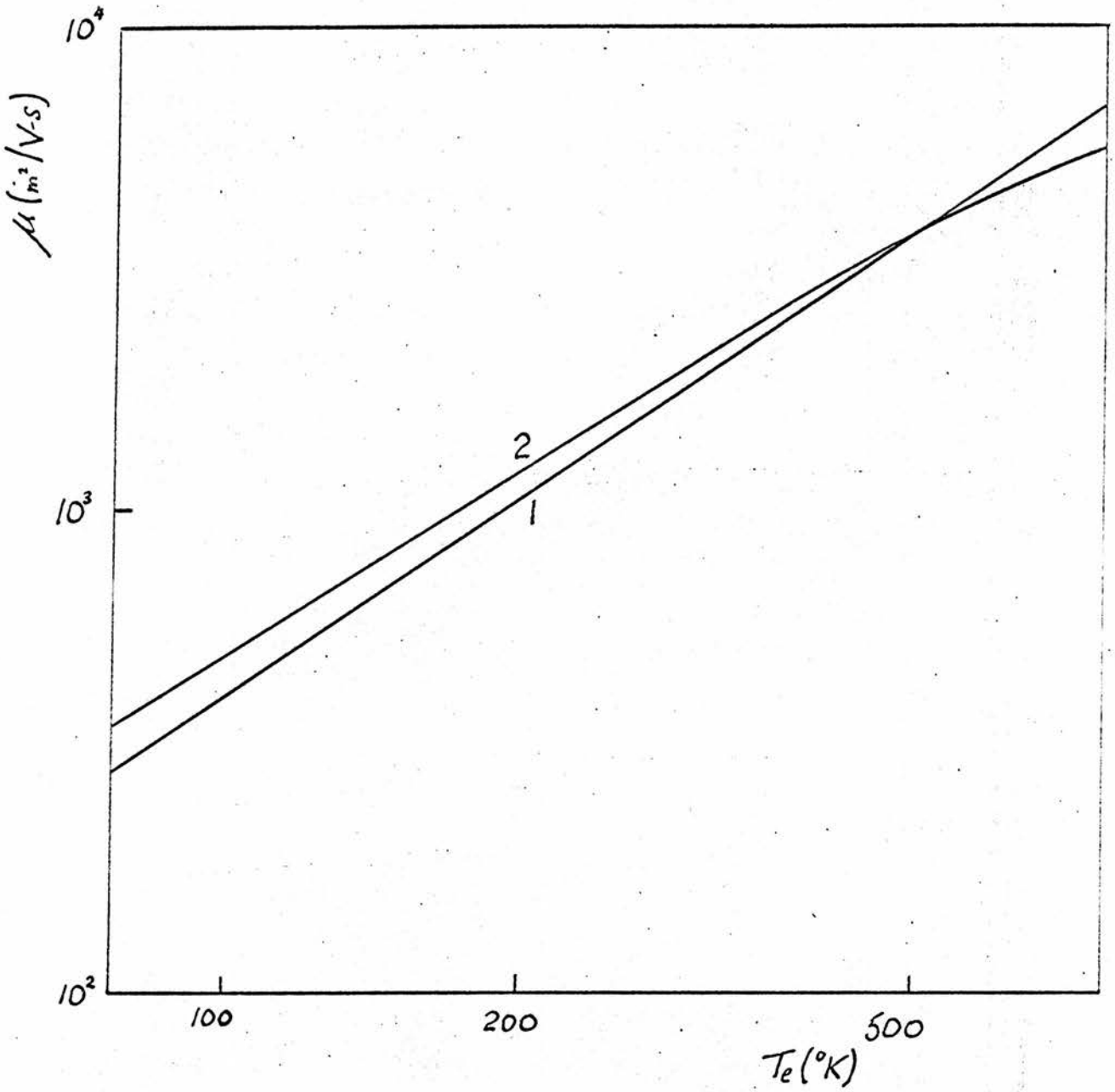

FIG. 8.

The variation of mobility with electron temperature for InSb at 77°K considering ionised impurity scattering ($N_I = 10^{20}/m^3$) for a parabolic band using Dingle's approximation in plot 1, and for a Kane (2) band structure in plot 2.

noted that the mobility resulting from ionised impurities is very insensitive to the electron concentration n .

3.3 Analysis of the Scattering Mechanisms of InSb at High and Low Fields

There is some confusion about the experimental value of the static dielectric constant of InSb [32-35]. Table 1 lists the low field polar mobility for InSb at 77°K for two different dielectric constants, 18.7 and 17.50 and the corresponding ~~Debye~~ temperatures of 260°K and 278°K given by references [33] and [35] respectively. Parabolic, Kane (1) and Kane (2) band structures with and without the inclusion of the s-type mixing of Bloch states are considered. The mobilities are given in $m^2/V-s$.

	ε_s	18.7	17.50
	θ	260	278
Parabolic		72.6	131.6
Kane (1)		53.2	94.8
Kane (2)		51.8	92.3
Kane (1)+s-p		62.0	111.5
Kane (2)+ s-p		61.2	109.5

Table 1.

Experimental values of the low field mobility of InSb at 77°K [8, 9, 30] range from 50-75$m^2/V-s$, the variation for different samples being due presumably to the different impurity concentrations. These values suggest that the dielectric constant of 17.50 leads to a more appropriate result for the polar mobility of 111.5, which is somewhat higher than the experimental values, as should be expected. The remaining calculations of this chapter for convenience will take a Kane (2) band structure with the inclusion of s-p mixing and spin-reversal scattering.

There is some doubt about the deformation potential of acoustic mode scattering. If the value of -30eV is taken [28, 36, 37], combining acoustic and polar scattering, the low field mobility of InSb at 77°K is about $67m^2/V-s$, which is rather low. Plot 1, Fig.9 shows the experimental high field characteristic given by Glicksman and Hicinbothem [9] for InSb at 77°K, plots 2 and 3 combine the effect of polar and acoustic scattering with deformation potentials of -7.2eV and -30eV respectively. Plot 2 also includes the effect of ionised impurities of concentration $1.4 \times 10^{20}/m^3$ which leads to good agreement with experiment up to $3 \times 10^4 V/m$. This suggests that -7.2eV is the more appropriate deformation potential.

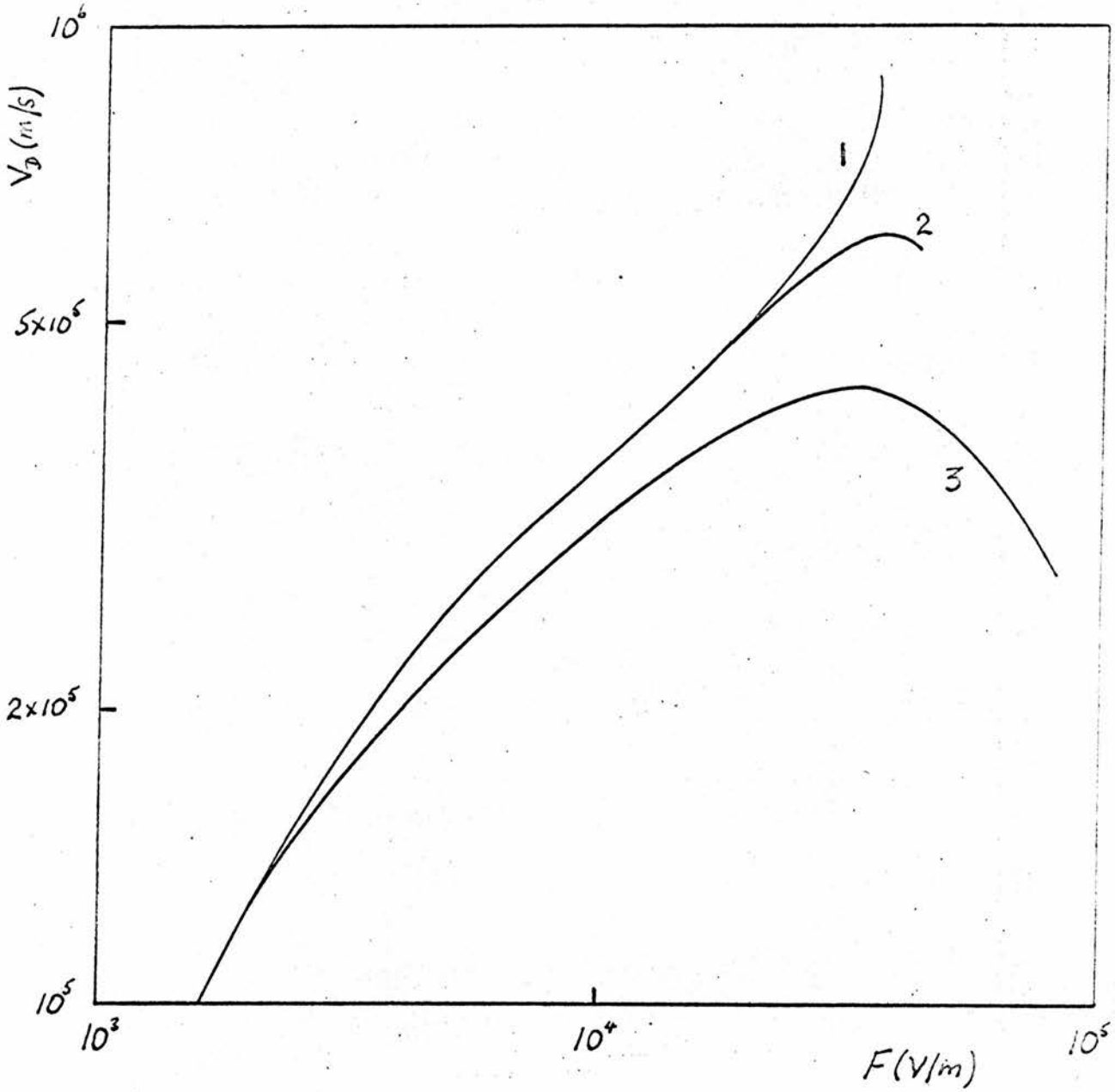

FIG. 9.

The variation of drift velocity with field for InSb at 77°K including polar, acoustic (and ionised impurities for plot 2) scattering, with an acoustic deformation potential of -7.2eV and -30eV for plots 2 and 3 respectively. Plot 1 is experimental [9].

Bok and Guthmann [8] give experimental data for InSb at 77°K and 20°K. Taking a deformation potential of -7.2eV, an impurity concentration of $3.3 \times 10^{20}/m^3$ is required to produce a low field mobility of $50 m^2/V\text{-}s$ at 77°K. The agreement at high fields is good. Also, the corresponding theoretical plot at 20°K given by Fig.10 is in good agreement with experiment, and has a low field mobility of $25 m^2/V\text{-}s$. It was not possible to explain the high field characteristics of InSb at 77°K and 20°K consistently with a deformation potential of -30eV.

An attempt was made to include the effects of electron-electron screening [22], but it appeared to make little difference at the electron concentrations stated for the experimental samples of references [8, 9, 30] for InSb at 77°K. Recent experimental evidence [45] has been obtained for very high fields above 5×10^4 V/m prior to the onset of carrier multiplication due to impact ionisation. At such fields electron energies are acheived which introduce the possibility of intervalley scattering. These effects will be discussed in chapters 4 and 5.

The experimental low field mobility of InSb over a wide range of lattice temperatures is given by Kinch [28] in plot 1, Fig.11. Plot 2 shows the theoretical mobility characteristic resulting from a combination of polar, acoustic (deformation potential -7.2eV) and ionised impurity scattering of concentration $3.3 \times 10^{20}/m^3$. Plot 3, Fig.11 shows the effect of electron-hole scattering as given by Ehrenreich [22]. If this is included in plot 2 it can be seen that good agreement with experiment would result at high and medium temperatures. Below 20°K the disagreement is explained by Kinch [28], and is due to electron-electron effects.

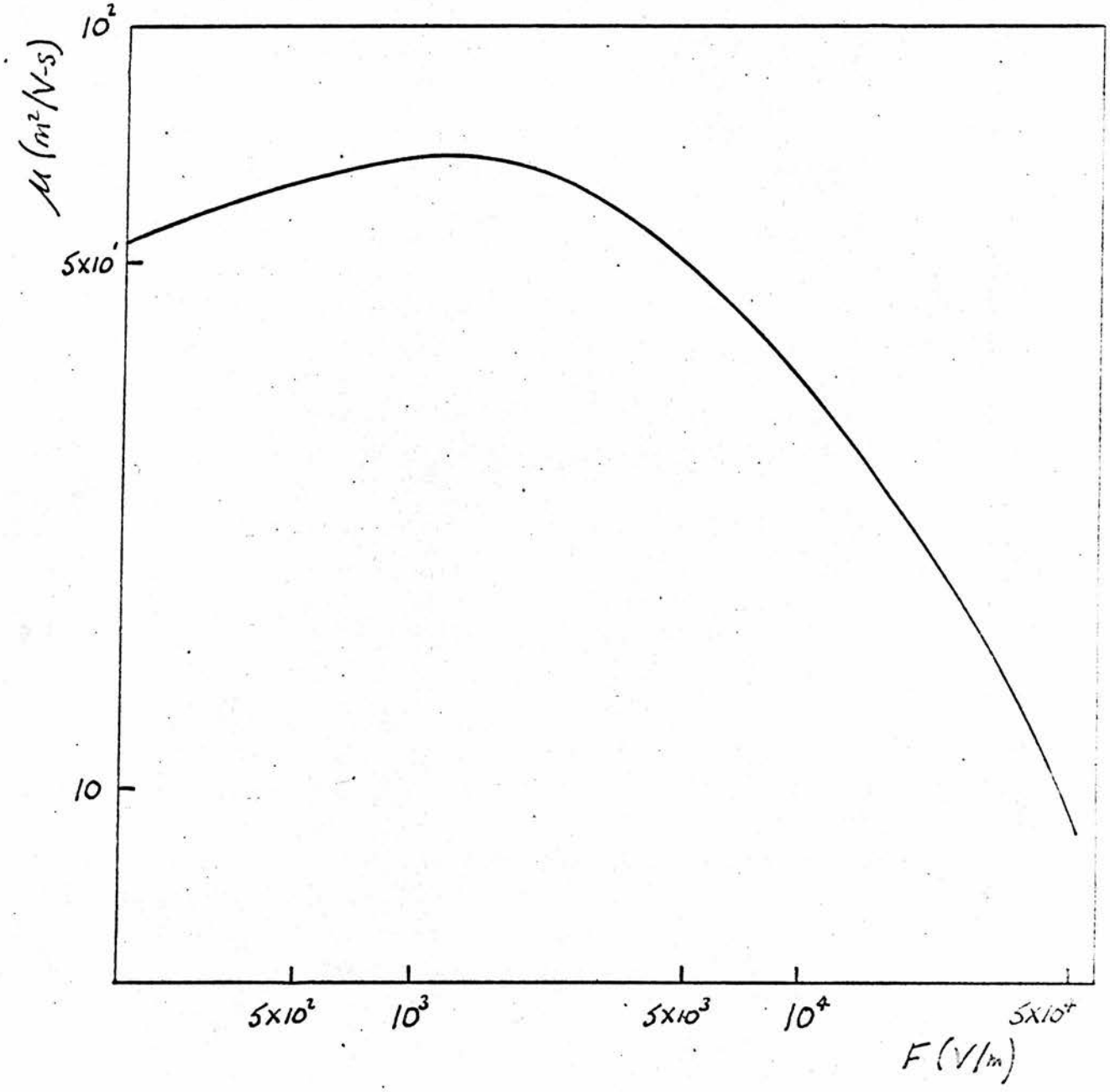

FIG. 10.

The variation of mobility with field for InSb at 20°K where a kane (2) band structure is assumed including s-p mixing, and polar, accustic, and ionised impurity scattering (N_I = 3.3 x $10^{20}/m^3$) are all taken into account.

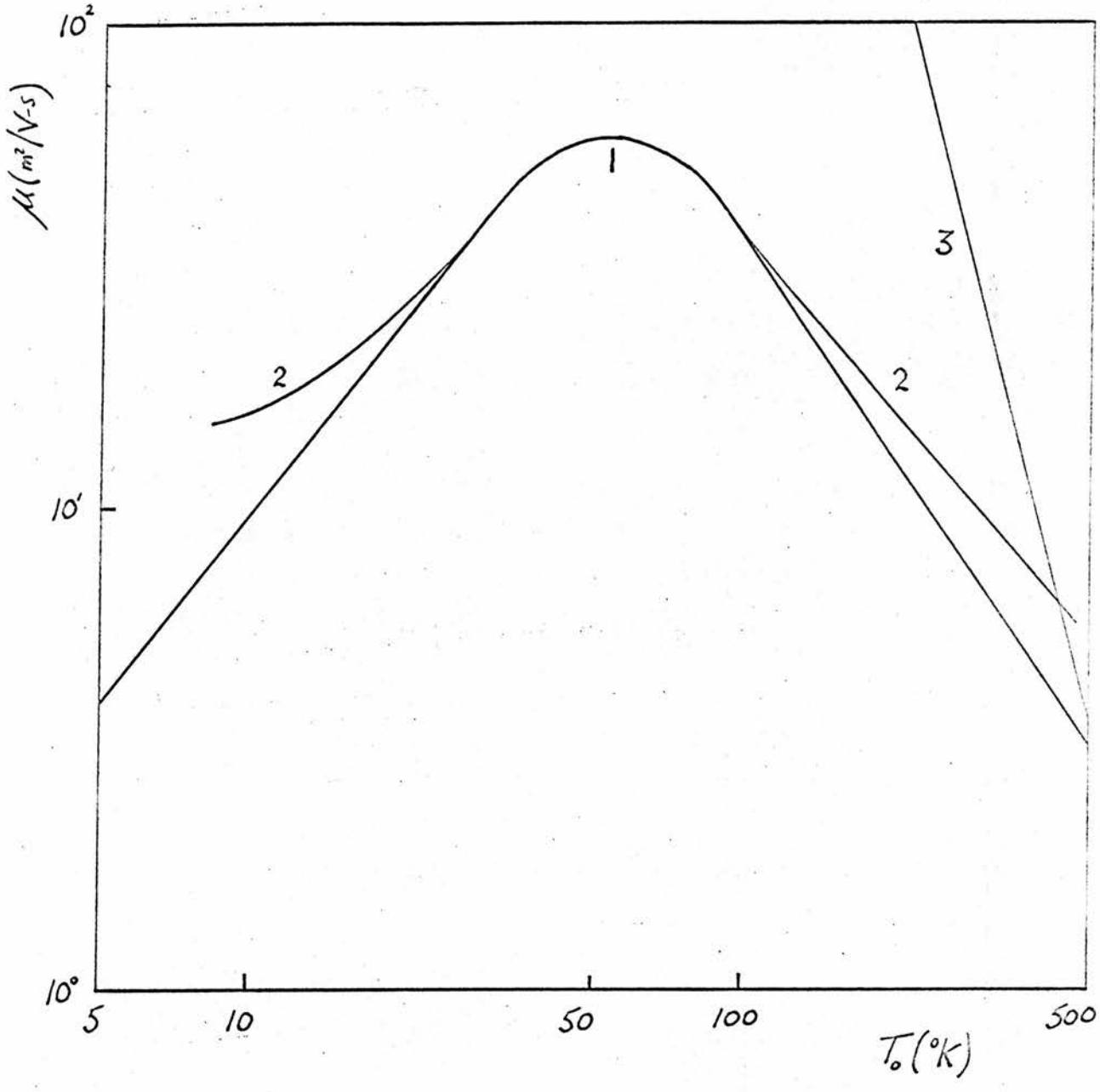

FIG. 11.

The variation of low field mobility with lattice temperature for InSb is shown by plots 1 and 2. Plot 1 is experimental [28], and plot 2 is theoretical where a Kane (2) band structure with s-p mixing is assumed and polar, acoustic, and ionised impurity scattering (N_I = $3.3 \times 10^{20}/m^3$) is included. Plot 3 is given by Ehrenreich [22] for electron-hole scattering.

CHAPTER 4

THE FORMULATION OF THE BOLTZMANN EQUATION AND THE DERIVATION OF THE COLLISION INTEGRALS FOR SMALL BAND GAP SEMICONDUCTORS

4.1 Introduction

The Boltzmann carrier transport equation can be written symbolically in its most general form as

$$\left(\frac{\partial f}{\partial t}\right)_F + \left(\frac{\partial f}{\partial t}\right)_c = 0. \qquad 4.1.1$$

The first term represents the variation of the distribution function $f(\underset{\sim}{k}, \underset{\sim}{r}, t)$ with time due to the application of a field, and the second term represents the variation due to carrier collisions. The distribution function is defined in the usual way with the normalisation condition given at any time t such that

$$\iint f(\underset{\sim}{k}, \underset{\sim}{r})\, d\underset{\sim}{k}\, d\underset{\sim}{r} = 1. \qquad 4.1.2$$

It is straightforward to deduce that

$$\left(\frac{\partial f}{\partial t}\right)_F = \frac{\partial f}{\partial t} + \dot{\underset{\sim}{k}} \cdot \frac{\partial f}{\partial \underset{\sim}{k}} + \underset{\sim}{v} \cdot \frac{\partial f}{\partial \underset{\sim}{r}} \qquad 4.1.3$$

where $\underset{\sim}{v}$ is the electron velocity as shown by Wilson [46].

The validity and justification for the use of Boltzmann's equation to describe low and high field transport in semiconductors is discussed in references [1,47,48]. The general conclusions reached are that provided the carrier concentration is sufficiently dilute such that the velocity of a carrier is uncorrelated with its position, and in the case where carrier-carrier energy exchange is large that the collisions are predominantly binary, then Boltzmann's equation is applicable. In the case of degenerate semiconductors the inclusion of the Pauli exclusion principle on the carrier-carrier interaction is an additional condition, but the following chapters are principally concerned with non-degenerate semiconductors.

There are two types of scattering processes which will be considered in the following sections of this chapter. Firstly there will be scattering due to phonons and ionised impurities, where the collision integral is of the form [1]

$$\left(\frac{\partial f_i(\underset{\sim}{k})}{\partial t}\right)_{ij} = \sum_{\underset{\sim}{q}} P_a(\underset{\sim}{k} \rightarrow \underset{\sim}{k}+\underset{\sim}{q}) f_j(\underset{\sim}{k}+\underset{\sim}{q}) + P_e(\underset{\sim}{k} \rightarrow \underset{\sim}{k}-\underset{\sim}{q}) f_j(\underset{\sim}{k}-\underset{\sim}{q}) - P_a(\underset{\sim}{k}-\underset{\sim}{q} \rightarrow \underset{\sim}{k}) f_i(\underset{\sim}{k}) - P_e(\underset{\sim}{k}+\underset{\sim}{q} \rightarrow \underset{\sim}{k}) f_i(\underset{\sim}{k}) \quad 4.1.4$$

the notation being the same as that used in 2.2, where P_a and P_e are the absorption and emission probabilities for an electron scattered through a momentum change $\pm\underset{\sim}{q}$. The subscripts i and j refer to the different valleys, with $f_i(\underset{\sim}{k})$ and $f_j(\underset{\sim}{k})$ defining the distribution functions corresponding to valleys labelled i and j respectively. The intervalley collision integral given by equation 4.1.4 reduces to the intravalley collision integral by taking $i=j$. The second type of collision integral to be considered will be that due to intravalley carrier-carrier collisions. This takes the form [49]

$$\left(\frac{\partial f(\underset{\sim}{k})}{\partial t}\right)_{e\text{-}e} = A_{e\text{-}e} \iiint [f(\underset{\sim}{k}_1') f(\underset{\sim}{k}') - f(\underset{\sim}{k}_1) f(\underset{\sim}{k})] \alpha(\chi, r) \sin\chi \, d\chi \, d\epsilon \, d\underset{\sim}{k}_1 \quad 4.1.5$$

where an electron with momentum $\underset{\sim}{k}$ is scattered into a state $\underset{\sim}{k}'$ due to collision with an electron of initial momentum $\underset{\sim}{k}_1$ and final momentum $\underset{\sim}{k}_1'$. This equation will be discussed in Section 4.5. The detailed evaluation of the relevant collision integrals will be performed in Sections 4.2-4.6.

4.2 Polar Optical Scattering

The collision integral for polar optical scattering assuming a parabolic band structure is discussed by Conwell [1], Chapter V. It will now be derived for a general band structure which is spherically symmetric in $\underset{\sim}{k}$ space.

Using first order perturbation theory the collision integral for intravalley scattering obtained from equation 4.1.4 becomes

$$\begin{aligned}\frac{\partial f(\underset{\sim}{k})}{\partial t} = \frac{2\pi}{\hbar}\sum_{\underset{\sim}{q}} & |(\underset{\sim}{k}|H'_{po}|\underset{\sim}{k}+\underset{\sim}{q})|^2\,\delta(E_{\underset{\sim}{k},N+1}-E_{\underset{\sim}{k}+\underset{\sim}{q},N})f(\underset{\sim}{k}+\underset{\sim}{q}) \\ & + |(\underset{\sim}{k}|H'_{po}|\underset{\sim}{k}-\underset{\sim}{q})|^2\,\delta(E_{\underset{\sim}{k},N-1}-E_{\underset{\sim}{k}-\underset{\sim}{q},N})f(\underset{\sim}{k}-\underset{\sim}{q}) \\ & - |(\underset{\sim}{k}-\underset{\sim}{q}|H'_{po}|\underset{\sim}{k})|^2\,\delta(E_{\underset{\sim}{k}+\underset{\sim}{q},N+1}-E_{\underset{\sim}{k},N})f(\underset{\sim}{k}) \\ & - |(\underset{\sim}{k}+\underset{\sim}{q}|H'_{po}|\underset{\sim}{k})|^2\,\delta(E_{\underset{\sim}{k}+\underset{\sim}{q},N-1}-E_{\underset{\sim}{k},N})f(\underset{\sim}{k})\end{aligned} \qquad 4.2.1$$

The notation is the same as that used in Chapter 2 where the polar optical phonon matrix element is defined by equation 2.2.3 for the case of carriers possessing s-type wave functions. Thus, transforming the summation over $\underset{\sim}{q}$ to an integral in the usual way and substituting the matrix element produces

$$\begin{aligned}\frac{\partial f(\underset{\sim}{k})}{\partial t} = \frac{e^2(\hbar\omega)}{(4\pi\varepsilon_0)2\pi\hbar}\left(\frac{1}{\varepsilon_\infty}-\frac{1}{\varepsilon_s}\right)\iiint\Big[& (N+1)\,\delta(E(k^2)-E((\underset{\sim}{k}+\underset{\sim}{q})^2)+\hbar\omega)f(\underset{\sim}{k}+\underset{\sim}{q}) \\ & + N\,\delta(E(k^2)-E((\underset{\sim}{k}-\underset{\sim}{q})^2)-\hbar\omega)f(\underset{\sim}{k}-\underset{\sim}{q}) \\ & - (N+1)\,\delta(E((\underset{\sim}{k}-\underset{\sim}{q})^2)-E(k^2)-\hbar\omega)f(\underset{\sim}{k}) \\ & - N\,\delta(E((\underset{\sim}{k}+\underset{\sim}{q})^2)-E(k^2)+\hbar\omega)f(\underset{\sim}{k})\Big]\sin\theta\,dq\,d\theta\,d\phi.\end{aligned} \qquad 4.2.2$$

Consider the first term in the integral where

$$I_1 = \iiint \delta(E(k^2)-E((\underset{\sim}{k}+\underset{\sim}{q})^2)+\hbar\omega)f(\underset{\sim}{k}+\underset{\sim}{q})\sin\theta\,dq\,d\theta\,d\phi,$$

the polar axis being in the direction $\underset{\sim}{k}$. The integration over θ can be performed in the usual way by defining the function $k^2 = F(E)$ (2.2). It is convenient to define the function $f(\underset{\sim}{k})$ in terms of the carrier energy E and an angle γ, where $\cos\gamma = \hat{k}\cdot\hat{k}_F$, $\hat{k}_F$ defining the unit vector in the direction of the field. The function $f(\underset{\sim}{k}+\underset{\sim}{q})$ can be obtained since

$E(|\underset{\sim}{k}+\underset{\sim}{q}|^2) = E(k^2) + \hbar\omega$, and $\hat{k}_F \cdot (\widehat{\underset{\sim}{k}+\underset{\sim}{q}}) = \dfrac{k\cos\theta + q(\hat{k}_F \cdot \hat{q})}{|\underset{\sim}{k}+\underset{\sim}{q}|}$

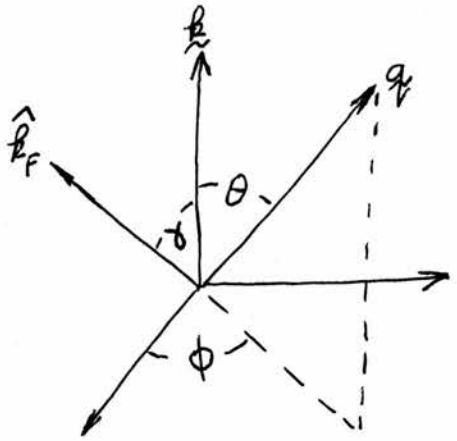

where $\hat{k}_F \cdot \hat{q} = \cos\theta\cos\gamma + \sin\theta\sin\gamma\cos\phi$ as can be seen from the diagram. Hence integrating over θ gives

$$I_1 = \frac{F'(E+\hbar\omega)}{\sqrt{F(E)}} \int_0^{\pi} \int_{q_{min}}^{q_{max}} \frac{f(E+\hbar\omega, \cos\gamma^+)}{q} \, dq \, d\phi ,$$

where

$$\cos\gamma^+ = \sqrt{\frac{F(E)}{F(E+\hbar\omega)}} \left\{ \cos\gamma + \frac{1}{2\sqrt{F(E)}} \left\{ [F(E+\hbar\omega) - F(E) - q^2]\cos\gamma \right.\right.$$

$$\left.\left. + \sqrt{4F(E)q^2 - [F(E+\hbar\omega) - F(E) - q^2]^2}\sin\gamma\cos\phi \right\}\right\} ,$$

and

$$q_{min}^{max} = \sqrt{F(E+\hbar\omega)} \pm \sqrt{F(E)}$$

The second term of the integral on the right-hand side of equation 4.2.2 can be evaluated in a similar manner, and the third and fourth terms can be evaluated resulting in terms not unlike those of equation 2.2.9. Thus, the collision integral reduces to

$$\frac{\partial f(\underset{\sim}{k})}{\partial t} = \frac{e^2 \hbar\omega N}{16\pi^2 \varepsilon_0 \hbar} \left(\frac{1}{\varepsilon_\infty} - \frac{1}{\varepsilon_s} \right) \left\{ e^{\theta/T} 2F'(E+\hbar\omega) \iint \frac{f(E+\hbar\omega, \cos\gamma^+)}{q} \, dq \, d\phi \right.$$

$$+ 2F'(E-\hbar\omega) \iint \frac{f(E-\hbar\omega, \cos\gamma^-)}{q} \, dq \, d\phi - 2\pi \left[\frac{F'(E+\hbar\omega)}{\sqrt{F(E)}} \right. \qquad 4.2.3$$

$$\left.\left. \times \log \frac{\sqrt{F(E+\hbar\omega)} + \sqrt{F(E)}}{\sqrt{F(E+\hbar\omega)} - \sqrt{F(E)}} + e^{\theta/T} \frac{F'(E-\hbar\omega)}{\sqrt{F(E)}} \log \frac{\sqrt{F(E)} + \sqrt{F(E-\hbar\omega)}}{\sqrt{F(E)} - \sqrt{F(E-\hbar\omega)}} \right] f(E, \cos\gamma) \right\} ,$$

where the limits of integration over ϕ are $0 \rightarrow \pi$, the limits

of integration over q are $q_{min}^{max} = \sqrt{F(E+\hbar\omega)} \pm \sqrt{F(E)}$ and $q_{min}^{max} = \sqrt{F(E)} \pm \sqrt{F(E-\hbar\omega)}$ for the first and second integrals respectively, and

$$\cos\gamma^{\pm} = \sqrt{\frac{F(E)}{F(E\pm\hbar\omega)}} \left\{ \cos\gamma + \frac{1}{2\sqrt{F(E)}} \left(\left[F(E\pm\hbar\omega) - F(E) - q^2 \right] \cos\gamma \right.\right.$$
$$\left.\left. + \sqrt{4F(E)q^2 - \left[F(E\pm\hbar\omega) - F(E) - q^2 \right]^2} \sin\gamma\cos\phi \right) \right\}$$

It is assumed that the function $F(E)$ is taken as zero if its argument becomes negative.

The inclusion of the mixing of Bloch states and spin-reversal scattering can be performed in a manner similar to that shown in Section 2.2.(d) by the insertion of the function $G(k,k',y)$ in the matrix element. It can be seen from the derivation of equation 2.2.19 that the integrands in equation 4.2.3 require an additional multiplicative factor

$$Q(k,k') - R(k,k')q^2 + S(k,k')q^4$$

where $k' = \sqrt{F(E\pm\hbar\omega)}$. The third and fourth terms on the right-hand side of equation 4.2.3 require their logarithms replaced by the factor

$$Q(k,k') \log\frac{k'+k}{|k'-k|} - 2R(k,k')kk' + 2S(k,k')kk'(k'^2+k^2)$$

Thus the full effect of the lattice periodicity is taken into account in the derivation of the polar optic mode collision integral.

4.3 Acoustic Phonon Scattering

The derivation of the acoustic phonon collision integral follows closely that of the polar optical phonon collision integral. It is necessary to use the matrix element defined by equation 2.3.1, and substitute it into equation 4.2.1 in the usual manner. Thus, using the fact that the δ -function is even

$$\frac{\partial f(\underline{k})}{\partial t} = \frac{E_1^2}{8\pi^2 \rho u^2 \hbar} \iiint \hbar u q \Big[\{(N+1) f(\underline{k}+\underline{q}) - N f(\underline{k})\} \delta(E(\underline{k}+\underline{q}) - E(\underline{k}) - \hbar u q) + \{N f(\underline{k}-\underline{q}) - (N+1) f(\underline{k})\} \delta(E(\underline{k}-\underline{q}) - E(\underline{k}) + \hbar u q) \Big] \times q^2 \sin\theta \, dq \, d\theta \, d\phi. \quad 4.3.1$$

where $N = (\exp(\hbar\omega / k_B T_0) - 1)^{-1}$ and $\hbar\omega = \hbar u q$. It will be assumed that the phonon energy is much less than the carrier energy throughout as in 2.3.

Consider the second term of the integrand and

$$I = \iiint (k_B T_0 - \tfrac{1}{2}\hbar u q) \delta(E(\underline{k}+\underline{q}) - E(\underline{k}) - \hbar u q) q^2 \sin\theta \, dq \, d\theta \, d\phi,$$

which can be integrated over θ in the usual way by defining $k^2 = F(E)$ resulting in

$$I = \frac{1}{2\sqrt{F(E)}} \int_0^{2\pi} \int_0^{q_{max}} (k_B T_0 - \tfrac{1}{2}\hbar u q)(F'(E) + \hbar u q F''(E)) q \, dq \, d\phi,$$

$q_{max} = 2\sqrt{F(E)} + \hbar u q$ as given by equation 2.3.2. Integrating, and disregarding terms above second order in the phonon energy produces

$$I = \frac{\pi}{\sqrt{F(E)}} \Big\{ 4 k_B T_0 F(E) F'(E) + \hbar u \big(2 k_B T_0 \sqrt{F(E)} F'^2(E) + \tfrac{8}{3} F^{3/2}(E) [k_B T_0 F''(E) - \tfrac{1}{2} F'(E)] \big) + (\hbar u)^2 \big(\tfrac{1}{2} k_B T_0 F'^3(E) + 4 F(E) F'(E) [k_B T_0 F''(E) - \tfrac{1}{2} F'(E)] - 2 F''(E) F^2(E) \big) \Big\}.$$

It is necessary to retain second order terms in order to include the contribution of the spherically symmetric part of the distribution function in the collision integral. This is discussed in Conwell p.218 [1]. Thus integrating the remaining terms in the integrand of equation 4.3.1 and

$$\frac{\partial f(\underline{k})}{\partial t} = \frac{E_1^2}{8\pi^2 \rho u^2 \hbar} \Big\{ \frac{1}{\sqrt{F(E)}} \int_0^{\pi} \int_0^{q_{max}} (k_B T_0 + \tfrac{1}{2}\hbar u q)(F'(E) + \hbar u q F''(E)) f(E + \hbar u q, \cos\gamma') q \, dq \, d\phi + \frac{1}{\sqrt{F(E)}} \int_0^{\pi} \int_0^{q_{max}} (k_B T_0 - \tfrac{1}{2}\hbar u q)(F'(E) - \hbar u q F''(E)) f(E - \hbar u q, \cos\gamma') q \, dq \, d\phi$$

$$-\frac{2\pi}{\sqrt{F(\epsilon)}}\left\{4k_BT_0F(\epsilon)F'(\epsilon)+(\hbar u)^2\left(\tfrac{1}{2}k_BT_0F'^3(\epsilon)+4F(\epsilon)F'(\epsilon)\left[k_BT_0F''(\epsilon)\right.\right.\right.$$
$$\left.\left.\left.-\tfrac{1}{2}F'(\epsilon)\right]-2F''(\epsilon)F^2(\epsilon)\right)\right\}f(E,\cos\gamma)\Big\}, \qquad 4.3.2$$

where the upper limit of the integration over q is given by $q_{max}=2\sqrt{F(\epsilon)}\pm\hbar u F'(\epsilon)$ for the first and second terms respectively. Also

$$\cos\gamma'=\left(1-\frac{q^2}{2F(\epsilon)}\right)\cos\gamma+\frac{q}{\sqrt{F(\epsilon)}}\sqrt{1-\frac{q^2}{4F(\epsilon)}}\sin\gamma\cos\phi, \qquad 4.3.3$$

which can be derived in a similar manner to equation 4.2.3.

If a strong energy relaxation mechanism exists, as in the case of a polar semiconductor at sufficiently high temperatures, it may be that the acoustic phonon field only affects the momentum relaxation of the carriers significantly. In this situation the higher order terms involving the phonon energy may be neglected resulting in a simplified collision integral of the form

$$\frac{\partial f(k)}{\partial t}=\frac{E_i^2k_BT_0F'(\epsilon)}{4\pi^2\rho u^2\hbar\sqrt{F(\epsilon)}}\left\{\int_0^{\pi}\int_0^{2\sqrt{F(\epsilon)}}f(E,\cos\gamma')q\,dq\,d\phi-4\pi F(\epsilon)f(\epsilon,\cos\gamma)\right\}. \qquad 4.3.4$$

The inclusion of the mixing of Bloch states can be performed in the manner decribed in Section 2.3.(c) and is straightforward but produces a rather lengthy expression for equation 4.3.2. For equation 4.3.4 an additional factor of

$$1-\frac{q^2}{2F(\epsilon)}(C+2G)+\frac{q^4}{4F^2(\epsilon)}G$$

appears in the integral, and the final term requires multiplying by $1-\frac{1}{3}(3C+2G)$ where C and G are defined in Appendix 1.

4.4 Ionised Impurity Scattering

The derivation of the rate of loss of momentum for ionised impurity scattering given in Section 2.4, was based on the assumption that the impurities could be regarded as infinitely massive and stationary with respect to the lattice. Consequently the carriers could not gain momentum as a result of being scattered by an impurity. This assumption will also be made in the derivation of the appropriate collision integral. Hence, substituting the matrix element given by equation 2.4.1 into equation 4.1.4 for the case of intravalley scattering gives

$$\frac{\partial f(\underset{\sim}{k})}{\partial t} = \frac{4e^4 N_I}{(4\pi\varepsilon_o\varepsilon_s)^2 \hbar} \left\{ \iiint \frac{1}{(\lambda^2+q^2)^2} \left[f(\underset{\sim}{k}-\underset{\sim}{q})\,\delta(E((\underset{\sim}{k})^2) - E((\underset{\sim}{k}-\underset{\sim}{q})^2)) \right.\right.$$
$$\left.\left. - f(\underset{\sim}{k})\,\delta(E((\underset{\sim}{k}+\underset{\sim}{q})^2) - E(\underset{\sim}{k}^2)) \right] q^2 \sin\theta\, dq\, d\theta\, d\phi$$

all the parameters being previously defined. Consider the second term in the integral, where

$$I = \iiint \frac{q^2}{(\lambda^2+q^2)^2}\,\delta(E((\underset{\sim}{k}+\underset{\sim}{q})^2) - E(\underset{\sim}{k}^2))\sin\theta\, d\theta\, dq\, d\phi$$

which can be integrated over θ and ϕ giving

$$I = \frac{\pi F'(E)}{\sqrt{F(E)}} \int_0^{q_{max}} \frac{q}{(\lambda^2+q^2)^2}\, dq .$$

$q_{max} = 2\sqrt{F(E)}$ as given in the derivation of equation 2.4.2.

Thus,

$$I = \frac{\pi F'(E)}{\sqrt{F(E)}} \cdot \frac{2F(E)}{\lambda^2(\lambda^2+4F(E))} ,$$

and

$$\frac{\partial f(\underset{\sim}{k})}{\partial t} = \frac{4e^4 N_I F'(E)}{(4\pi\varepsilon_o\varepsilon_s)^2 \hbar \sqrt{F(E)}} \left\{ \int_0^{\pi} \int_0^{2\sqrt{F(E)}} \frac{q}{(\lambda^2+q^2)^2} f(E,\cos\gamma')\, dq\, d\phi \right.$$
$$\left. - \frac{2\pi F(E)}{\lambda^2(\lambda^2+4F(E))} f(E,\cos\gamma) \right\} \qquad 4.4.1$$

where $\cos\gamma'$ is defined by equation 4.3.3.

As can be seen from equation 2.4.3, Section 2.4.(b) the inclusion of the mixing of Bloch states requires the additional factor $(1 - Rq^2 + Sq^4)$ in the integrand of the first term of equation 4.4.1. In the second term $2F(E)/(\lambda^2(\lambda^2+4F(E)))$ needs replacing by

$$\frac{2F(E)}{\lambda^2(\lambda^2+4F(E))}(1+\lambda^2 R+\lambda^4 S) - \log\left(1+\frac{4F(E)}{\lambda^2}\right).(R+\lambda^2 S) + 4F(E)\,S$$

where R and S are defined in Appendix 1.

4.5 Intervalley Scattering

The intervalley collision integral is defined by equation 4.1.4. In order to include the full effects of intervalley scattering it is necessary to sum the collision integrals for equivalent and inequivalent intervalley scattering, over all the allowed transitions. In some cases this may involve very many terms [50]. The appropriate matrix element is given by Conwell, p.154 [1], and is

$$|(\underset{\sim}{k}\pm\underset{\sim}{q}|H'_{iv}|\underset{\sim}{k})|^2 = \frac{\Xi_{ij}^2\,\hbar\,Z_j}{2V\rho\omega_{ij}}\left(N+\tfrac{1}{2}\mp\tfrac{1}{2}\right) \qquad 4.5.1$$

where Ξ_{ij} is the intervalley coupling constant, Z_j the number of equivalent valleys of type j, ω_{ij} the intervalley phonon frequency, and $N=[\exp(\hbar\omega_{ij}/k_BT_0)-1]^{-1}$ is the phonon occupation number.

Thus, assuming Ξ_{ij} and ω_{ij} as constants, substituting 4.5.1 into 4.1.4 produces

$$\left(\frac{\partial f_i(\underset{\sim}{k})}{\partial t}\right)_{ij} = \frac{\Xi_{ij}^2 Z_j}{8\pi^2\rho\omega_{ij}}\iiint\Big[\left\{(N+1)f_j(\underset{\sim}{k}+\underset{\sim}{q})-Nf_i(\underset{\sim}{k})\right\}\delta(E_j((\underset{\sim}{k}+\underset{\sim}{q})^2)-E_i(k^2)+\hbar\omega_{ij}) \qquad 4.5.2$$

$$+\left\{Nf_j(\underset{\sim}{k}-\underset{\sim}{q})-(N+1)f_i(\underset{\sim}{k})\right\}\delta(E_j((\underset{\sim}{k}-\underset{\sim}{q})^2)-E_i(k^2)+\hbar\omega_{ij})\Big]$$
$$\times q^2\sin\theta\,dq\,d\theta\,d\phi$$

where E_i and E_j represent energy states for carriers in valleys i and j respectively. The energy bands can be expressed in the usual generalised formalism by taking

$$(\underset{\sim}{k}-\underset{\sim}{R}_i)^2 = F_i(E_i-\Delta_i) \qquad 4.5.3$$

where $\underset{\sim}{R}_i$ is the relative displacement of the i th valley from the centre of the B.Z. and Δ_i is the energy of the valley minimum.

Consider the first term of the integrand on the right-hand side of equation 4.5.2 and

$$I = \iiint\delta(E_j((\underset{\sim}{k}+\underset{\sim}{q})^2)-E_i(k^2)-\hbar\omega_{ij})f_j(\underset{\sim}{k}+\underset{\sim}{q})q^2\sin\theta\,dq\,d\theta\,d\phi,$$

Let

$$x = E_j((\underset{\sim}{k}+\underset{\sim}{q})^2)-E_i-\hbar\omega_{ij}$$

therefore

$$(\underset{\sim}{k}+\underset{\sim}{q}-\underset{\sim}{R}_j)^2 = F_j(E_i+\hbar\omega_{ij}-\Delta_j+x)$$

Choosing the polar axis directed along $\underset{\sim}{k}-\underset{\sim}{R}_j$ results in

$$-2|\underset{\sim}{k}-\underset{\sim}{R}_j|q\sin\theta\,d\theta = F_j'(E_i+\hbar\omega_{ij}-\Delta_j+x)\,dx$$

Thus, substituting and integrating over x produces

$$I = \frac{F_j'(E_i+\hbar\omega_{ij}-\Delta_j)}{2\sqrt{F_j(E_j-\Delta_j)}} \iint f_j(\underset{\sim}{k}+\underset{\sim}{q})\, q\, dq\, d\phi$$

where the limits for the q integration are given by the conditions defined in the argument of the δ function

$$E_j((\underset{\sim}{k}+\underset{\sim}{q})^2) = E_i + \hbar\omega_{ij}$$

which are

$$q_{min}^{max} = \sqrt{F_j(E_i+\hbar\omega_{ij}-\Delta_j)} \pm \sqrt{F_j(E_j-\Delta_j)}$$

The energy E is defined as zero at the bottom of the i th valley and $E' = E + \Delta_i - \Delta_j$, therefore

$$I = \frac{F_j'(E'+\hbar\omega_{ij})}{2\sqrt{F(E)}} \int_0^{2\pi}\int_{q_{min}}^{q_{max}} f_j(\underset{\sim}{k}+\underset{\sim}{q})\, q\, dq\, d\phi$$

where $q_{min}^{max} = \sqrt{F_j(E'+\hbar\omega_{ij})} \pm \sqrt{F_j(E')}$, and $E' = E + \Delta_i - \Delta_j$

Hence

$$\left(\frac{\partial f_i(\underset{\sim}{k})}{\partial t}\right)_{ij} = \frac{\Xi_{ij}^2 N Z_j}{8\pi\rho\omega_{ij}} \left\{ \exp\left(\frac{\hbar\omega_{ij}}{k_B T_0}\right) \frac{F_j'(E'+\hbar\omega_{ij})}{2\sqrt{F_j(E')}} \iint f_j(E'+\hbar\omega_{ij}, \cos\gamma^+)\, q\, dq\, d\phi \right.$$

$$+ \frac{F_j'(E'-\hbar\omega_{ij})}{2\sqrt{F_j(E')}} \iint f_j(E'-\hbar\omega_{ij}, \cos\gamma^-)\, q\, dq\, d\phi - 2\pi \left\{ F_j'(E'+\hbar\omega_{ij}) \right. \quad 4.5.4$$

$$\left. \left. \times \sqrt{F_j(E'+\hbar\omega_{ij})} + \exp\left(\frac{\hbar\omega_{ij}}{k_B T_0}\right) F_j'(E'-\hbar\omega_{ij}) \sqrt{F_j(E'-\hbar\omega_{ij})} \right\} f_i(E', \cos\gamma) \right\}$$

where the limits of integration over ϕ are $0 \to 2\pi$, and those over q are $q_{min}^{max} = \sqrt{F_j(E'+\hbar\omega_{ij})} \pm \sqrt{F_j(E')}$ for the first integral,

and $q_{min}^{max} = \sqrt{F_j(E')} \pm \sqrt{F(E'-\hbar\omega_{ij})}$ for the second integral.

$$\cos\gamma^{\pm} = \sqrt{\frac{F_j(E')}{F_j(E'\pm\hbar\omega_{ij})}} \left\{ \cos\gamma + \frac{1}{2F_j(E')} \left(\left[F_j(E'\pm\hbar\omega_{ij}) - F_j(E') - q^2\right]\cos\gamma \right. \right.$$

$$\left. \left. + \sqrt{4F_j(E')q^2 - \left[F_j(E'\pm\hbar\omega_{ij}) - F_j(E') - q^2\right]^2}\, \sin\gamma\cos\phi \right) \right\}$$

where $E' = E + \Delta_i - \Delta_j$. This derivation is similar to that given for equation 4.2.3. The inclusion of the mixing of Bloch states is straightforward but somewhat lengthy and follows closely that given in Sections 2.2.(d) and 4.2.

4.6. Electron-electron Scattering

The carrier-carrier collision integral defined by equation 4.1.5 was derived by Chapman and Cowling [49]. It has been applied to the transport properties of semiconductors by Appel [51], and found to have little effect at low fields. However Hasegawa and Yamashita [52] considered the warm electron problem and found that at sufficiently high electron densities, electron-electron collisions make a significant difference to the conductivity of n-type germanium. Their derivation was concerned with the spherically symmetric part of the collision integral. It will now be generalised to include the non-symmetric part of the collision integral and band structure non-parabolicity.

The collision integral will initially be derived for a parabolic band structure. Equation 4.5.1 can be written in a suitable form as

$$\frac{\partial f(\underset{\sim}{k})}{\partial t} = \frac{n A_0 \sqrt{\pi}\, \hbar^3}{2(2\pi m^* k_B T_0)^{3/2}} \iiint [f(\underset{\sim}{k}')f(\underset{\sim}{k}_1') - f(\underset{\sim}{k})f(\underset{\sim}{k}_1)]\, \alpha(\chi, r) \times \sin\chi \, d\chi \, d\epsilon \, d\underset{\sim}{k}_1' \qquad 4.6.1$$

where electrons with momenta $\underset{\sim}{k}$ and $\underset{\sim}{k}_1$ mutually scatter into states $\underset{\sim}{k}'$ and $\underset{\sim}{k}_1'$, with relative momenta $\underset{\sim}{r} = \underset{\sim}{k}_1 - \underset{\sim}{k}$ and $\underset{\sim}{r}' = \underset{\sim}{k}_1' - \underset{\sim}{k}'$. χ is the angle between $\underset{\sim}{r}$ and $\underset{\sim}{r}'$, ϵ specifies the orientation of $\underset{\sim}{r}'$, $\alpha(\chi, r) = |\sigma(\chi, r)|^2 \hbar r / m^*$, where $\sigma(\chi, r)$ is the differential cross-section and n is the electron concentration. The constant which appears before the integral in equation 4.6.1 arises from the definition of the distribution function given by equation 4.1.2. Chapman and Cowling [49] define their distribution function as the occupation number per unit volume of configuration space.

The collision integral can be evaluated by using the conservation equations of momentum and energy which apply to electrons in a parabolic band. These are

$$\underset{\sim}{k}_1 + \underset{\sim}{k} = \underset{\sim}{k}_1' + \underset{\sim}{k}',$$

and

$$k_1^2 + k^2 = k_1'^2 + k'^2$$

It is easy to show that the magnitudes of the relative momenta r and r' before and after the collision respectively, are equal.

A transformation of coordinates to the system (r, θ, ϕ) will be made choosing the origin of the coordinate system at $\underset{\sim}{k}_1 = \underset{\sim}{k}$, and the polar axis directed along $\underset{\sim}{k}$. Thus

$$\frac{\partial f(\underset{\sim}{k})}{\partial t} = \frac{n A_0 \sqrt{\pi}\, \hbar^3}{2(2\pi m^* k_B T_0)^{3/2}} \iiint [f(\underset{\sim}{k}')f(\underset{\sim}{k}_1') - f(\underset{\sim}{k})f(\underset{\sim}{k}_1)] \propto(\chi, r) \sin\chi \, d\chi \, d\epsilon \, r^2 \sin\theta \, dr \, d\theta \, d\phi ,$$

where

$$\left.\begin{aligned} \underset{\sim}{k}_1 &= \underset{\sim}{k} + \underset{\sim}{r} \quad , \\ \underset{\sim}{k}' &= \underset{\sim}{k} + (\underset{\sim}{r} - \underset{\sim}{r}')/2 \, , \\ \underset{\sim}{k}_1' &= \underset{\sim}{k} + (\underset{\sim}{r} + \underset{\sim}{r}')/2 \, . \end{aligned}\right\} \qquad 4.6.2$$

and

These equations can be squared to produce

$$\left.\begin{aligned} k_1^2 &= k^2 + 2kr\cos\theta + r^2 \quad , \\ k'^2 &= k^2 + kr(\cos\theta - \cos\theta') + r^2(1-\cos\chi)/2 \, , \\ k_1'^2 &= k^2 + kr(\cos\theta + \cos\theta') + r^2(1+\cos\theta)/2 \, . \end{aligned}\right\} \qquad 4.6.3$$

and

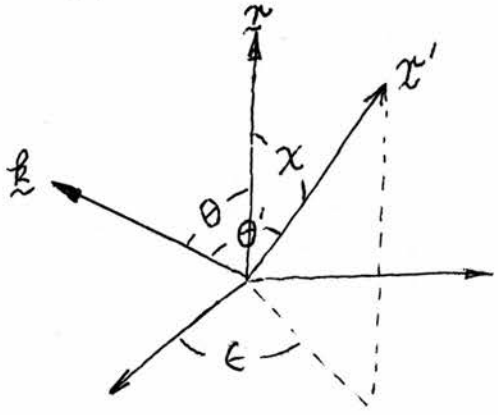

It can be seen from the diagram that

$$\cos\theta' = \cos\theta\cos\chi + \sin\theta\sin\chi\cos\epsilon .$$

The distribution function will be defined so that $f(\underset{\sim}{k}) = f(E, \cos\gamma)$ the angle γ being defined with respect to the unit vector $\hat{k}_F$ in the direction of the applied field. Hence, multiplying equations 4.6.2 by the vector $\hat{k}_F$ gives

$$\left.\begin{aligned} k_1 \cos\gamma_1 &= k\cos\gamma + r\cos\beta \quad , \\ k'\cos\gamma' &= k\cos\gamma + r(\cos\beta - \cos\beta')/2 \, , \\ k_1'\cos\gamma_1' &= k\cos\gamma + r(\cos\beta + \cos\beta')/2 \, . \end{aligned}\right\} \qquad 4.6.4$$

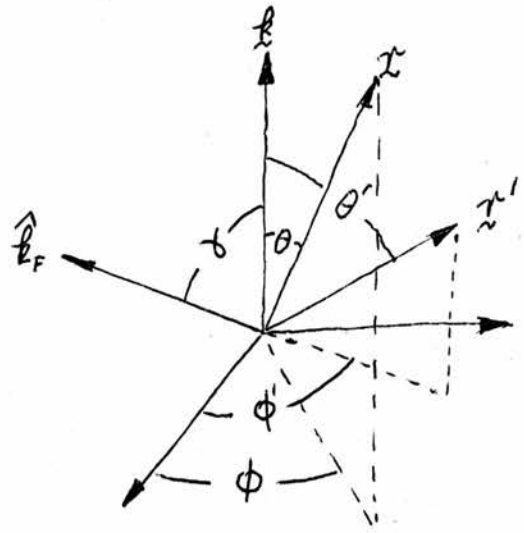

where

$$\cos\beta = \cos\theta\cos\gamma + \sin\theta\sin\gamma\cos\phi ,$$

and

$$\cos\beta' = \cos\theta'\cos\gamma + \sin\theta'\sin\gamma\cos\phi' .$$

$\cos\phi'$ can be obtained from the equation

$$\cos\chi = \cos\theta\cos\theta' + \sin\theta\sin\theta'\cos(\phi-\phi')$$

Redefining the distribution function in energy space such that $E = \frac{\hbar^2k^2}{2m^*}$ and taking $X = \frac{\hbar\chi}{\sqrt{2m^*}}$ gives

$$\left.\begin{aligned} E_1 &= E + 2\sqrt{E}X\cos\theta + X^2 \quad , \\ E' &= E + \sqrt{E}X(\cos\theta - \cos\theta') + X^2(1-\cos\chi)/2 \quad , \\ E_1' &= E + \sqrt{E}X(\cos\theta + \cos\theta') + X^2(1+\cos\chi)/2 \quad . \end{aligned}\right\} \quad 4.6.5$$

and

$\cos\theta'$ being given in equations 4.6.3. Similarly,

$$\left.\begin{aligned} \cos\gamma_1 &= \frac{1}{\sqrt{E_1}}\left\{\sqrt{E}\cos\gamma + X\cos\beta\right\} \quad , \\ \cos\gamma' &= \frac{1}{\sqrt{E'}}\left\{\sqrt{E}\cos\gamma + \frac{X}{2}(\cos\beta - \cos\beta')\right\} \quad , \\ \cos\gamma_1' &= \frac{1}{\sqrt{E_1'}}\left\{\sqrt{E}\cos\gamma + \frac{X}{2}(\cos\beta + \cos\beta')\right\} \quad , \end{aligned}\right\} \quad 4.6.6$$

$\cos\beta$ and $\cos\beta'$ being defined in equations 4.6.4. The collision integral reduces to

$$\frac{\partial f(E)}{\partial t} = \frac{n A_0}{2\pi (k_B T_0)^{3/2}} \int_0^{2\pi}\int_0^{\pi}\int_0^{\infty}\int_0^{2\pi}\int_0^{\pi} \left[f(E',\cos\gamma') f(E_1',\cos\gamma_1') - f(E,\cos\gamma) f(E_1',\cos\gamma_1') \right] \qquad 4.6.7$$

$$\times \alpha(\chi,x) \sin\chi \, d\chi \, d\epsilon \, x^2 \sin\theta \, dx \, d\theta \, d\phi .$$

$$\alpha(\chi,x) = \frac{\sqrt{2}\, e^4 m^{*3/2} x}{\left[4\pi \varepsilon_0 \varepsilon_s \hbar \left(\lambda^2 + 2m^* x \sin^2\left(\frac{\chi}{2}\right)/\hbar^2 \right) \right]^2}$$

as given by Conwell [1]. The derivation of $\alpha(\chi,x)$ is based on the Born approximation with λ^2 defined by equation 3.2.6.

It was possible for the collision integrals arising from carrier-phonon interactions to include the effects of band structure non-parabolicity in a very general way. In the case of the carrier-carrier collision integral this is not possible. However, by choosing a simplified Kane band structure of the form $k^2 = 2m^* E(1+E/G)/\hbar^2$, which has been discussed in Section 3.1, with some additional assumptions, the calculation can be performed.

The angle χ defined in the collision integral (equation 4.5.1) refers to the angle between the relative velocities of the carriers before and after collision. In the case of a parabolic band this is also the angle between the relative momenta of the carriers before and after collision. For a non-parabolic band this is no longer the case and care has to be taken to choose χ correctly.

The effective mass of a carrier in an energy band of the above form is $m^*(1+2E/G)$, so the relative velocity of the carriers with momenta $\underset{\sim}{k}_1$ and $\underset{\sim}{k}$ is given by

$$\frac{\hbar}{m^*} \left\{ \frac{\underset{\sim}{k}_1}{\left(1+\frac{2E_1}{G}\right)} - \frac{\underset{\sim}{k}}{\left(1+\frac{2E}{G}\right)} \right\} = \frac{\hbar}{m^*} \underset{\sim}{\gamma} ,$$

the parameters being defined in a manner analogous to the parabolic case. From this equation it is straightforward to deduce that

$$E_1 = \frac{G}{2} \left\{ \sqrt{1 + \frac{4T}{G-4T}} - 1 \right\} ,$$

where

$$T = \frac{E\left(1+\frac{E}{G}\right)}{\left(1+2\frac{E}{G}\right)^2} + 2x \frac{\sqrt{E\left(1+\frac{E}{G}\right)}}{\left(1+\frac{2E}{G}\right)} \cos\theta + x^2 ,$$

E_1 and X being defined in the usual way. These equations reduce to the parabolic expressions when G is large.

Consideration of the relative velocity after collision leads to

$$\left(1+\frac{2E_1'}{G}\right)\left(1+\frac{2E'}{G}\right)\underset{\sim}{k}' = \left(1+\frac{2E'}{G}\right)\underset{\sim}{k}_1' - \left(1+\frac{2E_1'}{G}\right)\underset{\sim}{k}'$$

which, after the inclusion of energy and momentum conservation necessitates the solution of a quartic equation in order to find E' and E_1'. However, the problem reduces to the solution of a quadratic equation if it is assumed that

$$E_1 + E \gg \frac{E_1 E}{G} \qquad 4.6.8$$

This condition is satisfied reasonably well for fields which produce average carrier energies corresponding to small fractions of the energy gap. In the case of InSb the average carrier energy is about 0.05eV at 3×10^4 V/m (see Ch. 5). The band gap of InSb is 0.23eV as given in Ch. 2, so E_1+E is roughly a factor of 10 greater than E_1E/G. This approximation is least valid for collisions between very energetic electrons.

Another consequence of the above assumption is that the relative velocity has a constant magnitude throughout the collision process, as in the parabolic case. Therefore after some calculation

$$E' = \frac{G}{2\left(1-\frac{4u}{G}\right)}\left\{\sqrt{1-\frac{4}{G}(u-v)-\frac{16}{G^2}(uv-w^2)} - \left(1-\frac{4}{G}(u-w)\right)\right\},$$

and

$$E_1' = \frac{G}{2\left(1-\frac{4u}{G}\right)}\left\{\sqrt{1-\frac{4}{G}(u-v)-\frac{16}{G^2}(uv-w^2)} - \left(1-\frac{4}{G}(u+w)\right)\right\},$$

where

$$u = 4E\left(\frac{1+\frac{E_1+E}{G}}{1+\frac{2E}{G}}\right)^2 + 4\sqrt{E}\,x\cos\theta\left(\frac{1+\frac{2E_1}{G}}{1+\frac{2E}{G}}\right)\left(1+\frac{E_1+E}{G}\right)+\left(1+\frac{2E_1}{G}\right)^2x^2,$$

$$v = \left[1+\frac{2(E_1+E)}{G}\right]^2x^2,$$

and

$$w = \left[1+\frac{2(E_1+E)}{G}\right]\left\{2\sqrt{E}\,x\cos\theta'\left(\frac{1+\frac{E_1+E}{G}}{1+\frac{2E}{G}}\right)+\left(1+\frac{2E}{G}\right)x^2\cos\chi\right\}$$

The cosines of the angles γ_1, γ' and γ_1' can be obtained in a similar manner to those defined by equations 4.6.**6**.

To include the effects of non-parabolicity on the mixing of Bloch states in the differential scattering cross-section $\sigma(\chi,\chi)$ requires the insertion of the function $G(k,k',\gamma)$ defined by equation 2.2.17. It should be noted that the condition defined by equation 4.6.8 has the effect of keeping the reduced mass of the inter-carrier collision process constant.

CHAPTER 5

SOLUTION OF THE BOLTZMANN EQUATION BY ITERATION AND ITS APPLICATION TO InSb AT 77°K

5.1 Introduction

A number of methods have recently been suggested for the iterative solution of the high field Boltzmann transport equation [6,53,54]. They involve the reformulation of Boltzmann's equation in such a manner that its solution can be generated from an initial trial function. The development of these approaches originated from the desire to evaluate the transport properties for realistic models of semiconductors to a required degree of accuracy. Consequently numerical considerations of the problem in question are of prime importance, since analytic solutions rarely exist in all but the simplest cases. This chapter is concerned with the theory of Rees' iterative solution of Boltzmann's equation and its application to InSb, with both the time dependent and time independent cases being discussed.

The time dependent Boltzmann equation which describes a non-degenerate semiconductor at high fields was derived in Chapter 4, and can be written in a general form as

$$\frac{\partial f}{\partial t} + \frac{e\underline{E}}{\hbar} \cdot \frac{\partial f}{\partial \underline{k}} = \bar{C}f \qquad 5.1.1$$

where $\bar{C}f$ represents the appropriate collision integral. It has been assumed in this equation that the problem under consideration is spatially homogeneous, and that only electric fields are present. The simplest possible iterative scheme for solving this equation can be obtained by a "stepwise" integration with respect to time. Since

$$\frac{\partial}{\partial t} f(\underline{k},t) = \lim_{\Delta t \to 0} \frac{f(\underline{k},t+\Delta t) - f(\underline{k},t)}{\Delta t},$$

equation 5.1.1 can be written in the form

$$f(\underline{k},t+\Delta t) = \left\{ 1 + \Delta t \left(-\frac{e\underline{E}}{\hbar} \cdot \frac{\partial}{\partial \underline{k}} + \bar{C} \right) \right\} f(\underline{k},t) \qquad 5.1.2$$

This equation could be used to evaluate the time development of the

distribution function provided Δt is sufficiently small. If the collision integral and the applied field are time independent, then a steady state solution can exist; it would be expected that after enough "steps in time" the distribution function would stabilise, and thus satify the time independent Boltzmann equation, which is given by equating the final term in equation 5.1.2 to zero. It should be noted that

$$f(\underset{\sim}{k} - \frac{e\Delta t \underset{\sim}{E}}{\hbar}) \doteq f(\underset{\sim}{k}) - \Delta t \frac{e\underset{\sim}{E}}{\hbar} \frac{\partial f(\underset{\sim}{k})}{\partial t}$$

therefore to first order in Δt

$$f(\underset{\sim}{k}, t+\Delta t) = \left\{ (1 + \Delta t \bar{C}) f(\underset{\sim}{k}, t) \right\}_{\underset{\sim}{k} \to \underset{\sim}{k} - \frac{e\Delta t}{\hbar}\underset{\sim}{E}} \qquad 5.1.3$$

where $\underset{\sim}{k} \to \underset{\sim}{k} - \frac{e\Delta t}{\hbar}\underset{\sim}{E}$ symbolises the projection of the function in braces along its collision free trajectory for a period Δt . This equation, with the inclusion of higher order terms in Δt , has been discussed by Kwok and Schultz [55,56], who also considered other approaches for generating the solution of Boltzmann's equation in such a manner. However, it is essential that the method chosen should be amenable to easy numerical evaluation, and the uniqueness of the resultant solution be known. Recently a method has been developed by Rees which possesses both of these qualities. This approach is initially concerned with the solution of the time independent transport problem, and will now be discussed.

The time independent Boltzmann equation is given by equation 5.1.1 when the distribution function can be expressed solely in terms of $\underset{\sim}{k}$. A reformulation of this equation can conveniently be obtained by adding a term linear in $f(\underset{\sim}{k})$. Thus

$$\frac{e\underset{\sim}{E}}{\hbar} \cdot \frac{\partial f(\underset{\sim}{k})}{\partial \underset{\sim}{k}} + \alpha(\underset{\sim}{k}) f(\underset{\sim}{k}) = \tilde{C} f(\underset{\sim}{k}) \qquad 5.1.4$$

This can be solved by introducing the integrating factor e^{G} , such that

$$\frac{e\underset{\sim}{E}}{\hbar} \cdot \frac{\partial}{\partial \underset{\sim}{k}} (e^{G} f) = e^{G} \tilde{C} f \quad , \qquad 5.1.5$$

where G can be obtained from the equation

$$\frac{e}{\hbar}\underset{\sim}{F}\cdot\frac{\partial G}{\partial \underset{\sim}{k}} = \alpha(\underset{\sim}{k}) \qquad 5.1.6$$

The inverse of an operator can conveniently be defined so that

$$p^{-1} = \int_0^\infty ds\, e^{-ps}, \quad \text{for} \quad Re\, p > 0$$

This facilitates the solution of equation 5.1.6 giving

$$G(\underset{\sim}{k}) = \left\{\int_0^\infty ds\, \exp\left(-\frac{es}{\hbar}\underset{\sim}{F}\cdot\frac{\partial}{\partial \underset{\sim}{k}}\right)\right\}\alpha(\underset{\sim}{k})$$

which after application of the translation operator produces

$$G(\underset{\sim}{k}) = \int_0^\infty ds\, \alpha\left(\underset{\sim}{k} - \frac{es}{\hbar}\underset{\sim}{F}\right)$$

where $G(\infty)$ is chosen to be zero. The solution of equation 5.1.5 can be obtained in a similar manner leading to

$$f(\underset{\sim}{k}) = \int_0^\infty \exp\left(-\int_0^t \alpha\left(\underset{\sim}{k} - \frac{es}{\hbar}\underset{\sim}{F}\right)ds\right)\tilde{C}f\left(\underset{\sim}{k} - \frac{et}{\hbar}\underset{\sim}{F}\right).dt \qquad 5.1.7$$

The above derivation of this integral equation was given by Vassell [57].

The collision integral for many problems of physical interest may be expressed as a linear functional of $f(\underset{\sim}{k})$. A collision integral of such a form is given by equation 4.1.4, which may be taken as

$$\bar{C}f(\underset{\sim}{k}) = -\int\left[f(\underset{\sim}{k}')P(\underset{\sim}{k}',\underset{\sim}{k}) - f(\underset{\sim}{k})P(\underset{\sim}{k},\underset{\sim}{k}')\right]d\underset{\sim}{k}'.$$

The second term in the integrand may be integrated so that

$$\bar{C}f(\underset{\sim}{k}) = \lambda(\underset{\sim}{k})f(\underset{\sim}{k}) - \int f(\underset{\sim}{k}')P(\underset{\sim}{k}',\underset{\sim}{k})\,d\underset{\sim}{k}' \qquad 5.1.8$$

Thus by substituting equation 5.1.8 into equation 5.1.7, a homogeneous Fredholm integral equation of the second kind is obtained such that

$$f(\underset{\sim}{k}) = \int_0^\infty \exp\left(-\int_0^t \alpha\left(\underset{\sim}{k} - \frac{es}{\hbar}\underset{\sim}{F}\right)ds\right)\left\{\left[\alpha(\underset{\sim}{k}) - \lambda(\underset{\sim}{k})\right]f(\underset{\sim}{k}) + \int f(\underset{\sim}{k}')P(\underset{\sim}{k}',\underset{\sim}{k})\,d\underset{\sim}{k}'\right\}dt \qquad 5.1.9$$

$$\underset{\sim}{k} \to \underset{\sim}{k} - \frac{et}{\hbar}\underset{\sim}{F}$$

Rees has discussed this equation in some detail and considered the "self scattering" rate $\alpha(\underset{\sim}{k})$, which has no physical significance since it involves the scattering of a carrier with no change of momentum, and chose it to remain a constant value. Therefore, with $\alpha(\underset{\sim}{k}) = \Gamma$,

$$f(\underset{\sim}{k}) = \int_0^\infty e^{-\Gamma t} \left\{ [\Gamma - \lambda(\underset{\sim}{k})] f(\underset{\sim}{k}) + \int f(\underset{\sim}{k}') P(\underset{\sim}{k}', \underset{\sim}{k}) d\underset{\sim}{k}' \right\} dt \qquad 5.1.10$$

$$\underset{\sim}{k} \rightarrow \underset{\sim}{k} - \frac{e t}{\hbar} \underset{\sim}{E}$$

It was known to Rees that when Γ is large this equation generates the time evolution of the distribution function. This can be shown simply by assuming that the second factor in the integral varies slowly when Γ is large, and can be removed from the integral choosing its argument at the time corresponding to the average value for the remaining integral. The remaining exponential can be integrated and equation 5.1.10 reduces to the time evolution form given by equation 5.1.3. Consequently Rees intuitively deduced that by appealing to the stability of the steady state, provided the total "self scattering" rate $\Gamma - \alpha(\underset{\sim}{k})$ is positive, equation 5.1.10 generates the Boltzmann time independent solution. This condition has been given mathematical justification by Vassell [57] who proved that when the kernel of the integral equation is positive and linear, and the initial trial iterate is also positive, then the unique steady state solution to the Boltzmann equation 5.1.1 can be obtained. More recently Kwok and Schultz [55,56], and Rees [7] have shown that the speed of convergence of equation 5.1.10 can be increased in many cases by choosing a "self scattering" rate that can be negative.

By taking $\alpha(\underset{\sim}{k}) = \lambda(\underset{\sim}{k})$ in equation 5.1.9 we obtain the iterative method which has been introduced by Budd [53] and Price [54]. Budd applied the method to a specific problem where the scattering processes are independent of the change in momenta of the carriers. Consequently it was possible to express the anisotropic part of the distribution function in terms of the symmetric part, thus expressing the problem wholly in terms of a one dimensional integral equation. This transformation is not possible for the important scattering processes which arise in a polar semiconductor, which is the problem of interest here.

A theorem from functional analysis proved by Banach [58] and concerning the properties of continuous operators in metric spaces will now be introduced, bearing in mind consideration of the numerical solution of the integral equation 5.1.9.

Theorem

If a contraction operator U maps a complete metric space X into itself, then we have a unique fixed point and this point can be obtained by the method of successive approximation from any point $X_0 \in X$. The contraction operator U given in the metric space X is defined such that a positive constant $\alpha < 1$ exists for any $x', x'' \in X$ where

$$\rho(Ux', Ux'') \leq \alpha \rho(x', x'')$$

$\rho(x', x'')$ defines the "distance" between x' and x''. The fixed point x^* is defined by the condition $Ux^* = x^*$. This theorem can be applied directly to the numerical solution of the integral equations discussed previously by defining the metric space X as the complete set of positive functions with the property

$$\lim_{|\xi| \to \infty} f(\xi) = 0$$

The distance between any two functions f', f'' can be defined as

$$\rho(f', f'') = \text{Max} \, | f' - f'' |$$

Consequently, if the metric distance between successive iterates is monotonically decreasing, the theorem above proves that convergence to a unique fixed point is obtained.

The reason for introducing this theorem is twofold: Firstly, the uniqueness of the solution to the Boltzmann equation can be proved numerically irrespective of the linearity of the kernel of the chosen integral equation; and secondly, the rate of convergence of the iterative process can quickly be ascertained. By consideration of the drift velocity or average energy of the successive distribution functions generated by the integral equation 5.1.10, it may take time to decide whether the process is convergent or weakly divergent, and it is of some importance that Γ be chosen as small as is consistent with generating a steady state convergent solution. Otherwise a great deal of unnecessary computational effort will be involved. However, the application of the above theorem readily gives the rate of convergence after some few iterations.

The remaining sections of this chapter will be concerned with the application of the theoretical methods discussed in this section to InSb.

5.2 Time Dependent and Time Independent Solutions for n-InSb at 77°K

Rees' method for solving the Boltzmann equation given by 5.1.10 will now be applied to InSb for combinations of the scattering mechanisms discussed in Chapter 4. The calculations presented in Chapter 3, which gave a good qualitative account of the main features of the transport properties of InSb, were based on an approximate method. Evidence was provided for the strength of the coupling constants for the different scattering mechanisms, and, as a consequence, the values of certain material constants of InSb. It is convenient to choose these values for the exact solution of the Boltzmann equation for InSb.

Recent experimental evidence [59,60] suggests that at very high fields the effects of intervalley scattering become significant. In previous calculations concerning intervalley scattering and the transport properties of GaAs [61,63] the application of the drifted Maxwellian approach has proved unsatisfactory when comparison with more exact calculations is made. (A more detailed discussion will be presented in section 5.3). However, since the approach discussed in section 5.1 is essentially exact, intervalley scattering can be included with confidence. A Monte-Carlo calculation recently reported by Fawcett and Ruch [62] on InSb has included these effects: The material constants for describing the higher valleys and intervalley scattering which this calculation was based on will also be used here, and the constants for the central (000) valley as described previously.

The application of Rees' iterative method can conveniently be performed in two stages. Firstly, the appropriate collision integral can be evaluated leading to

$$g(\underset{\sim}{k}) = [\Gamma - \lambda(\underset{\sim}{k})] f(\underset{\sim}{k}) + \int f(\underset{\sim}{k}') P(\underset{\sim}{k}', \underset{\sim}{k}) d\underset{\sim}{k}' \qquad 5.2.1$$

and secondly, the resulting function is projected along the collision free trajectory of a carrier, followed by an additional integration

$$f(\underset{\sim}{k}) = \int_0^\infty e^{-\Gamma t} g(\underset{\sim}{k} - \frac{e t}{\hbar} \underset{\sim}{E}) \, dt. \qquad 5.2.2$$

The inclusion of the effects of band structure non-parabolicity to the evaluation of equation 5.2.1 have been given in Chapter 4. Its inclusion for equation 5.2.2 will now be discussed.

In evaluating the collision integrals of Chapter 4 it was found convenient to define the distribution function as $f(\underline{k}) = f(E,\cos\gamma)$. Consequently to perform the operation defined by equation 5.2.2 it is necessary to find expressions for E' and $\cos\gamma'$, where

$$g(\underline{k} - \frac{e\xi}{\hbar}\underline{F}) = g(E',\cos\gamma')$$

For the band structure $k^2 = F(E)$,

$$F(E') = (\underline{k} - \frac{e\xi}{\hbar}\underline{F}) \quad , \text{ and } \cos\gamma' = \hat{k}_F \cdot (\underline{k} - \frac{e\xi}{\hbar}\underline{F})$$

Therefore

$$F(E') = F(E) - 2\sqrt{F(E)}\,\frac{e\xi F}{\hbar}\cos\gamma + \left(\frac{e\xi F}{\hbar}\right)^2 \qquad 5.2.3$$

and

$$\cos\gamma' = \left(\sqrt{F(E)}\cos\gamma - \frac{e\xi F}{\hbar}\right)/\sqrt{F(E')}$$

To solve equation 5.2.3 the inverse of the function $F(E')$ must be known and it may be necessary to do this numerically. However, the calculations of Chapter 3 show that a good approximation to the band structure of InSb is given by

$$F(E) = 2m^*E(1 + E/G)/\hbar^2$$

which has an inverse

$$E = \frac{G}{2}\left(\sqrt{1 + \frac{4\hbar^2 F(E)}{2m^* G}} - 1\right). \qquad 5.2.4$$

The solution of equation 5.2.3 is obtained by substitution. A brief description of the numerical solution of the problem described above will now be given.

A representative programme is listed in Appendix 2 which calculates the polar mobility, including the full effects of the lattice periodicity, for InSb at 77°K and a field of 10^4 V/m. The distribution function was given by a matrix of 500 points in the $(E, \cos\gamma)$ plane to produce an accuracy of greater than 1% for the corresponding drift velocity and average energy. The integration over the phonon field parameters q and ϕ were evaluated using a 10 step Gaussian integration method for each, taking the appropriate values for the distribution function using a three point Lagrange interpolation formula. No interpolation over the energy is necessary since the original values for the distribution function were judiciously chosen as integral fractions of the phonon energy. The final stage of the iterative process described by equation 5.2.2 was accomplished by using a 20 step Gaussian integration method for ξ over an appropriate range,

and using a six point bivariate interpolation formula on the logarithm of the distribution function. This part of the calculation is very much quicker than the first part, and the accuracy of the resultant drift velocity and average energy is greater than 2% over the whole calculation. In Appendix 2 the first listing shows the variation of drift velocity and average energy of the electrons as they evolve from thermal equilibrium to the steady state value for 10^4V/m. It was necessary to choose a small value of $1/\Gamma$ initially corresponding to 0.2 picoseconds in order to obtain convergence, but a larger value of 0.75ps was possible when the distribution function was nearer the steady state solution. A convenient way of making the convergence process more rapid can be obtained by choosing an appropriate distribution function near the expected solution. In the example given by the second listing shown in Appendix 2 an exact drifted Maxwellian distribution function with an average energy and drift velocity close to the expected solution was chosen, resulting in rapid convergence. The uniqueness of the solutions for the two above calculations is evident from the distance between successive iterates through consideration of Banach's theorem stated in the previous section of this chapter. To include the effects of intervalley scattering, which will now be discussed, it was necessary to improve the efficiency of the above programme.

Table 2

	(000) valley	⟨111⟩ valleys
m^*	0.013m	0.2m
Acoustic deformation potential	7.2eV	10eV
Optical deformation potential	0	1×10^{11}eV/m
Band Gap	0.23eV	
Spin orbit splitting of valence band	∞	
Static dielectric constant	15.68	
High frequency dielectric constant	17.50	
Debye temperature	278°K	
Crystal density	5.79×10^3 Kg/m^3	
Sound velocity	3.7×10^3 m/s	
Lattice spacing	6.48Å	

Table 2 lists the material constants for the central (000) valley and the four satellite ⟨111⟩ valleys for InSb used in the calculations which follow. The intervalley scattering process was assumed to take place between inequivalent valleys by interaction with longitudinal acoustic phonons at the ⟨111⟩ edge of the B.Z. with an energy of 12.7meV [64,65]. The ⟨111⟩ valley was assumed to be 0.45eV above the conduction band edge, and the intervalley coupling constant was taken as 5×10^{10} eV/m. Plot 1, Fig. 12 shows the drift velocity field characteristic for the model described. Plot 2 and the points (⊛) of Fig. 12 indicate the theoretical calculation by Fawcett and Ruch [62] and the experimental results by Neukerman and Kino [45]. Fig. 13 shows the average electron energy (bold line) and the fraction of electrons in the (000) valley (dotted line) for InSb at 77°K. The strength of the scattering by the polar phonon field resulting from the material constants of InSb chosen by Fawcett and Ruch is greater than in the present calculation and produces a lower population of the higher valleys. Convergence of the iterative process is slow at low fields but the low field mobility is estimated to be about 1.8×10^{2} m²/V-s.

Figs. 14 and 15 show the first four terms of the spherical harmonic expansion of the distribution function corresponding to fields 1×10^{4} V/m and 5×10^{4} V/m respectively. The Legendre functions are normalised such that $P_n(1) = 1$. At a field of 1×10^{4} V/m the distribution function is streamed in the direction of the field as would be expected since the average carrier energy is about the same as the polar phonon energy. The change in slope of the spherically symmetric part of the distribution function is due to the onset of polar phonon emission. At high fields the carrier energy increases with respect to the polar phonon energy, and the higher terms in the spherical harmonic expansion begin to decrease as can be seen in Fig. 15. The average carrier energy is still only seven times the polar phonon energy at 5×10^{4} V/m. At energies above 0.45eV the distribution function rapidly decreases due to intervalley transfer.

The inclusion of electron-electron scattering was considered in the above calculation for the spherically symmetric part of the distribution function. It was found to have a small effect of the order of a few percent for carrier concentrations in the range 10^{19}–10^{20} m^{-3} and was subsequently ignored. This conclusion was also reached by Rees [6].

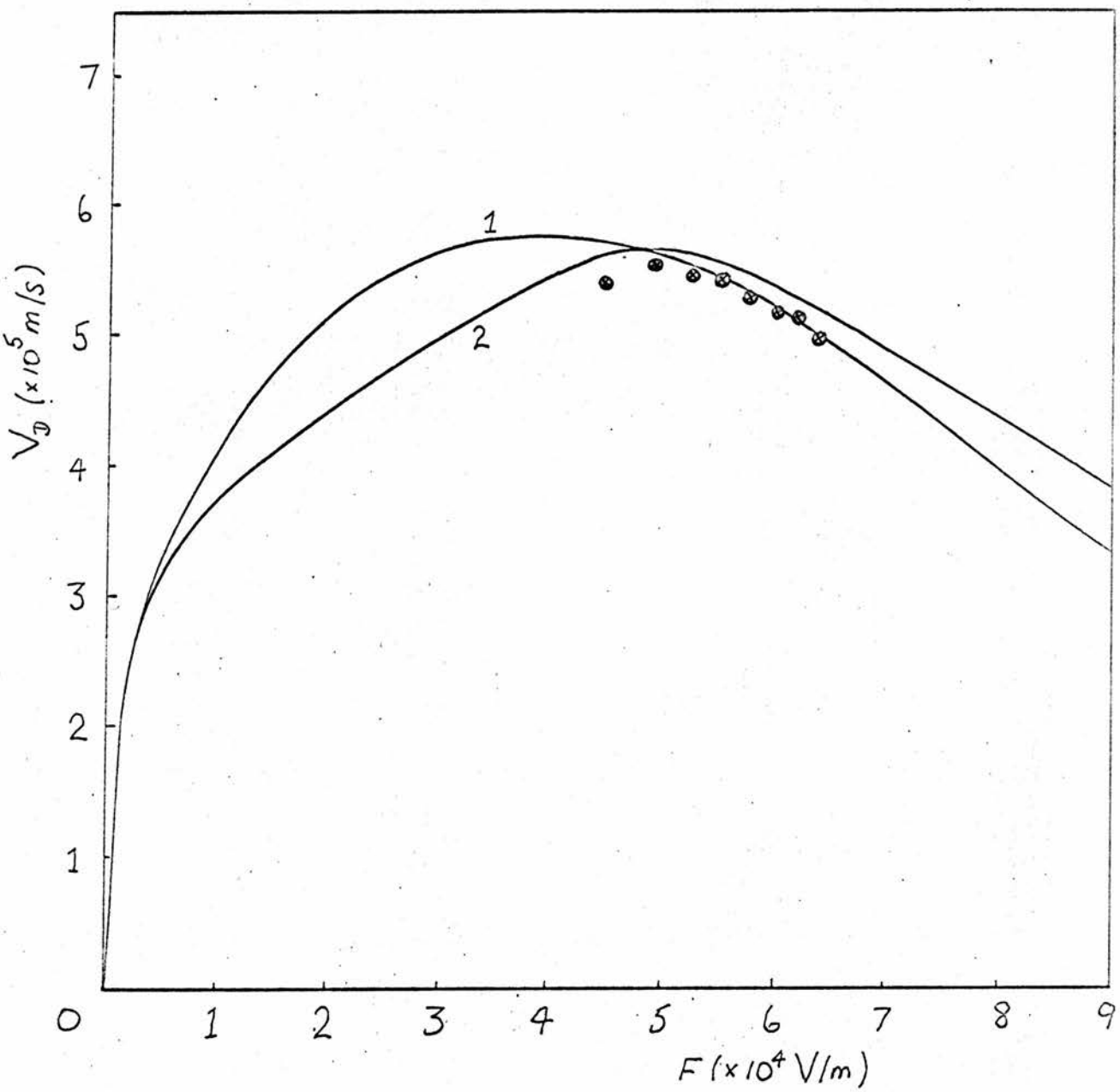

FIG. 12

The variation of drift velocity with field for InSb at 77°K for the present calculation in plot 1, and in a similar calculation by Fawcett and Ruch [62] in plot 2. The experimental points (⊛) are given by Neukerman and Kino [45]. ($E \parallel [100]$)

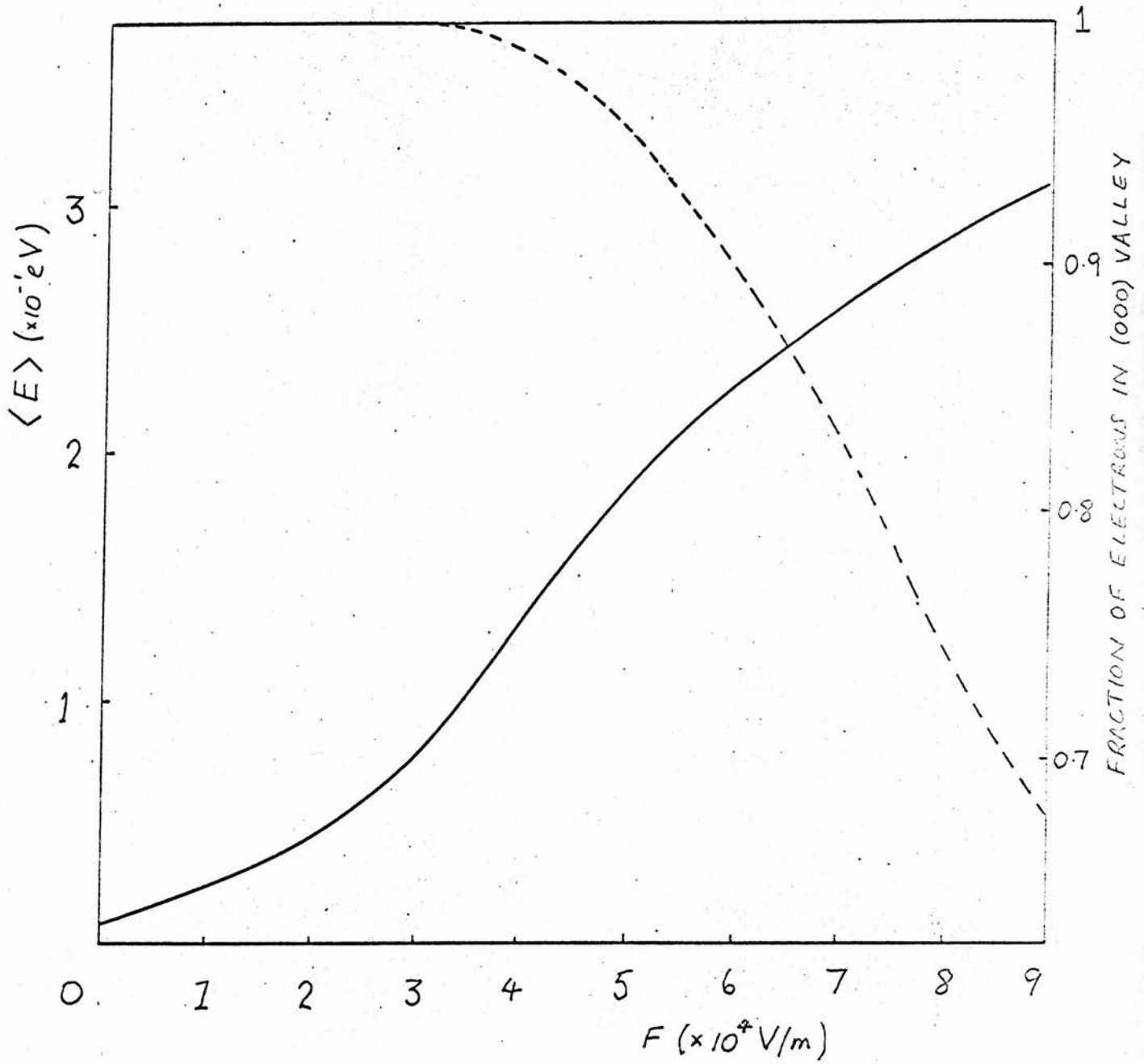

FIG. 13

The variation of average electron energy (bold line) and fraction of electrons in the (000) valley (dotted line) with field for InSb at 77°K.

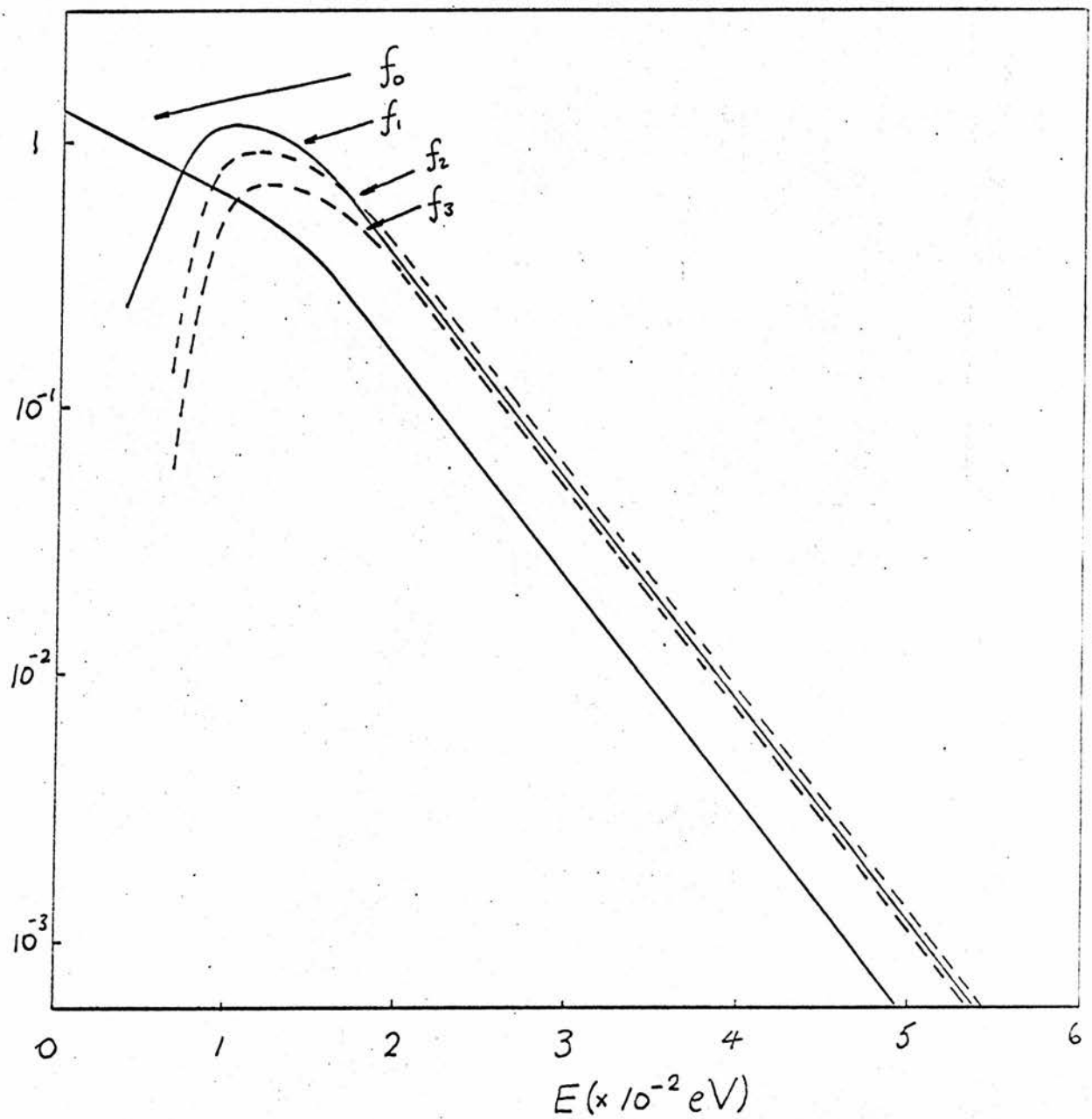

FIG. 14

The spherical harmonic expansion of the distribution function for a field of 10^4 V/m for InSb at 77° K.

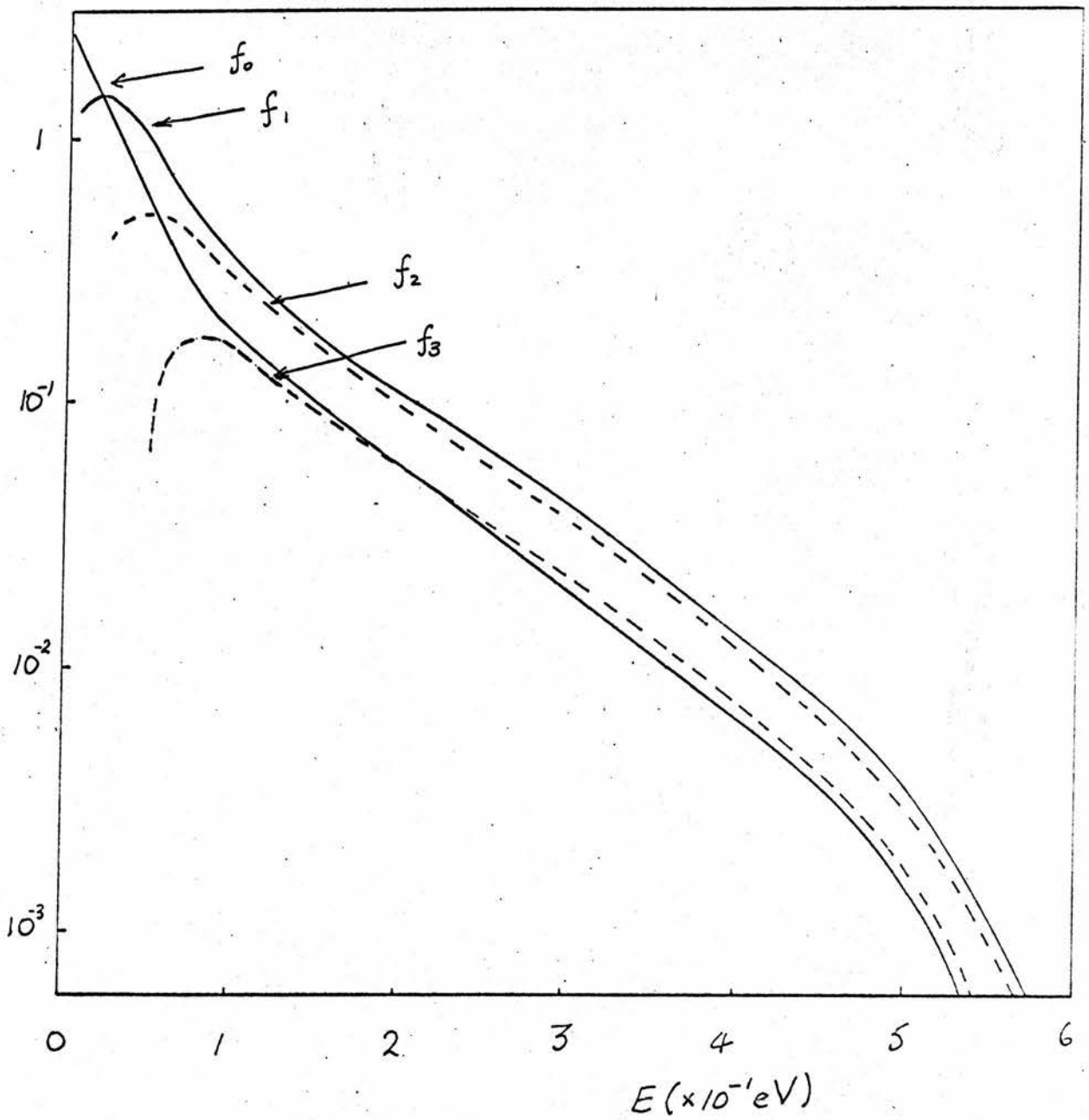

FIG. 15

The spherical harmonic expansion of the distribution function for a field of 5×10^4 V/m for InSb at 77° K.

By choosing a suitably large value of Γ the time evolution of the distribution function can be obtained from equation 5.1.10. Appendix 2 lists the time evolution of the drift velocity and average carrier energy for a field of 1×10^4 V/m. This is represented by plot 2, Figs. 16 and 17. Plots 1 and 3, Figs. 16 and 17 show the drift velocity and average energy evolution for the application of fields 1×10^3 V/m and 4×10^4 V/m; only polar scattering has been included for convenience. As has been pointed out by Rees, at higher fields the carrier drift velocity overshoots its steady state value, reaches a maximum value and then decreases. The approach to the steady state at the lowest field is slow.

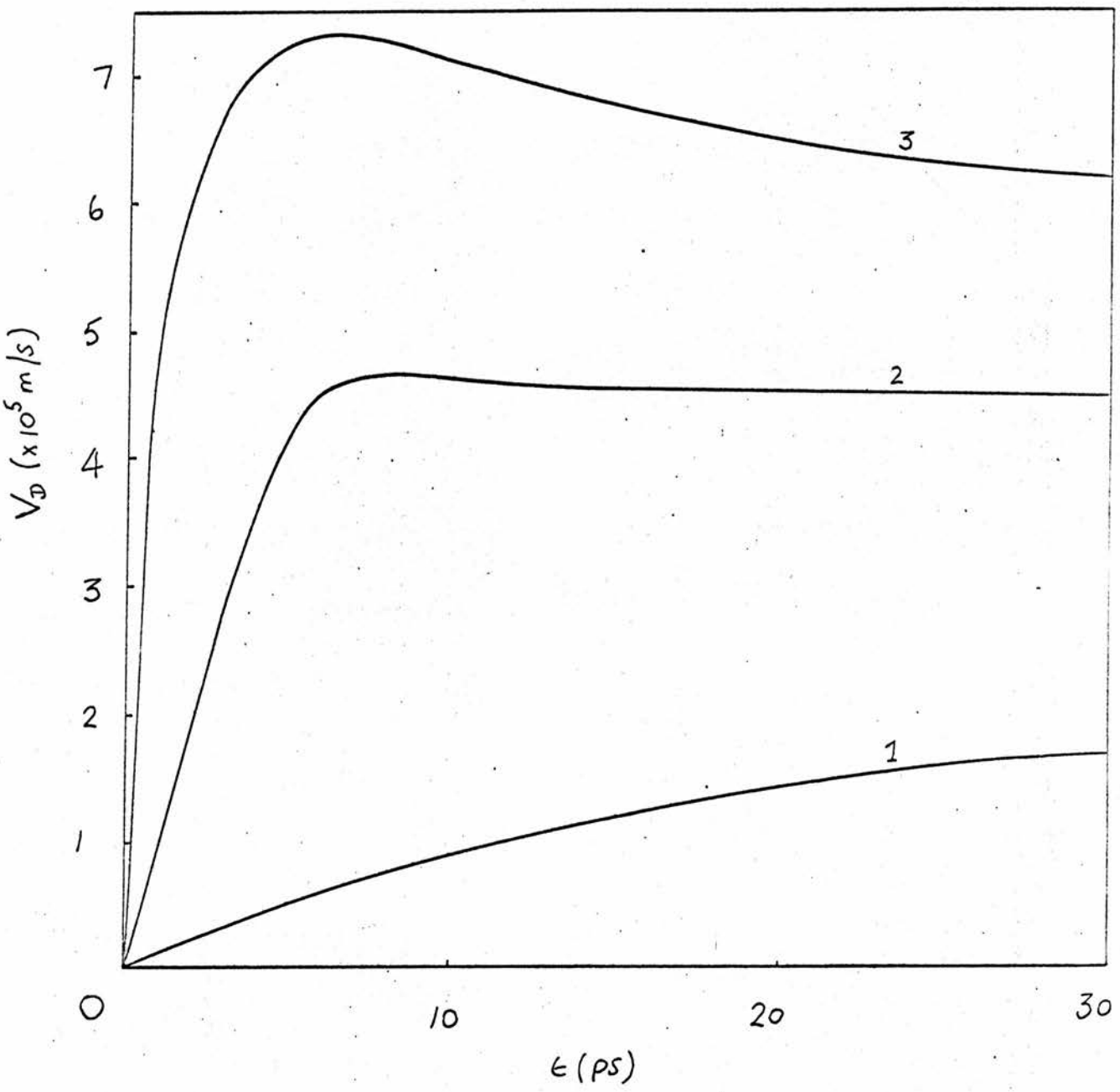

FIG. 16

The evolution of the drift velocity in time for electrons in InSb at 77°K for fields of 10^3 V/m, 10^4 V/m, and 4 x 10^4 V/m in plots 1, 2, and 3 respectively. Only polar scattering is included.

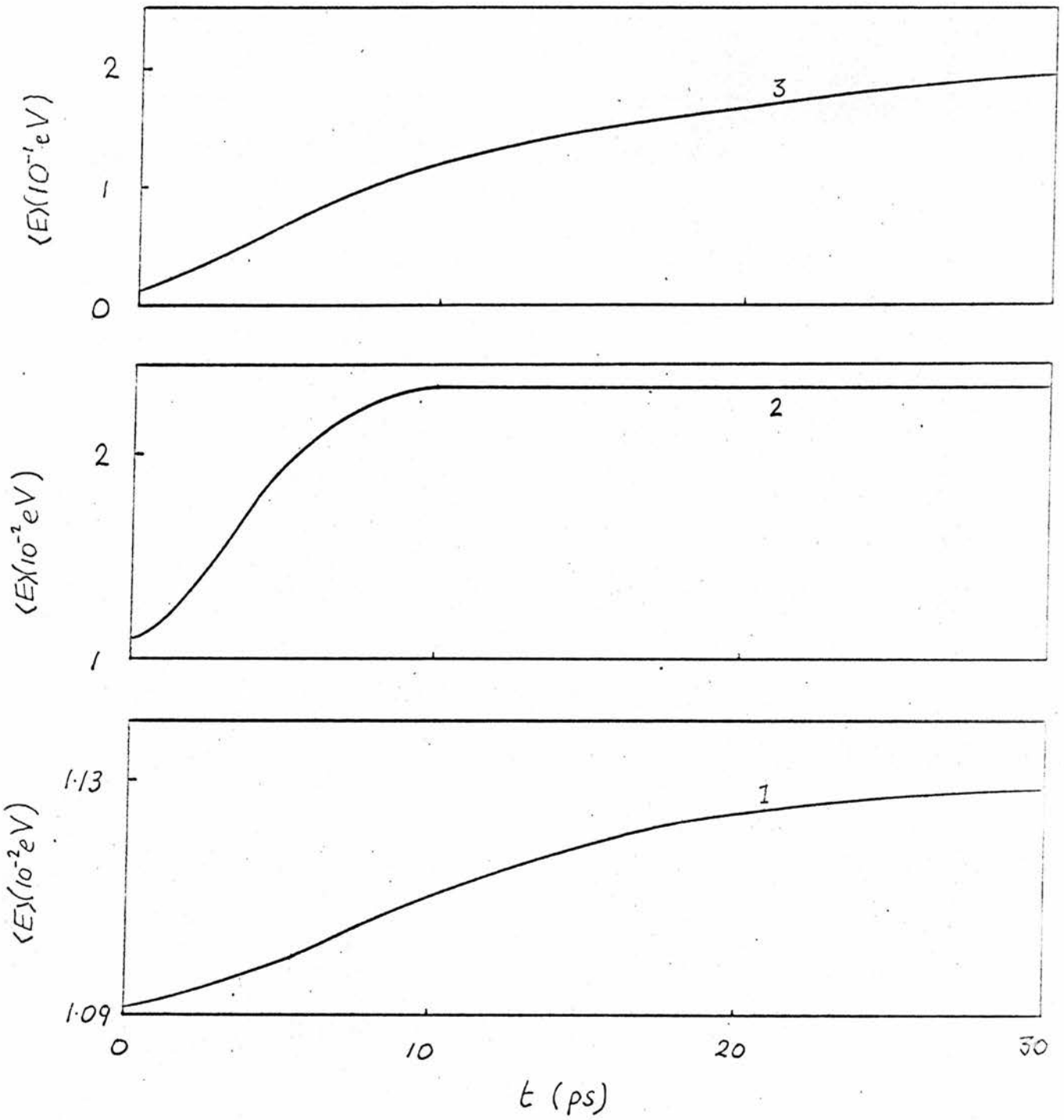

FIG. 17

The evolution of the average energy in time for electrons in InSb at 77°K for fields of 10^3 V/m, 10^4 V/m, and 4 x 10^4 V/m in plots 1, 2, and 3 respectively. Only polar scattering is included.

5.3 Comparison of the Drifted Maxwellian Approach with the Boltzmann Solution

The solution of a particular problem by the drifted Maxwellian approach is considerably easier than by the exact methods previously discussed, and consequently has some value for qualitative or perhaps semiquantitative analysis. It is estimated that the computational effort involved in satisfying the one dimensional simultaneous equations for the drifted Maxwellian solution is about two or three orders of magnitude easier than the integral equation methods. Consequently it is of considerable interest to discuss the limitations of the former approach through comparison with the exact Boltzmann solution.

The drift velocity-field characteristic, including polar scattering only and the full effects of the lattice periodicity, are shown for the solution of Boltzmann's equation in plot 1, Fig. 18, and for the drifted Maxwellian solution in plot 2, Fig. 18. The material constants for InSb at 77°K are those discussed previously. It can be shown that the agreement for fields between 1 and 4×10^4 V/m is very good, the two solutions differing by only 10%; at higher fields the difference increases somewhat. The mobility for the Boltzmann solution at low fields is estimated to be about 1.9×10^2 $m^2/V\text{-}s$; the drifted Maxwellian approach is about 40% lower. This large difference can be understood by considering the onset of polar phonon emission: At low fields the average electron energy is about half the polar phonon energy, thus the polar phonon emission produces a rapid decrease in the exact distribution function at higher energies. The corresponding drifted Maxwellian solution attempts to approximate the rapidly varying function by a smoothly varying function. This produces a corresponding inaccuracy in the resulting mobility. At higher fields the average electron energy increases, and the exact distribution is able to accommodate the onset of polar phonon emission. Consequently, as can be seen from Figs. 14 and 15, the distribution function varies less rapidly and the drifted Maxwellian is more able to represent the Boltzmann solution.

In plots 1 and 2, Fig. 19, the average energy and field are given for the exact and drifted Maxwellian solution for carriers scattered by polar phonons in InSb as discussed above. Very good agreement between the two theories is obtained. The reason for this is because at energies above the onset of polar phonon emission the corresponding

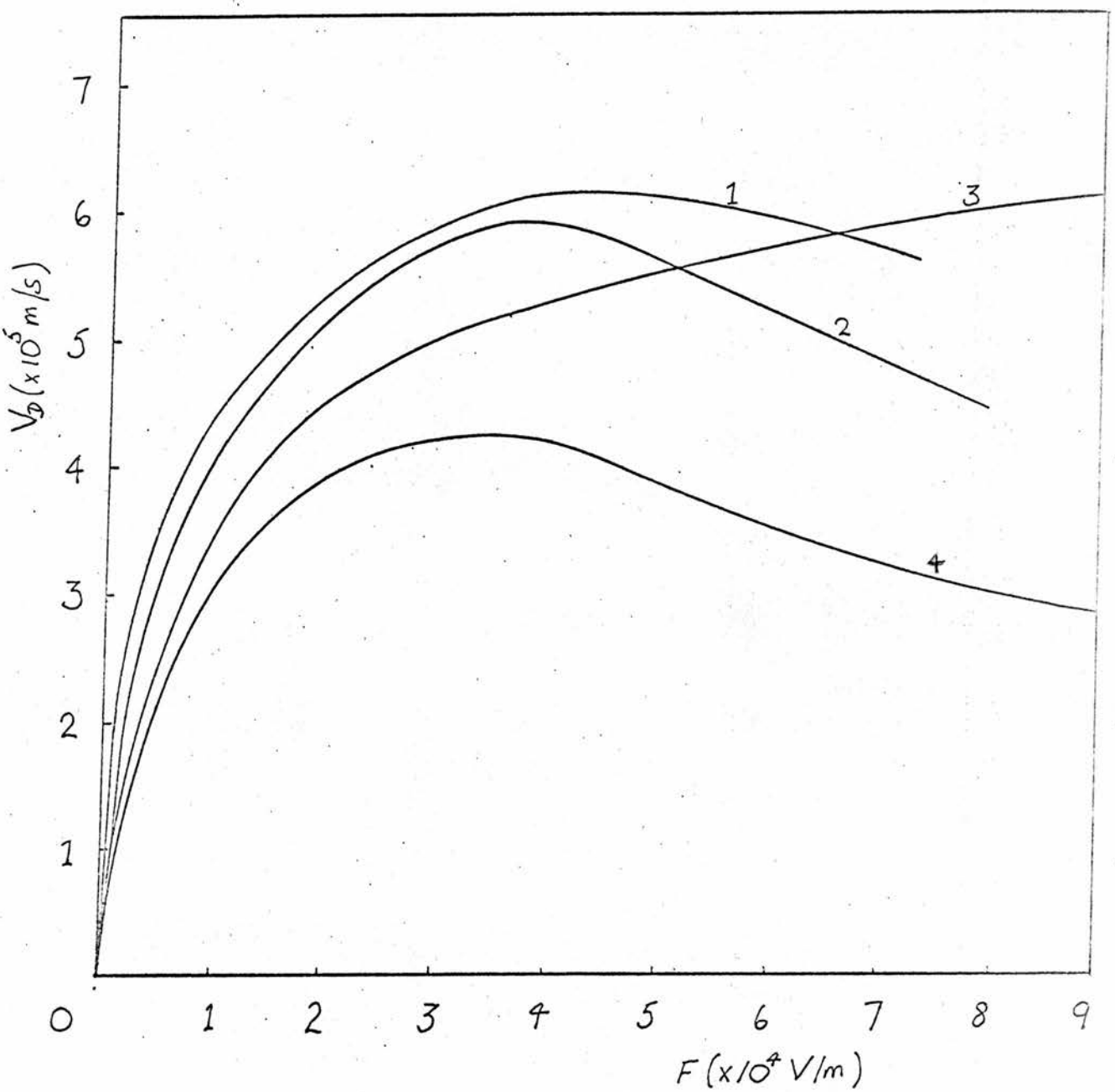

FIG. 18

The variation of drift velocity with field for InSb at 77°K is given for the exact calculation in plot 1 and the corresponding drifted Maxwellian calculation in plot 2, with the exclusion of acoustic and intervalley scattering. Plots 3 and 4 are the same calculation as for plots 1 and 2 but with the inclusion of acoustic scattering with a deformation potential of -30eV.

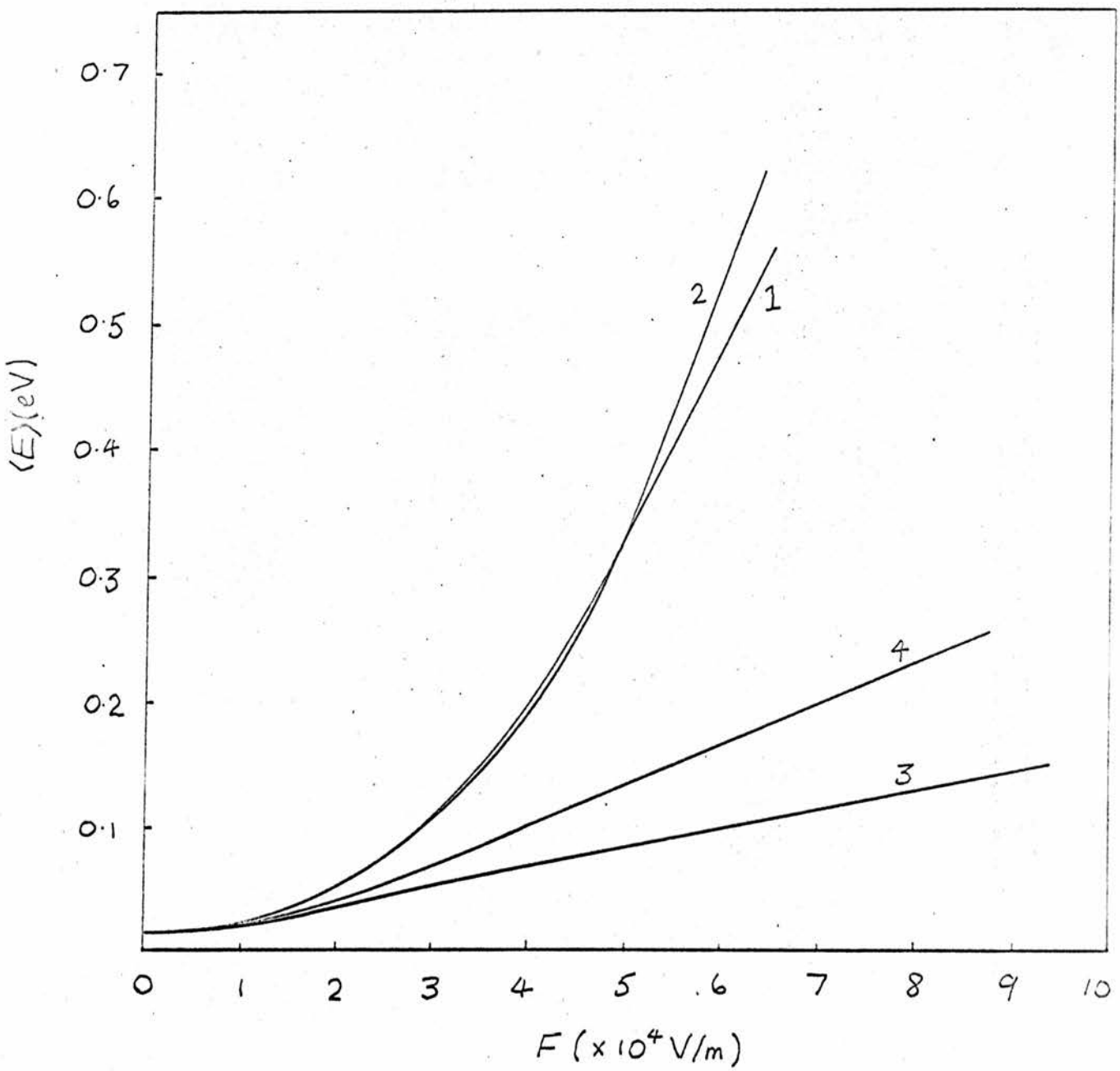

FIG: 19

The variation of the average energy with field for InSb at 77°K is given for the exact calculation in plot 1 and the corresponding drifted Maxwellian calculation in plot 2, with the exclusion of acoustic and intervalley scattering. Plots 3 and 4 are the same calculation as for plots 1 and 2 but with the inclusion of acoustic scattering with a deformation potential of -30eV.

relaxation time is given by a slowly varying function, as can be seen from equation 2.2.20, and since the average carrier energy depends directly on the spherically symmetric part of the distribution function which is least affected by the detailed peculiarities of the distribution function, the drifted Maxwellian is able to give a good approximation to the exact solution. Fig. 20 compares the spherically symmetric parts of the distribution functions corresponding to the exact solution for plot 1, and the drifted Maxwellian solution in plot 2, at a field of 5×10^4 V/m. The average energy for the two functions is close, but the detailed form is different. This is due to the weakening of polar scattering at high energies as has been discussed by Fawcett et al [63] in connection with intervalley scattering, and the inadequacies of the drifted Maxwellian approach to represent the inclusion of these effects.

Plots 3 and 4, Figs. 18 and 19, describe the properties of the above system for InSb, with the inclusion of acoustic phonon scattering taking a deformation potential of -30eV, for the exact and drifted Maxwellian solutions respectively. Reasonable agreement exists between the two treatments up to about 3×10^4 V/m, and the low field mobility for the exact solution is estimated to be 1.0×10^2 m^2/V-s, and the corresponding drifted Maxwellian solution about 30% less. However, the solutions at higher fields are very different. It can be seen from equation 2.3.8 that the relaxation time for acoustic scattering rapidly decreases with increasing energy. From the above discussion this is precisely a situation in which the drifted Maxwellian distribution function has difficulty representing the exact solution. Consequently the drifted Maxwellian treatment overestimates the average electron energy at high fields.

Interpretation of the inadequacies of the drifted Maxwellian theory is not straightforward since the resulting solution depends simultaneously on the average energy loss and the average momentum loss of the carriers. However, some insight into the nature of the approximation can be obtained by a detailed study of the relaxation mechanisms present as indicated above. The solution of more realistic models for semiconductors involving spatial inhomogeneity for example, cannot be solved by the iterative method discussed here at the present time, since it

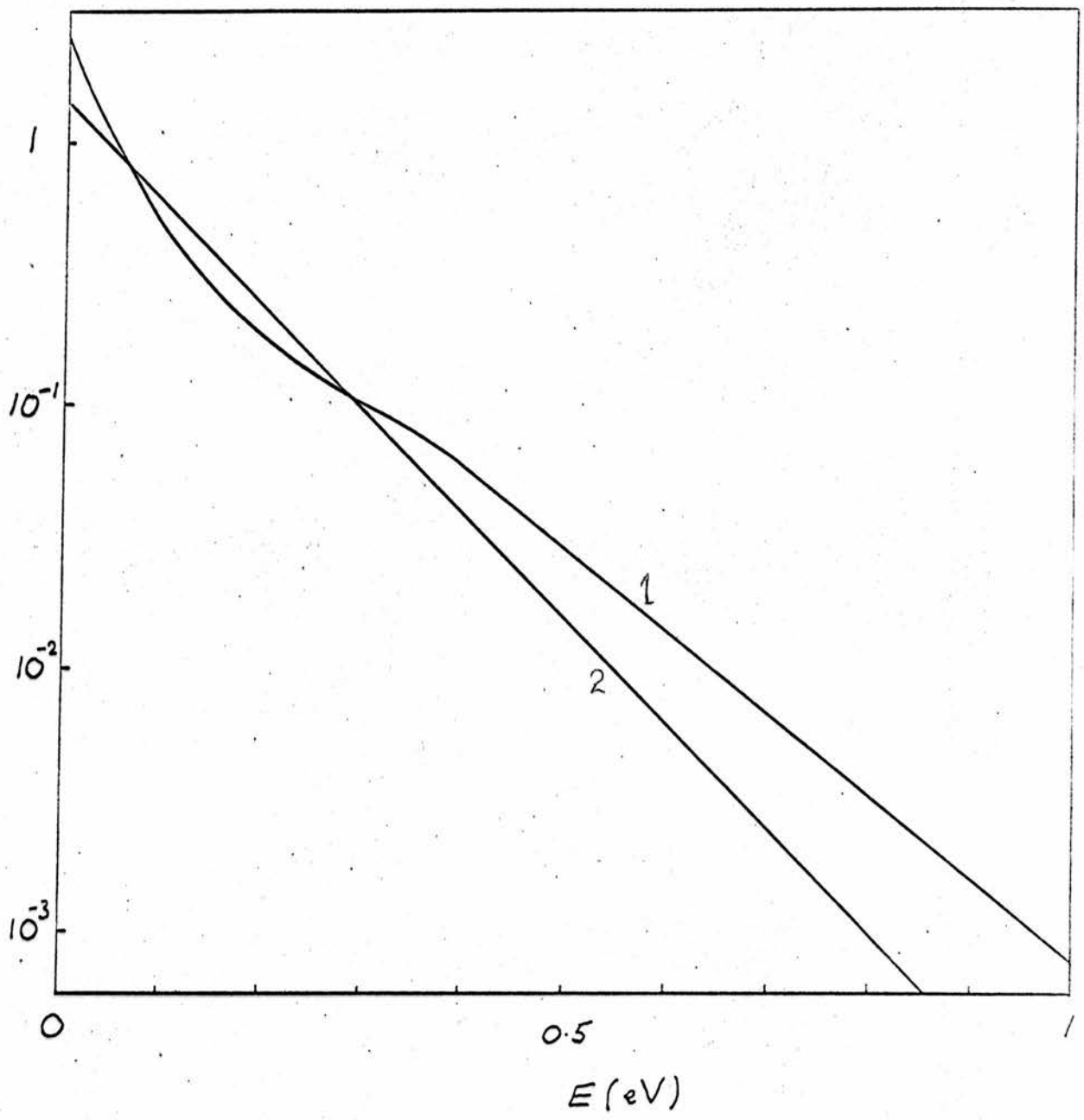

FIG. 20.

The spherically symmetric part of the distribution function for electrons scattered by polar phonons in InSb at 77°K for an exact calculation in plot 1, and the corresponding drifted Maxwellian calculation in plot 2.

would involve at least an order of magnitude more computation than can reasonably be carried out by existing computers. The application of a set of drifted Maxwellian distribution functions suitably modified to represent the corresponding spatially homogeneous Boltzmann solutions could prove a useful starting point for such a calculation.

APPENDIX 1

A summary of the relevant results from Kane's [19] $\underset{\sim}{k}.p$ band structure calculation of InSb will now be given.

Equation 10 of Kane's paper gives the functional form of the conduction band of InSb as

$$\frac{\hbar^2 k^2}{2m^*} = \frac{E'(E'+G)(E'+G+\Delta)(G+\frac{2}{3}\Delta)}{G(G+\Delta)(E'+G+\frac{2}{3}\Delta)} \qquad \text{A1.1}$$

where $E' = E - \hbar^2k^2/2m^*$, G is the band gap, Δ the spin orbit splitting of the valence band, m^* the effective mass at the centre of the B.Z., and m the free electron mass. Since $E \sim \hbar^2k^2/2m^*$ and $m^* \sim 0.013m$ it is a good approximation to replace E' by E in equation A1.1. The coefficients for the inclusion of the terms arising from the mixing of Bloch states and spin-reversal scattering are given by equation 15 in Kane's paper and can be written as

$$\left.\begin{aligned} a_k &= \frac{kP(E+G+2\Delta/3)}{\sqrt{(k^2P^2+E^2)(E+G+\frac{2}{3}\Delta)^2 + 2\Delta^2E^2/9}}, \\ b_k &= \frac{\sqrt{2}\,\Delta E/3}{\sqrt{(k^2P^2+E^2)(E+G+\frac{2}{3}\Delta)^2 + 2\Delta^2E^2/9}}, \end{aligned}\right\} \qquad \text{A1.2}$$

and

$$c_k = \frac{E(E+G+2\Delta/3)}{\sqrt{(k^2P^2+E^2)(E+G+\frac{2}{3}\Delta)^2 + 2\Delta^2E^2/9}},$$

where

$$k^2P^2 = \frac{E(E+G)(E+G+\Delta)}{(E+G+2\Delta/3)} .$$

The spin orbit splitting for InSb $\Delta \sim 1eV$, and a reasonable approximation for equations A1.1 and A1.2 arise from the assumption $E, G \ll \Delta$. This leads to

$$\frac{\hbar^2k^2}{2m^*} = E(1+E/G),$$

and

$$\left.\begin{aligned} a_k &= \sqrt{(1+E/G)/(1+2E/G)}, \\ b_k &= \sqrt{E/(3(G+2E)} = c_k/\sqrt{2} . \end{aligned}\right\} \qquad \text{A1.3}$$

To incorporate the effects of equations A1.3 for the case of acoustic phonon scattering it is necessary to replace E by $E \pm \hbar u q$ and expand the resulting function to first order in $\hbar u q$. Thus, taking $X = E/G$,

$$a_{k'} = \sqrt{\frac{1+X}{1+2X}}\left(1 \mp \frac{\hbar u q}{2G(1+X)(1+2X)}\right),$$

$$b_{k'} = \sqrt{\frac{X}{3(1+2X)}}\left(1 \pm \frac{\hbar u q}{2GX(1+2X)}\right),$$

and

$$c_{k'} = \sqrt{\frac{2X}{3(1+2X)}}\left(1 \pm \frac{\hbar u q}{2GX(1+2X)}\right).$$

Therefore

$$\beta(k,k') = \frac{1}{(1+2X)^2}\left(1+2X+\frac{5}{4}X^2 \mp \frac{\hbar u q\,(1+\frac{3}{4}X)}{G(1+2X)}\right) = A \pm \hbar u q\, B,$$

$$\rho(k,k') = \frac{2X(1+X)}{(1+2X)^2}\left(1 \mp \frac{\hbar u q}{2GX(1+2X)(1+X)}\right) = C \pm \hbar u q\, D,$$

and

$$\alpha(k,k') = \frac{3X^2}{4(1+2X)^2}\left(1 \pm \frac{\hbar u q}{GX(1+2X)}\right) = G \pm \hbar u q\, H,$$

in the notation previously defined. It is straightforward to obtain the factors resulting from the inclusion of lattice periodicity.

APPENDIX 2

PROGRAMME FOR CALCULATING THE POLAR MOBILITY OF INSB AT HIGH ELECTRIC FIELDS.

```
      DIMENSION WG(12),F(3),DF(3),GM(16),GN(16),BF(40,15),AA(3),BB(3),
     1WN(20),EN(20)
      COMMON BG(40,15), BT(40,15), WY(45), GG(15),WX(40),WZ(40)
      READ(5,101) (GN(I),WG(I),I=2,11)
      READ(5,103) (WY(I),WY(16-I),I=1,8)
      READ(5,104) (WX(I),WX(I+1),I=2,10,2)
      READ(5,105) (EN(I),WN(I),I=1,20)
      PI=3.1416
      GAMMA=1./0.2E-12
      N=6
      DO 5 I=1,15
      GG(I)= -1.+(I-1)/7.
      GM(I+1)=COS(PI/2.*(1.-GN(I+1)))
    5 CONTINUE
      DO 6 I=1,15
      WX(   I)=WY(I)
    6 CONTINUE
      DO 77 I=1 ,15
      WY(30-I)=WY(I)
      WY(28+I)=WY(I)
   77 CONTINUE
      WY(15)=2.*WY(15)
      WY(29)=WY(29)*2.
      THETA=2.78E+2
      EM=0.13E-1
      T=7.7E+1
      EG=2.3E-1
      TEX=EXP(THETA/T)
      FIN=5.093E+8*THETA*SQRT(EM)/(TEX-1.)
      VD=0.
      ELEC=1.E+4
      TEMP=7.7E+1
      C1=1./(8.617E-5*TEMP)
      B1=3.37E-6*SQRT(EM)
      D2=4./EG
      C2=3.37E-6*C1*VD*SQRT(EM)
      A=8.617E-5*THETA
      C3=1.
      C5=3.37E-6*SQRT(EM)*VD
      AZ=7.
  100 FORMAT (15E12.4)
  977 FORMAT (E12.4)
  101 FORMAT (2E12.4)
  103 FORMAT(2F10.7)
  104 FORMAT (2F10.7)
  105 FORMAT (2F9.6)
  106 FORMAT (1X,'THE VALUE OF GAMMA IS',E12.4)

      TABULATION OF TRIAL FUNCTION

      DO 7 I=1,30
      E=(I-1)*A/N
```

```
      XX=EXP(-E*C1)*C3
      XY=SQRT(E+E*E/EG)*C2
      DO 9 J=1,15
      BT(I,J)=XX*EXP(XY*GG(J))
    9 CONTINUE
    7 CONTINUE
      TEM=EXP(THETA/TEMP)
      TEMX=EXP(THETA/(N *TEMP))
      LL=1
      CALL VELO(LL,B1,EG,A,N)

      MAIN PROGRAMME

      NN=29+N
      DO 3 KK=1,2
      TD=ELEC/GAMMA/B1
      WRITE (6,106) GAMMA
      DO 999 LL=2,25
      DO 98 J=1,15
      IU=29+N
      DO 99 I=30,IU
      BG(I,J)=BG(29,J)/TEMX**(I-29)
   99 CONTINUE
   98 CONTINUE
      DO 15 I=2,29
      E=(I-1)*A/N
      IF (I.GT.N+1) GOTO 17
      IN=2
      GOTO 19
   17 IN=3
   19 E=E+A
      DO 21 M=1,IN
      F(M)=E+E*E/EG
      DF(M)=1.+2.*E/EG
      SF=SQRT(1.+E/EG)
      SDF=SQRT(DF(M))
      AA(M)=SF/SDF
      BB(M)=SQRT(E/(3.*EG))/SDF
      E=E-A
   21 CONTINUE
      F1=F(1)
      F2=F(2)
      A1=SQRT(F1)
      A2=SQRT(F2)
      A5=2.*A1*A2
      F4=(F1-F2)/(2.*F2)
      AP=AA(1)*AA(2)
      AP2=AP*AP
      BP=BB(1)*BB(2)
      BP2=BP*BP
      ALP=AP2+2.25*BP2
      BEP=6.*AP*BP
      GAP=6.75*BP2
      FAP=(F1+F2)/A5
      FAP2=FAP*FAP
```

```
      DEP=(ALP+FAP*BEP+FAP2*GAP)
      EPP=(BEP+2.*FAP*GAP)/A5
      ZEP=GAP/(4.*F1*F2)
      TR1=DF(1)*(DEP*ALOG((A2+A1)/(A1-A2))-A5*(EPP-A5*FAP*ZEP))
      TR3=0.
      H1=A2/A1
      Z1=DF(1)*PI*TEX
      IT=I+N
      IF (IN.LT.3) GOTO 23
      F3=F(3).
      A3=SQRT(F3)
      A6=2.*A2*A3
      F5=(F3-F2)/(2.*F2)
      AN=AA(2)*AA(3)
      AN2=AN*AN
      BN=BB(2)*BB(3)
      BN2=BN*BN
      ALN=AN2+2.25*BN2
      BEN=6.*AN*BN
      GAN=6.75*BN2
      FAN=(F2+F3)/A6
      FAN2=FAN*FAN
      DEN=ALN+FAN*BEN+FAN2*GAN
      EPN=(BEN+2.*FAN*GAN)/A6
      ZEN=GAN/(A6*A6)
      TR3=TEX*DF(3)*(DEN*ALOG((A2+A3)/(A2-A3))-A6*(EPN-A6*FAN*ZEN))
      H3=A2/A3
      Z2=DF(3)*PI*A3/A2
      ID=I-N
   23 REL=2.*PI/A2*(TR1+TR3)
   30 DO 25 J=1 ,15
      GC=GG(J)
      GS=SQRT(1.-GC*GC)
      SUL1=0.
      SUL3=0.
      DO 27 L=2,11
      Q1=A2*GN(L)+A1
      QP=DEP/Q1-Q1*(EPP-ZEP*Q1*Q1)
      Q2=Q1*Q1/F2
      R1=F4-0.5*Q2
      R2=SQRT(Q2-R1*R1)*GS*H1
      S1=H1*GC*(1.+R1)
      SUM1=0.
      IF (IN.LT.3) GOTO 29
      Q3=A2+GN(L)*A3
      QN=DEN/Q3-Q3*(EPN-ZEN*Q3*Q3)
      Q4=Q3*Q3/F2
      R3=F5-0.5*Q4
      R4=SQRT(Q4-R3*R3)*GS*H3
      S3=H3*GC*(1.+R3)
      SUM3=0.
   29 DO 33 M=2,11
      GM1=S1-GM(M)*R2
      R =7.0*GM1+8.0
      J1=R
```

```
      R=R-J1
      IF (R.LT.0.5) GOTO 71
      R=R-1.
      J1=J1+1
   71 IF (J1.EQ.1.OR.J1.EQ.15) GOTO 198
      GOTO 199
  198 J1=(8 +6*J1)/7
      R=(1.-ABS(R))*(J1-3)/IABS(J1-3)
  199 RR=R*R
      SUM1=SUM1+WG(M)* ((RR-R)/2.*BG(II,J1-1)+(1.-RR)*BG(II,J1)
     1+(RR+R)/2.*BG(II,J1+1))
      IF (IN.LT.3) GOTO 33
      GM3=S3+R4*GM(M)
      R =7.0*GM3+8.0
      J3=R
      R=R-J3
      IF (R.LT.0.5) GOTO 73
      R=R-1.
      J3=J3+1
   73 IF (J3.EQ.1.OR.J3.EQ.15) GOTO 298
      GOTO 299
  298 J3=(8 +6*J3)/7
      R=(1.-ABS(R))*(J3-3)/IABS(J3-3)
  299 RR=R*R
      SUM3=SUM3+WG(M)* ((RR-R)/2.*BG(ID,J3-1)+(1.-RR)*BG(ID,J3)
     1+(RR+R)/2.*BG(ID,J3+1))
   33 CONTINUE
      SUL1=SUL1+WG(L)*SUM1*QP
      IF (IN.LT.3) GOTO27
      SUL3=SUL3+WG(L)*SUM3*QN
   27 CONTINUE
      BF(I,J)=(Z1*SUL1+Z2*SUL3)*FIN+(GAMMA-REL*FIN)*BG(I,J)
      BF(I,J)=ALOG(BF(I,J)/GAMMA)
   25 CONTINUE
   15 CONTINUE

   PROJECTION ALONG COLLISION FREE TRAJECTORIES

      DO 398 J=1,15
      IU=29+N
      DO 399 I=30,IU
      BF(I,J)=BF(29,J)-A*C1*(I-29)
  399 CONTINUE
  398 CONTINUE
      DO 45 I=2,29
      E=(I-1)*A/N
      F1=E+E*E/EG
      A1=SQRT(F1)
      D1=1./(C1*A1)
      ET=SQRT(E)*2.
   89 DO 47 J=1 ,15
      CC=GG(J)
      XL=AZ*TD
      SUM=0.
      DO 49 NM=1,20
```

```
      TC=XL/2.*(1.+EN(NM))
      GD=F1-2.*GC*A1*TC+TC*TC
      Z=(SQRT(1.+D2*GD )-1.)*EG/2.
      RE=N *Z /A+1.
      I1=RE
      RE=RE-I1
      IF (I1.NE.1) GOTO 50
      RE=RE-1.
      I1=2
      IM=29+N
   50 IF (I1.LT.IM-1) GOTO 51
      I1=IM-1
      RE=1.
   51 GF=(A1*GC-TC)/SQRT(GD)
      I2=I1+1
      RG=7.0*GF+8.0
      J1=RG
      RG=RG-J1
      IF(J1.NE.1) GOTO 58
      RG=RG-1.
      J1=2
   58 IF(J1.NE.15) GOTO 59
      RG=1.
      J1=14
   59 J2=J1+1
      R1=RE/2.
      R2=RG/2.
      R3=RE*RE/2.
      R4=RG*RG/2.
      HF=RE*RG
      SUM=SUM
     1+WN(NM)*       EXP((R3-R1)*BF(I1-1,J1)+(R4-R2)*BF(I1,J1-1)+(1.+HF-2
     2.*(R3+R4))*BF(I1,J1)+(R3+R1-HF)*BF(I2,J1)+(R4+R2-HF)*BF(I1,J2)+HF*
     3BF(I2,J2)-TC/TD)
   49 CONTINUE
      BT(I,J)=SUM*B1/ELEC*XL/2.*GAMMA
   47 CONTINUE
   45 CONTINUE
      CALL VELO(LL,B1,EG,A,N)
  999 CONTINUE
      GAMMA=1./0.75E-12
    3 CONTINUE
      STOP
      END

      SUBROUTINE VELO(L,B1,EG,A,N)

      COMMON BG(40,15), BT(40,15), WY(45), GG(15),WX(40),WZ(40)
      DIMENSION V(100),XLP1(40),XLP2(40),XLP3(40),XLP4(40)
      TX=4.
      NN=21+N
      VEL=0.
      SUM2=0.
  200 FORMAT (I4,4E12.4)
  201 FORMAT (I4,2E12.4,12X,E12.4)
```

```
202 FORMAT(15F8.5)
    SUM3=0.
    SUM4=0.
    DO 5 I=1,29
    E=(I-1)*A/N
    F1=E+E*E/EG
    A1=SQRT(F1)
    DF=(1.+2.*E/EG)*A1
    SUMA=0.
    SUMB=0.
 66 DO 8 J=1 ,15
    ZG=BG(I,J)
    ZF=BT(I,J)
  9 BG(I,J)=ZF
    T=ABS(ZG-ZF)
    WW=WX(J)*ZF
    IF (T.LT.VEL) GOTO 13
    VEL=T
 13 SUMA=SUMA+WW*GG(J)
    SUMB=SUMB+WW
  8 CONTINUE
    IF (L.EQ.1.OR.L.EQ.20) GOTO 22
    GOTO 22
 23 K=I/2
    T=I-2*K
    IF (T.GT.0.1) GOTO 22
    WRITE(6,202) (BT(I,J),J=1,15)
 22 SUM2=SUM2+WY(I)*SUMA*F1
    TERM=WY(I)*SUMB*DF
    SUM3=SUM3+TERM
    SUM4=SUM4+TERM*E
  5 CONTINUE
    IF (L.EQ.1.OR.L.EQ.20) GOTO 56
    GOTO 56
 54 DO 51 I=2,30,2
    XLL1=0.
    XLL2=0.
    XLL3=0.
    XLL4=0.
    DO 53 J=1,15
    XMU=GG(J)
    DIF=BG(I,J)*WX(J)/0.250193
    XLL1=XLL1+DIF/2.
    XLL2=XLL2+DIF*3./2.*XMU
    XLL3=XLL3+DIF*5./2.*(3.*XMU*XMU-1.)/2.
    XLL4=XLL4+DIF*7./2.*XMU*(5.*XMU*XMU-3.)/2.
 53 CONTINUE
    XLP1(I)=XLL1
    XLP2(I)=XLL2
    XLP3(I)=XLL3
    XLP4(I)=XLL4
 51 CONTINUE
    WRITE (6,202) (XLP1(I),I=2,30,2)
    WRITE (6,202) (XLP2(I),I=2,30,2)
    WRITE (6,202) (XLP3(I),I=2,30,2)
```

```
      WRITE (6,202) (XLP4(I),I=2,30,2)
   56 VX=2.*SUM2/SUM3/B1
      AVE=SUM4/SUM3
      V(L)=VEL
      IF (L.LT.3) GOTO 10
      RAT=VEL/V(L-1)
      WRITE (6,200) L,VX,AVE,RAT,VEL
      GOTO 12
   10 WRITE (6,201) L,VX,AVE,VEL
   12 RETURN
      END
/DATA
-0.9739E+00  0.6667E-01
-0.8651E+00  0.1495E+00
-0.6794E+00  0.2191E+00
-0.4334E+00  0.2693E+00
-0.1489E+00  0.2955E+00
 0.1489E+00  0.2955E+00
 0.4334E+00  0.2693E+00
 0.6794E+00  0.2191E+00
 0.8651E+00  0.1495E+00
 0.9739E+00  0.6667E-01
 .0090242   .0090242
 .0710987   .0710987
- .0770721- .0770721
 .3501443   .3501443
- .6625093- .6625093
1.2630122 1.2630123
-1.6802270-1.6802270
1.9534439 1.9534439
0.0069028 0.0603652
-0.0926840 0.4301592
-1.0343692 2.2336420
-3.5331888 4.3920768
-3.7088370 1.5148337
- .993128   .017614
- .963972   .040601
- .912234   .062672
- .839117   .083277
- .746332   .101930
- .636054   .118195
- .510867   .131689
- .373706   .142096
- .227786   .149173
- .076527   .152753
 .076527   .152753
 .227786   .149173
 .373706   .142096
 .510867   .131689
 .636054   .118195
 .746332   .101930
 .839117   .083277
 .912234   .062672
 .963972   .040601
 .993128   .017614
```

Time evolution for a field of 1 x 10^4 V/m

The programme listed above will calculate the time evolution of the distribution function for InSb at a field of 1 x 10^4 V/m. For brevity, only the effects of polar phonon scattering has been included, but at this particular field it is the dominant scattering mechanism.

The following table lists the time evolution of the carrier drift velocity and average carrier energy for InSb at 77° K from equilibrium. The first column gives the number of the iterate, the second column the carrier drift velocity in m/s, the third column the average carrier energy in eV, the fourth column the maximum "distance" between two successive iterates, and the fifth column the ratio of successive "distances" between iterates:

```
 1  0.1404E 01  0.1092E-01  0.1000E 01

THE VALUE OF GAMMA IS 1./0.2E-12

 2  0.2417E 05  0.1096E-01  0.5235E-01
 3  0.4632E 05  0.1106E-01  0.5023E-01  0.9594E 00
 4  0.6744E 05  0.1122E-01  0.4806E-01  0.9569E 00
 5  0.8798E 05  0.1142E-01  0.4940E-01  0.1028E 01
 6  0.1081E 06  0.1165E-01  0.4979E-01  0.1008E 01
 7  0.1279E 06  0.1193E-01  0.4930E-01  0.9901E 00
 8  0.1473E 06  0.1224E-01  0.4804E-01  0.9746E 00
 9  0.1664E 06  0.1258E-01  0.4711E-01  0.9807E 00
10  0.1850E 06  0.1295E-01  0.4751E-01  0.1008E 01
11  0.2032E 06  0.1334E-01  0.4722E-01  0.9941E 00
12  0.2209E 06  0.1375E-01  0.4633E-01  0.9811E 00
13  0.2381E 06  0.1418E-01  0.4556E-01  0.9833E 00
14  0.2548E 06  0.1461E-01  0.4569E-01  0.1003E 01
15  0.2710E 06  0.1505E-01  0.4527E-01  0.9908E 00
16  0.2867E 06  0.1548E-01  0.4435E-01  0.9798E 00
17  0.3019E 06  0.1591E-01  0.4425E-01  0.9976E 00
18  0.3166E 06  0.1634E-01  0.4403E-01  0.9952E 00
19  0.3308E 06  0.1675E-01  0.4336E-01  0.9848E 00
20  0.3444E 06  0.1714E-01  0.4306E-01  0.9930E 00
21  0.3574E 06  0.1752E-01  0.4293E-01  0.9969E 00
22  0.3698E 06  0.1788E-01  0.4238E-01  0.9872E 00
23  0.3814E 06  0.1822E-01  0.4147E-01  0.9784E 00
24  0.3924E 06  0.1855E-01  0.4025E-01  0.9706E 00
25  0.4026E 06  0.1886E-01  0.3879E-01  0.9637E 00

THE VALUE OF GAMMA IS 1./0.75E-12

 2  0.4361E 06  0.2007E-01  0.1364E 00
 3  0.4498E 06  0.2095E-01  0.1139E 00  0.8355E 00
 4  0.4570E 06  0.2169E-01  0.9813E-01  0.8613E 00
 5  0.4603E 06  0.2225E-01  0.8339E-01  0.8498E 00
 6  0.4613E 06  0.2264E-01  0.6952E-01  0.8337E 00
 7  0.4612E 06  0.2292E-01  0.5767E-01  0.8295E 00
 8  0.4604E 06  0.2312E-01  0.4876E-01  0.8455E 00
```

9	0.4593E 06	0.2326E-01	0.4313E-01	0.8846E 00
10	0.4582E 06	0.2336E-01	0.4035E-01	0.9355E 00
11	0.4570E 06	0.2343E-01	0.3833E-01	0.9499E 00
12	0.4558E 06	0.2348E-01	0.3650E-01	0.9522E 00
13	0.4548E 06	0.2351E-01	0.3466E-01	0.9466E 00
14	0.4538E 03	0.2354E-01	0.3281E-01	0.9466E 00
15	0.4528E 06	0.2355E-01	0.3101E-01	0.9452E 00
16	0.4520E 06	0.2355E-01	0.2933E-01	0.9457E 00
17	0.4512E 06	0.2355E-01	0.2877E-01	0.9811E 00
18	0.4504E 06	0.2355E-01	0.2898E-01	0.1007E 01
19	0.4497E 06	0.2355E-01	0.2901E-01	0.1001E 01
20	0.4491E 06	0.2354E-01	0.2889E-01	0.9959E 00
21	0.4485E 06	0.2353E-01	0.2865E-01	0.9919E 00
22	0.4480E 06	0.2352E-01	0.2833E-01	0.9887E 00
23	0.4475E 06	0.2351E-01	0.2794E-01	0.9864E 00
24	0.4471E 06	0.2350E-01	0.2751E-01	0.9845E 00
25	0.4467E 06	0.2349E-01	0.2705E-01	0.9833E 00

Steady state for a field of 1 x 10^4 V/m

The corresponding steady state distribution function can be evaluated by choosing a suitable initial distribution function with the same average energy and drift velocity. In this case an exact drifted Maxwellian distribution function with an electron temperature of 95° K and drift velocity of 4.5 x 10^5 m/s was chosen for the initial function. The columns correspond to those previously defined:

1	0.4517E 06	0.2483E-01	0.2571E 01

THE VALUE OF GAMMA IS 1./0.75E-12

2	0.4464E 06	0.2477E-01	0.4800E 00	
3	0.4482E 06	0.2438E-01	0.3805E 00	0.7928E 00
4	0.4511E 06	0.2420E-01	0.2833E 00	0.7444E 00
5	0.4527E 06	0.2407E-01	0.1978E 00	0.6983E 00
6	0.4519E 06	0.2394E-01	0.1162E 00	0.5874E 00
7	0.4496E 06	0.2382E-01	0.6327E-01	0.5446E 00
8	0.4471E 06	0.2372E-01	0.3121E-01	0.4932E 00
9	0.4451E 06	0.2363E-01	0.2757E-01	0.8835E 00
10	0.4438E 06	0.2357E-01	0.2580E-01	0.9358E 00
11	0.4431E 06	0.2352E-01	0.2526E-01	0.9789E 00
12	0.4428E 06	0.2349E-01	0.2436E-01	0.9647E 00
13	0.4427E 06	0.2347E-01	0.2285E-01	0.9378E 00
14	0.4426E 06	0.2346E-01	0.2125E-01	0.9300E 00
15	0.4426E 06	0.2346E-01	0.1979E-01	0.9315E 00
16	0.4425E 06	0.2345E-01	0.1854E-01	0.9366E 00
17	0.4425E 06	0.2344E-01	0.1747E-01	0.9421E 00
18	0.4424E 06	0.2344E-01	0.1655E-01	0.9477E 00
19	0.4424E 06	0.2343E-01	0.1578E-01	0.9531E 00
20	0.4424E 06	0.2343E-01	0.1512E-01	0.9582E 00
21	0.4424E 06	0.2342E-01	0.1547E-01	0.9637E 00
22	0.4424E 06	0.2342E-01	0.1411E-01	0.9684E 00
23	0.4424E 06	0.2342E-01	0.1387E-01	0.9831E 00
24	0.4424E 06	0.2342E-01	0.1379E-01	0.9941E 00

References

[1] E.M. Conwell, High Field Transport in Semiconductors, Academic Press, New York/London 1967.

[2] H. Fröhlich and F. Seitz, Phys. Rev. 79, 526 (1950).

[3] H. Fröhlich and V.V. Paranjape, Proc. Phys. Soc. B69, 21 (1956).

[4] T. Kurosawa, J. Jap. Phys. Soc. 20, 937 (1965).

[5] A.D. Boardman, W. Fawcett and H.D. Rees, Sol. Stat. Comm. 6, 305 (1968).

[6] H.D. Rees, J. Phys. Chem. Sol. 30, 643 (1969).

[7] H.D. Rees, J. Phys. C: Sol. State Phys. 5, 641 (1972).

[8] J. Bok and C. Guthmann, phys. stat. sol. 6, 853 (1964).

[9] M. Glicksman and W.A. Hicinbothem, Jr., Phys. Rev. 129, 1572 (1963).

[10] C. Hammar and P. Weissglas, phys. stat. sol. 24, 531 (1967).

[11] T. Stokoe and J.F. Cornwell, phys. stat. sol. 49, 1, 209 (1972).

[12] T. Stokoe and J.F. Cornwell, phys. stat. sol. 49, 2, 651 (1972).

[13] I. Licea, phys. stat. sol. 25, 461 (1968).

[14] I. Licea, phys. stat. sol. 27, K137 (1968).

[15] I. Licea, phys. stat. sol. 37, 795 (1970).

[16] I. Licea, phys. stat. sol. 38, 841 (1970).

[17] E.M. Conwell, Phys. Rev. 143, 657 (1965).

[18] V.V. Paranjape, Phys. Rev. 150, 608 (1966).

[19] E.O. Kane, J. Phys. Chem. Sol. 1, 249 (1957).

[20] H. Fröhlich, Proc. Roy. Soc. A160, 230 (1937).

[21] R. Stratton, Proc. Roy. Soc. A246, 408 (1958).

[22] H. Ehrenreich, J. Phys. Chem. Sol. 2, 131 (1957).

[23] E.G.S. Paige, Prog. Semicond. 8, 62 (1964).

[24] L.L. Korenblit and V.E. Sherstobitov, Sov. Phys. Semiconductors 2. 5. 564 (1968).

[25] H. Brooks, Phys. Rev. 83, 879 (1951).

[26] R. Barrie, Proc. Phys. Soc. B69, 553 (1956).

[27] H.J. Hrostowski, F.J. Morin, T.H. Geballe and G.H. Wheatley, Phys. Rev. 98, 556 (1955).

[28] M.A. Kinch, Brit. J. Appl. Phys. 17, 1257 (1966).

[29] H. Miyazawa and H. Ikoma, J. Jap. Phys. Soc. 23, 290 (1967).

[30] E. Bonek and K. Richter, Bericht Nr. HL7, Institut für Hochfrequenztechnik der Technischen Hochschule, Wien (1967).

[31] W. Zawadzi and W. Symansky, J. Phys. Chem. Sol. 32, 1151 (1971).

[32] W.G. Spitzer and H.Y. Fan, Phys. Rev. 99, 1893 (1955).

[33] G.S. Picus, E. Burstein, B.W. Henvis and M. Hass, J. Phys. Chem. Sol. 8, 282 (1959).

[34] M. Hass and B.W. Henvis, J. Phys. Chem. Sol. 23, 1099 (1962).

[35] R.B. Sanderson, J. Phys. Chem. Sol. 26, 803 (1965).

[36] E. Haga and H. Kimura, J. Jap. Phys. Soc. 18, 777 (1963).

[37] I.M. Tsidilovski, phys. stat. sol. 8, 253 (1965).

[38] E. De Alba and J. Warman, J. Phys. Chem. Sol. 24, 531 (1967).

[39] D. Mukhopadhyay and B.R. Nag, Indian J. of Pure and App. Phys. 7, 616 (1969).

[40] O. Madelung, Physics of III-V Compounds, John Wiley and Sons Inc., New York (1964).

[41] V.V. Paranjape and T.P. Ambrose, Phys. Letters 8, 4, 223 (1964).

[42] V.V. Paranjape and E. De Alba, Proc. Phys. Soc. 85, 945 (1965).

[43] D. Matz, Phys. Rev. 168, 3, 843 (1968).

[44] R.B. Dingle, Phil. Mag. 46, 831 (1955).

[45] A. Neukerman and G.S. Kino, Appl. Phys. Letters 17, 102 (1970).

[46] A.H. Wilson, The Theory of Metals, Cambridge Univ. Press, London and New York 1953.

[47] A. Hasegawa and J. Yamashita, Phys. Chem. Sol. 23, 875 (1962).

[48] K. Huang, Statistical Mechanics, John Wiley and Sons, New York 1963.

[49] S. Chapman and T.G. Cowling, The Mathematical Theory of Non-uniform Gases, Cambridge Univ. Press, London and New York 1939.

[50] E.G.S. Paige, IBM J. Res. Develop. 562 (1969).

[51] J. Appel, Phys. Rev. 122, 1760 (1962).

[52] A. Hasegawa and J. Yamashita, J. Jap. Phys. Soc. 17, 1751 (1962).

[53] H. Budd, Phys. Rev. 158, 798 (1967).

[54] P.J. Price, IBM J. Res. Develop. 14, 12 (1970).

[55] P.C. Kwok and T.D. Schultz, Phys. Rev. 3, 4, 1180 (1971).

[56] P.C. Kwok and T.D. Schultz, Phys. Rev. 3, 4, 1189 (1971).

[57] M.O. Vassell, Jour. Math. Phys. 11, 2, 408 (1970).

[58] V. Vulich, Introduction to functional analysis for scientists and technologists, International Series of Monographs in Pure and Applied Maths., No. 32 Pergammon Press.

[59] S. Porowski, W. Paul, J.C. McGroddy, M.I. Natwin and J.E. Smith Jr., Sol. State Comm. 7, 905 (1969).

[60] J.E. Smith Jr., M.I. Nathan and J.C. McGroddy, Appl. Phys. Letters 15, 242 (1969).

[61] P.N. Butcher and W. Fawcett, Proc. Phys. Soc. 86, 1205 (1965).

[62] W. Fawcett and J.G. Ruch, Appl. Phys. Letters 15, 11, 368 (1969).

[63] W. Fawcett, A.D. Boardman and S. Swain, J. Phys. Chem. Sol. 31, 1963 (1970).

[64] J.L. Birman, M. Lax and R. Loudon, Phys. Rev. 145, 620 (1966).

[65] D.L. Stierwalt, J. Jap. Phys. Soc. Suppl. 21, 58 (1966).